

**DEVELOPMENT OF DESIGN TOOL FOR STATICALLY
EQUIVALENT DEEPWATER MOORING SYSTEMS**

A Thesis

by

IKPOTO ENEFIOK UDOH

Submitted to the Office of Graduate Studies of
Texas A&M University
in partial fulfillment of the requirements for the degree of

MASTER OF SCIENCE

December 2008

Major Subject: Ocean Engineering

**DEVELOPMENT OF DESIGN TOOL FOR STATICALLY
EQUIVALENT DEEPWATER MOORING SYSTEMS**

A Thesis

by

IKPOTO ENEFIOK UDOH

Submitted to the Office of Graduate Studies of
Texas A&M University
in partial fulfillment of the requirements for the degree of

MASTER OF SCIENCE

Approved by:

Chair of Committee,	Richard Mercier
Committee Members,	Harry Jones
	Jerome Schubert
Head of Department,	David V. Rosowsky

December 2008

Major Subject: Ocean Engineering

ABSTRACT

Development of Design Tool for Statically Equivalent Deepwater Mooring Systems. (December 2008)

Ikpoto Enefiok Udoh, B. Eng., University of Port Harcourt, Nigeria

Chair of Advisory Committee: Dr. Richard Mercier

Verifying the design of floating structures adequately requires both numerical simulations and model testing, a combination of which is referred to as the hybrid method of design verification. The challenge in direct scaling of moorings for model tests is the depth and spatial limitations in wave basins. It is therefore important to design and build equivalent mooring systems to ensure that the static properties (global restoring forces and global stiffness) of the prototype floater are matched by those of the model in the wave basin prior to testing.

A fit-for-purpose numerical tool called STAMOORSYS is developed in this research for the design of statically equivalent deepwater mooring systems. The elastic catenary equations are derived and applied with efficient algorithm to obtain local and global static equilibrium solutions. A unique design page in STAMOORSYS is used to manually optimize the system properties in search of a match in global restoring forces and global stiffness. Up to eight mooring lines can be used in analyses and all lines have the same properties. STAMOORSYS is validated for single-line mooring analysis using LINANL and Orcaflex, and for global mooring analysis using MOORANL and Orcaflex. A statically equivalent deepwater mooring system for a representative structure that could be tested in the Offshore Technology Research Center at Texas A&M University is then designed using STAMOORSYS and the results are discussed.

DEDICATION

This work is dedicated to the almighty God for his kindness and mercies.

ACKNOWLEDGEMENTS

The successful completion of my thesis was possible thanks to the support of many people, including my committee members, professors, friends and family. I give my sincere thanks to my committee chair, Dr. Richard Mercier, for the opportunity to be a part of this research and for inspiring me to work hard at it. His insistence on top quality work drove my ability to search deep for adequate solutions to research challenges. I appreciate Dr. Harry Jones for his support, guidance, and timely feedback during my research. I thank Dr. Jerome Schubert for honest feedback on my work and for serving effectively on my committee even under short notice. I thank Dr. Robert Randall for his guidance and counseling which helped me set a balance between research and other aspects of my academic pursuits. My thanks also go to Dr. Scott Socolofsky for his ideas which inspired me to explore possible routes in search of the best approaches to overcome some of my research challenges.

I thank my parents Hon. Justice and Barr. (Lady) Enefiok Udoh, for their immeasurable support during the entire course of my studies. I extend my gratitude to my love Agnes Iyoho, who encouraged me and stood by me through it all. I appreciate my brother Anyanya and my sisters Uduak and Ndifreke for their moral support and guidance whenever I needed to make difficult decisions.

I acknowledge my friends James Ofoegbu, Amir Izadparast, Suresh Rajendran, Adeniyi Olumide and Akan Ndey for making themselves available anytime it was necessary to have fun and ease the troubled research mind. Their pieces of advice and jokes made a world of difference in re-generating the strength and motivation to accomplish the goals of my research.

TABLE OF CONTENTS

	Page
ABSTRACT	iii
DEDICATION	iv
ACKNOWLEDGEMENTS	v
TABLE OF CONTENTS	vi
LIST OF FIGURES	viii
LIST OF TABLES	xiii
CHAPTER	
I INTRODUCTION: MOORING OF OFFSHORE STRUCTURES	1
1.1 Introduction	1
1.2 Objective of research	3
1.3 Truncated versus equivalent mooring systems	5
1.4 Scope of research project	23
1.5 Mooring lines and components of mooring systems	24
1.6 Offshore mooring systems	33
II DESIGN-RELATED LIMITATIONS OF EXISTING MOORING METHODOLOGIES	36
2.1 Challenges in deepwater model testing using equivalent mooring systems	36
2.2 Suitability of existing approaches for mooring line analysis	47

CHAPTER	Page
2.3 Engineering behavior and modes of failure of mooring lines	61
III FORMULATION OF STAMOORSYS	70
3.1 General principles in static analysis of spread catenary mooring systems	71
3.2 Algorithm used in STAMOORSYS for the design of statically equivalent spread mooring systems	84
3.3 A description of the features in STAMOORSYS	99
IV APPLICATION OF STAMOORSYS IN DESIGN OF STATICALLY EQUIVALENT MOORING SYSTEMS	109
4.1 Analysis of single line mooring systems using STAMOORSYS, Orcaflex and LINANL	109
4.2 Validation of STAMOORSYS for static global analysis of spread mooring systems	124
4.3 Design of statically equivalent deepwater mooring system	130
V SUMMARY AND CONCLUSIONS	140
5.1 Economic advantages of STAMOORSYS	141
5.2 Limitations of STAMOORSYS and up-coming modifications	142
5.3 Conclusions	144
REFERENCES	146
APPENDIX A	149
APPENDIX B	152
VITA	156

LIST OF FIGURES

FIGURE	Page
1.1 Sketch of truncated and full depth mooring systems	6
1.2 The hybrid approach to design verification	10
1.3 Discrepancies between full depth floater and model scale floater	13
1.4 Sketch of discrepancies between full depth and model scale systems	13
1.5 Dependence of uncertainties on model scale	17
1.6 Model tank station-keeping equipment	20
1.7 Static mooring line responses – prototype versus model	21
1.8 A sketch showing the use of point masses in truncated systems	22
1.9 Stainless steel cable	25
1.10 (a) Very flexible steel cable (b) Flexible steel cable	26
1.11 Studless mooring chain	27
1.12 Stud-linked mooring chain	27
1.13 Synthetic fiber rope	28
1.14 Anchor set-up for basin scale mooring	30
1.15 Clamping device for basin scale mooring line	30
1.16 Connectors for model scale mooring	31
1.17 Bending Shoe and Rotary Sheave fairleads	32
1.18 Pad-eye screw	33

FIGURE	Page
1.19 Classification of spread mooring systems	34
1.20 Spread mooring systems	34
2.1 OTRC wave basin and FPSO model	37
2.2 Prototype (a) and Equivalent (b) mooring system layouts	38
2.3 Vertical profile of catenary mooring system – full depth system	41
2.4 Vertical profile of equivalent system	41
2.5 Total restoring force (in kN) and single line static characteristics of systems – full depth system versus equivalent ...	42
2.6 Free body diagram of considered mooring system	47
2.7 Representation of floating unit with eight mooring lines	51
2.8 Representation of mooring lines by means of non-linear springs ...	52
2.9 (a) Initial mooring pattern (b) Final mooring pattern	54
2.10 Mooring stiffness curves for the Brazilian FPSO	58
2.11 Free body diagram of elastic cable connecting points A and B	59
2.12 Static stiffness test	65
2.13 Mean load steps and cycling tests	66
2.14 Loading mechanisms on offshore mooring chains	67
2.15 Fatigued sections of a mooring chain	68
2.16 Stress range – No. of cycles relationship	68
3.1 Sketch of spread mooring system with 4 mooring lines in elevation	71
3.2 Single-segment mooring	72

FIGURE	Page
3.3 Free body diagram of elemental section	73
3.4 Sketch of single line mooring showing offset and departure	85
3.5 A summary of the computation procedure in STAMOORSYS	86
3.6 Sample layout of 4-line and 8-line system for zero offset case	88
3.7 Numerical procedure in STAMOORSYS	90
3.8 Simple sketch of 3-segment mooring line	91
3.9 Equilibrium configuration found with touchdown point within segment 3	92
3.10 Equilibrium configuration when touchdown point is at end of segment 3	92
3.11 Equilibrium configuration found with touchdown point within segment 2	93
3.12 Equilibrium configuration when touchdown point is at end of segment 2	93
3.13 Equilibrium configuration found with touchdown point within segment 1	94
3.14 Equilibrium configuration when touchdown point is at end of segment 1	94
3.15 Challenge in using higher order interpolation in STAMOORSYS	95
3.16 Verification of linear interpolation accuracy	96
3.17 A 4-line mooring system with $X_{off} > 0, Y_{off} > 0$ offset	97
3.18 STAMOORSYS offset error prompt	100
3.19 Tasks executed by different user controls in set-up page	101
3.20 Tasks executed by different user controls in design page	106

FIGURE	Page
3.21 Summary of recommended approach in the use of STAMOORSYS	107
4.1 Problem set-up for single line analysis using STAMOORSYS, Orcaflex and LINANL	109
4.2 Restoring forces versus departures for Case 1	110
4.3 Restoring forces versus fairlead tensions for Case 1.....	113
4.4 Restoring forces versus tensions at the anchor for Case 1	113
4.5 Suspended lengths versus restoring forces for Case 1	114
4.6 Lengths on the sea floor versus restoring forces for Case 1	114
4.7 Restoring forces versus departures for Case 2	115
4.8 Restoring forces versus fairlead tensions for Case 2	116
4.9 Restoring forces versus tensions at the anchor for Case 2	116
4.10 Suspended lengths versus restoring forces for Case 2	117
4.11 Lengths on the sea floor versus restoring forces for Case 2	117
4.12 Restoring forces versus departures for Case 3	118
4.13 Restoring forces versus fairlead tensions for Case 3	119
4.14 Restoring forces versus tensions at the anchor for Case 3	119
4.15 Suspended lengths versus restoring forces for Case 3	120
4.16 Lengths on the sea floor versus restoring forces for Case 3	120
4.17 Restoring forces versus departures for Case 4	122
4.18 Fairlead tensions versus departures for Case 4.....	123
4.19 MOORANL and STAMOORSYS x-axis global restoring force curves	125

FIGURE	Page
4.20 MOORANL and STAMOORSYS y-axis global restoring force curves	126
4.21 MOORANL and STAMOORSYS x-axis global stiffness curves	126
4.22 MOORANL and STAMOORSYS y-axis global stiffness curves	127
4.23 Orcaflex and STAMOORSYS x-direction global restoring force curves	129
4.24 Orcaflex and STAMOORSYS x-direction global stiffness curves	129
4.25 Plan view sketch of prototype mooring system	131
4.26 Plan view sketch of equivalent mooring set-up	132
4.27 Equivalent and prototype global restoring forces for design solution 1	134
4.28 Equivalent and prototype global stiffness for design solution 1	135
4.29 Equivalent and prototype global restoring forces for design solution 2	138
4.30 Equivalent and prototype global stiffness for design solution 2.....	138

LIST OF TABLES

TABLE	Page
2.1 Comparison of effective system stiffness contribution due to presence of risers	57
3.1 Summary of major equations used in obtaining static equilibrium solutions	83
3.2 Display of check related to preliminary and computed departures	102
3.3 Sample display of check related to grid resolution	102
4.1 Mooring line properties for hypothetical problem	111
4.2 Results for single line analysis, Case 1	112
4.3 Results for single line analysis, Case 2	112
4.4 Results for single line analysis, Case 3	112
4.5 Properties of mooring system components for test Case 4	121
4.6 Fairlead and anchor coordinates for example problem	125
4.7 Mooring line properties for global analysis validation using Orcaflex	128
4.8 Mooring line coordinates for global analysis validation using Orcaflex	128
4.9 Properties of first equivalent mooring design solution	136
4.10 Properties of second equivalent mooring design solution	137

CHAPTER I

INTRODUCTION: MOORING OF OFFSHORE STRUCTURES

1.1 INTRODUCTION

Consistent demand for offshore resources has seen the industry to an era of increasing applications of deep water technology and concepts for better engineering productivity. The sustained drive to improve the harvests from offshore oil exploration, production and transportation has led to the existence of various structures, designed to meet the specific needs of the industry under peculiar circumstances. In ocean depths widely defined as deep water (500m up to 3000m) floating structures find most use in offshore operations as the construction and performance of fixed structures for such depths would be enormously expensive, and of very high engineering risks.

Floating offshore vessels, like any other, require stability to be operational especially under extreme environmental conditions. Mooring systems are therefore required to provide such stability against vessel dynamics, while ensuring allowable excursions. With so much depending on the mooring systems of these floating structures, it is worthwhile to understand to a high degree of accuracy the performance of each of the system components and the global response of the mooring system. The performance of any mooring system is typically a function of the type and size of the vessel in use, the operational water depth, environmental forces acting, sea bed (soil) conditions, and the competence of the mooring lines and anchors / clump weights. These different factors must be closely complimentary for a mooring system to harness its full potential against environmental loads which are predominant offshore.

This thesis follows the style of ASME Journals.

At prototype scale, designing a mooring system for floating structures requires careful considerations of all factors, keeping in mind the implications of the failure of the system. Understanding the behavior of the structure under operational loads is essential for a competent design. Considerations in design must include maximum permissible excursions of the vessel, proper choice of mooring lines, anchors and clump weights (if used), design life, cost and failure modes such as snapping of mooring lines and fatigue damage.

Of equal (if not greater) importance is the verification of the global analysis performed in the design of floating structures and their moorings. Conscious of the fact that such structures will be exposed to great environmental forces offshore, measures must be taken to ensure that their designs are appreciably reliable. One way to verify the analysis performed in the prototype design process is by model testing. A model of the designed floater is built and subjected to the same environmental loads in the wave basin as those used in the prototype design. During testing, the responses of the floater to various forcing due to wind, wave and current are measured and compared to those obtained in the design of the prototype floater. For as long as the testing procedure is conceptually and practically correct, the results obtained independently represent the performance to be expected of the prototype floater under the given loading conditions, if it is installed in the field. Therefore the role of model testing in the verification of designs for floating structures is truly unique.

A more highly appreciated method of verifying the design of floating structures is one called the hybrid approach. This approach involves the combination of model testing with numerical simulation, to obtain the response of the floater at model scale. The hybrid method has been proven to reduce the uncertainties in the verification process significantly, as opposed to an isolated physical model

testing approach. Details of the hybrid approach are given in section 1.3.1 of this document.

Conducting model tests requires wave basins, which are typically limited in depth and spatial dimensions. Although the model floater is typically much smaller than the prototype system, depending on the model scale chosen, basin dimensions may not be sufficiently large to accommodate the directly scaled mooring system. Consequently, the size of the floater and the accompanying mooring system are reduced such that they adequately fit into the test facility. The test engineer has a primary task to replicate the static behavior of the prototype system on the model to be tested in the wave basin. Essentially, the effects of the mooring system in the wave basin on the model floater must be equal to those which the prototype mooring system has on the full-depth floater. This introduces the need for equivalent mooring systems to represent the moorings of the full depth system. In many publications, the terms “equivalent mooring systems” and “truncated mooring systems” are interchangeably used, but doing so defiles their individual definitions. In a later section of this report, a proper distinction between the two is drawn for clarity.

1.2 OBJECTIVE OF RESEARCH

The challenge of understanding the behavior of a floating structure under environmental loads is quite a hand full, and producing designs of mooring systems with high integrity requires the ability to isolate the various behaviors of the system as induced by different loads acting. The dynamic response of a vessel would most often over-shadow its static response. For this reason, it is considered good practice to study the static and dynamic responses of floating vessels independently in design, to allow a clear attribution of observed results to the correct vessel responses.

It is therefore pertinent to resort to physical model tests as an important aspect of the design of offshore structures. Model tests provide a competent approach to validate computer-aided designs of mooring systems. However, a major challenge to model testing is the limited depth and dimension of available model basins. This limitation poses the challenge of developing truncated mooring systems of static equivalence to that which the considered full depth floaters will be connected. The designer thus ensures through this process that the static global behavior of the prototype floater mooring system is most appropriately represented. Without this representation, the basis for comparing the two systems (prototype and model) is compromised, and so static equivalence provides an agreement in static global responses between model and prototype prior to measurement of dynamic responses.

This research provides a designer-friendly software / program for the design of statically equivalent mooring systems for model testing purposes. The reader will find in this text discussions portraying the relevance of suitable software in the design of such mooring systems. Although many softwares exist that perform static analysis of mooring systems, most are by far more cumbersome to use for the mentioned objective. While the designer seeks an optimum statically equivalent mooring system that reflects a replication of the prototype floating vessel, flexibility is required in computer-aided design for easy alteration of design parameters for sensitivity analysis.

General discussions on mooring of offshore structures can be found later in this chapter, including mooring lines, mooring components and various offshore mooring systems in contemporary use. The second chapter of this text discusses previous works related to model testing using equivalent mooring systems, exposing further the relevance of this research. Within the third chapter, discussions on the formulation of the software produced in this research can be found. The application of the formulated tool in the design of statically

equivalent mooring systems using possible test cases is reported in the fourth chapter. Comparisons are also made with existing programs widely used in mooring analysis. A summary and conclusions follow in the last chapter of this text, highlighting the economic significance of this project and probable future modifications to the software.

1.3 TRUNCATED VERSUS EQUIVALENT MOORING SYSTEMS

Throughout this text a truncated mooring systems refers to a mooring system which has been reduced in size due to basin depth or spatial limitations as suggested by fig 1.1. In other words the actual mooring system is shortened to allow physical model testing, used in the verification of design of any considered floating structure. It is worthy of emphasis that though the truncation of mooring systems is inevitable based on spatial limitations, the optimum objective is to have the model's mooring system produce an equivalent performance to the already-designed prototype system. Therefore a mooring system which has been reduced in size and which matches the static properties of the full depth system in the same number of rigid body degrees of freedom and over some specified range of loads or offsets is best described as a “statically equivalent mooring system”. Such a system is the focus of this research, and beyond this point, it shall in some contexts within this text be simply referred to as an “equivalent mooring system”. An equivalent mooring system used in model tests makes the following tasks achievable:

- A demonstration of the competence of the applied concepts in analysis and design of the mooring system
- Exposing and isolating the system behaviors (dynamic and static), to enable accurate attribution of various results to the correct loads inducing them
- Evaluation of the accuracy of assumptions, factors and allowances considered in the analysis and design process for floating systems

- Identification of possible unexpected behaviors of the system, which may not be accounted-for in the design.

A truncated mooring system simply implies terminating the mooring at the available depth without modifying the properties of the retained segments. With such a system, static equivalence is impossible hence the need to modify the properties of the retained segments to obtain static behaviors similar to those of the prototype floater.

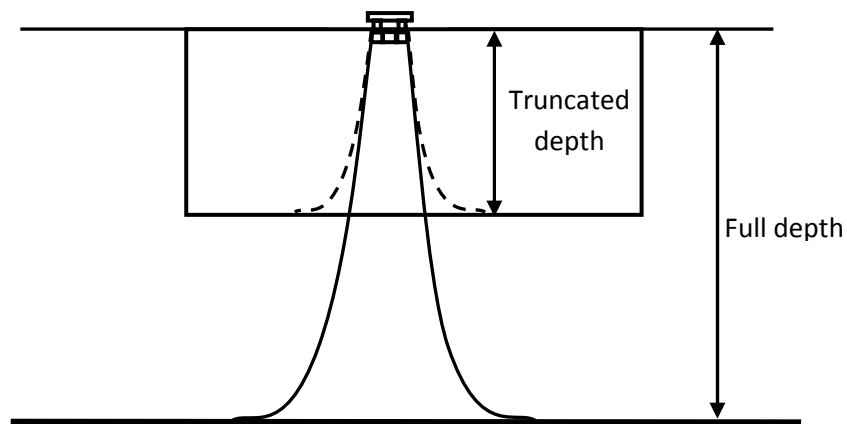


Fig. 1.1: Sketch of truncated and full depth mooring systems

It is necessary to mention that the successful verification of designs using model testing with equivalent mooring systems requires competent tools and experienced testing engineers. Even with such tools and competent engineers, there may be design issues that cannot be predicted by model testing with a high degree of accuracy. This implies that numerical simulation models must be validated and calibrated using conditions as close as possible to the original (full depth) system. Once this is guaranteed, extrapolation to the full depth system using the validated model is justified.

Considering that the use of both model testing and numerical simulation together will increase the tendency to produce more optimal and reliable designs, the argument that simulation softwares be as designer-friendly as possible is

bolstered. A reduction in the complexity of numerical simulation software reduces the probability of producing incorrect calibration results. If calibration results are inaccurate, then the basis for comparison of computer-aided designs with the results of model testing using equivalent mooring systems is almost completely flawed and this research is essentially aimed at providing a tool which focuses only on static design, making it easier to formulate a fit-for-purpose tool.

Certain criteria must be satisfied for a numerical model to be considered validated by a calibration process; in comparison with model test results obtained using equivalent mooring systems.

- If the target of the numerical model is to simulate static response of the floater / mooring system, then it must be able to reproduce all statically measured responses (global restoring forces, horizontal offsets, tensions, etc.) from offset tests performed with the same conditions used in the numerical model simulation.
- For the simulation of dynamic response, the coupled numerical model should be able to reproduce measured floater / mooring system responses of damping tests, wind / current forces, regular waves and random wave tests.

In validating numerical models with model testing, it is important to identify and apply a testing procedure that assists the verification process. A widely accepted procedure is to start off with static offset tests, then damping tests, force calibration tests, regular wave tests, and so on.

1.3.1 DESIGN CONSIDERATIONS FOR EQUIVALENT MOORING SYSTEMS

Discussions here reflect contributions from a wealth of experienced design and model testing engineers, some of whose works are discussed in the literature review (second chapter). Important aspects of the verification of mooring

designs for deep water floating structures are described. After the scaled physical model of the floater / mooring system is built, a numerical model of this physical model is built with the same numerical modeling procedures as the prototype system. This process is described as “modeling the model”. The design of the statically equivalent mooring system is performed in such a manner as to optimize the “needs” for static equivalence of the model system to be used in the testing project.

System verification tests then proceed and all observations of system parameters that deviate from the initial model-of-the-model are incorporated in the model, thereby updating it to meet the “as-built” conditions. The integrity of the updating process depends greatly on the ability to identify inconsistencies in the numerical and physical models. Discrepancies may be found in parameters such as static offsets (for statics tests) and free vibration behavior of floater, wave radiation and diffraction effects (for dynamics tests). Feeding a correction of these discrepancies back into the equivalent design model increases the accuracy of model testing. After the tests are concluded the measured responses at model scale are extrapolated to the full depth size of the floater / mooring system using the model-of-the-model, for comparison with the response from the design of the prototype floater system. The “modeling-the-model” process is depicted as part of fig.1.2.

An important parameter to be considered in the development options for equivalent mooring systems is the ratio between the truncated depth (measured from the fairlead or top attachment point) and the full (original) water depth of the designed system. This parameter is defined as the truncation factor, and is denoted γ .

$$\text{Truncation factor } (\gamma) = \frac{\text{WaterDepth}_{\text{Full}}}{\text{WaterDepth}_{\text{Truncated}}} \quad (1.1)$$

The truncation factor is used in computations that guide the selection of mooring components for equivalent mooring design. An example is the computation of the total length of equivalent mooring lines $L_{total_equivalent}$, as:

$$L_{total_equivalent} = \gamma * L_{total_full} \quad (1.2)$$

where L_{total_full} is the total length of the mooring lines at full depth.

Considering the modeling process described earlier, designing an equivalent mooring system can be described as an optimization process, the results of which are known before the analysis. The designer faces the challenge of selecting a combination of mooring components with specific properties that produce the same static results (global restoring forces and static stiffness) for the equivalent mooring system as in the prototype system, at least with acceptable tolerance errors.

Certain factors not considered in the optimization process, but which are usually accounted for in the making of engineering judgments while comparing the measured response from model tests to those of the prototype design of the floater, include the following:

- Uncertainties regarding the model scale and those introduced by the truncation of the system.
- Interaction effects between mooring system and floater motions.
- Possibility of unknown effects.
- Checking which loading effects are predominant under applied / prevailing conditions.

It is important to further explain the hybrid approach of design verification, and in doing so emphasize how this research affects this approach. The explanations that follow are intended to offer a more explicit understanding of the processes in fig.1.2.

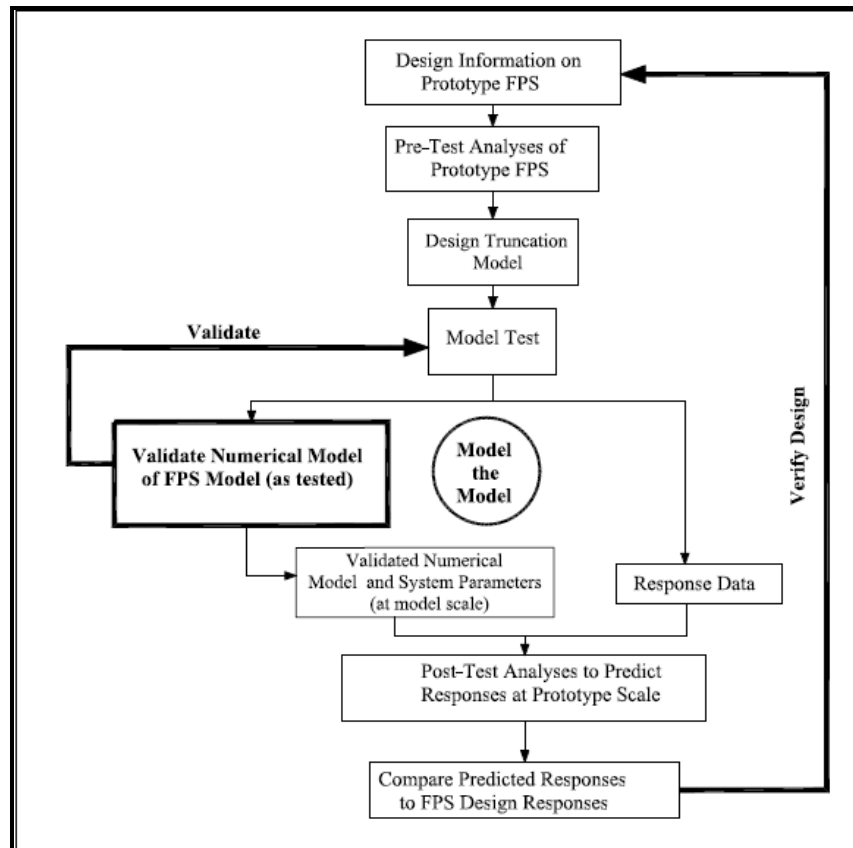


Fig. 1.2: The hybrid approach to design verification
Source: Stansberg and others [1]

- After acquiring the design information on the prototype floater (the design of which is to be verified) pre-test analyses are performed to obtain the criteria on static and dynamic parameters which must also apply to the model to be tested. Such parameters will typically include static global restoring forces and global stiffness in some specified number of rigid body degrees of freedom, and over some specified loads or offsets. Other parameters typically included are natural frequencies of the free vibration of the floater.
- Designing the statically equivalent mooring system follows. It is possible to use the same numerical tool to both model the model which is to be tested, and design the statically equivalent mooring system. However,

this research is providing a fit-for-purpose tool to handle the design of the equivalent system. At this point one may consider this development to be a division of tasks, which will not only increase the accuracy of the results from each task, but also increase the efficiency of the design process.

- With the designed statically equivalent mooring system in place with the model floater in the wave basin, model testing commences. A competent numerical tool is used to represent the floater model, and this numerical model is validated and updated to include known observed deviations from the target conditions to which the model floater must comply. Updates to the model of the statically equivalent mooring system are generally required to account for deviations between designed and as-built mooring components (springs, chains, etc.) and other adjustments to the mooring system to compensate for imperfections in the model floater (weight, buoyancy, trim). In addition the updating process relies on a verification of the agreement between the physical model and numerical model in dynamic effects such as free vibration behavior, as well as linear wave radiation and diffraction effects. Response data is also collected independent of the numerical software used in modeling the model.
- At the end of the testing process, the responses simulated by the validated numerical model should be essentially the same as those collected independent of the numerical tool. Using the validated / updated numerical model, post-test analyses involving the extrapolation of results to predict responses at the prototype scale are performed. The extrapolated responses are then compared to the responses obtained for the designed prototype floater.

So the primary effect of this research on the hybrid modeling process is providing a numerical tool (the development of which is described herein) to design the statically equivalent mooring system. This implies that a separate numerical tool would be needed to model the model.

Applying the hybrid method of model testing and numerical modeling to the design of equivalent mooring systems in such a manner that a reliable verification is performed involves some simplifying assumptions. These assumptions include:

- The method of analysis adopted in modeling-the-model accurately replicates the model test performed. One with appreciable level of experience in model testing and design of equivalent mooring systems would agree that this assumption is not farfetched if modeling tools are competent.
- Primary system responses produced by the equivalent mooring system are large enough to be measured for the validation and calibration of the analytical models.
- Extrapolation of model outputs to prototype water depth is performed using accurate numerical schemes.
- No unknowns occur between the equivalent moorings at model test water depth and the prototype mooring system at full depth.

Compensating for these assumptions in the design of truncated mooring systems is almost impossible. This gives a feel for the fact that there are limitations to the hybrid approach of FPS design verification, and that the integrity of the verification process depends greatly on how well the risks of errors and uncertainties are reduced. Most problems encountered in the modeling process associated with the design of these systems are due to practical imperfections rather than scale effects. As such there will be a variation in the integrity of different design projects involving testing engineers with comparable levels of experience.



Fig. 1.3: Discrepancies between full depth floater and model scale floater
Source: Experimental methods in marine hydrodynamics (NTNU) [2]

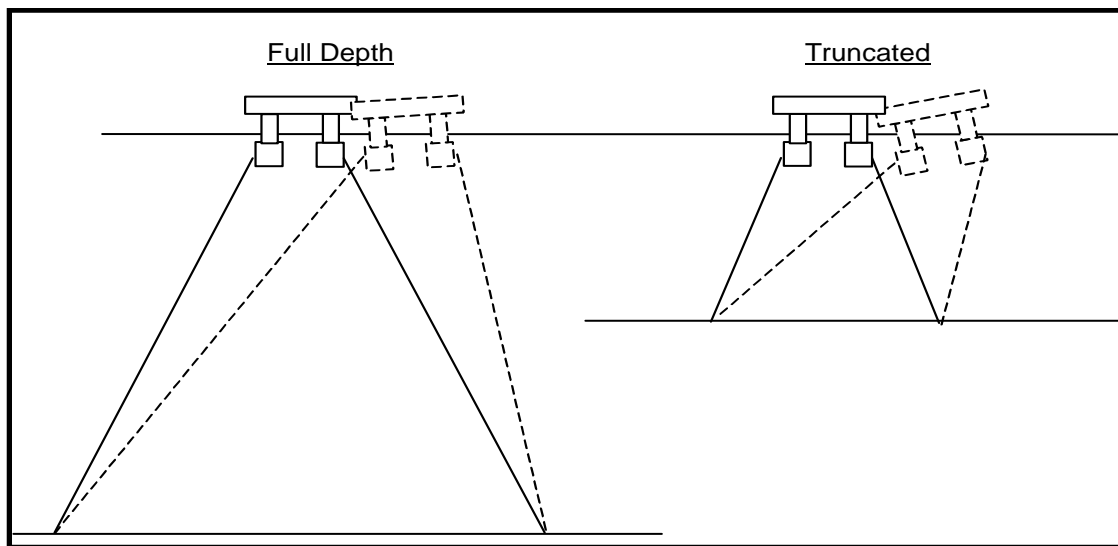


Fig. 1.4: Sketch of discrepancies between full depth and model scale systems

The truncation (not equivalence) of a mooring system at model scale can induce discrepancies compared to the prototype system. To illustrate some discrepancies between a full depth floater-mooring system and a truncated system which are inherently existent in design, the floating structures in figs. 1.3 and 1.4 may be considered. The semi-submersible platform in fig.1.4

experiences a horizontal offset as well as rolling motions in the vertical plane. Clearly, the vessel roll response is magnified in the truncated system with respect to the full depth system. Designing statically equivalent deepwater mooring systems thus requires making sound engineering judgments in an effort to compensate for such lapses.

In view of the tools and limitations discussed, the requirements and alternatives in deep water model test projects should be considered simultaneously. Selecting an acceptable verification method may depend on several factors including the type of floating structure to be modeled, the type of mooring system to be used, the primary parameters of interest and the environmental conditions. Typical alternative testing methods in the design of mooring systems include:

- Ultra small scale testing of complete system; achievable in wave basins.
- Outdoor testing in fjords or lakes. The major limitation in the use of this method is that the environmental conditions given by nature are uncontrollable and can therefore not be used on a routine basis as a verification tool. However, with outdoor testing the compromise on scale and system simplifications is greatly reduced.
- Hybrid method, combining model testing with numerical modeling - the steps of which have been appreciably discussed earlier in this section.

1.3.2 MAJOR PARAMETERS IN DESIGN OF STATICALLY EQUIVALENT DEEPWATER MOORING SYSTEMS

In general, the parameters of great significance in the design of statically equivalent mooring systems are listed below.

- Vertical calm water equilibrium position of the floater in wave basin
- Horizontal offset of floating structure in response to prevailing static loads
- Design water depth (at wave basin scale)

- Mooring line characteristics (axial stiffness, submerged weight, length)
- Total global horizontal and vertical restoring forces exerted by mooring system
- Hydrostatic and mooring contributions to the stiffness matrix for the floating structure.

Depending on the designer's interest, some parameters are of greater significance than others in specific projects. Considering that this research addresses static equivalence, dynamic parameters are not at play. Having the capability to understand the effect that each parameter has on the overall design is interesting. Sensitivity analyses ensure optimum design, and with such capability optimal design outputs can be obtained and the most critical aspects of interest in a given project can be addressed. Using such analysis guides the compensation of a non-equivalent parameter to achieve a desired response. For instance, in an effort to obtain the correct natural periods of the statically equivalent floater-mooring system, if the correct pitch stiffness cannot be achieved and the designer considers this to be important for the floater response, then an option may be considered where the pitch stability could be used to compensate inadequate pitch stiffness. In other words, if the longitudinal metacentric height (GM_L) of the structure is great enough such that the pitch motions do not affect the stability of the floating structure, then this effect could compensate the inadequate pitch stiffness. Although such improvising strategies are acceptable to some testing engineers, they may not necessarily qualify as decent practice to others. Overall, the global behavior of the floater is the deciding factor – this cannot be compromised, regardless of the strategies used in attaining equivalence.

The reader may have observed that “clump weights” or “clump masses” is not included in the list of parameters considered in the design of equivalent mooring systems. Experienced designers consider modeling with clump weights “not

ideal". An even distribution of mooring lines and properties makes modeling easy and the validation and calibration processes of numerical models is greatly simplified if clump weights are not used. Without the use of clump weights, there is also less complexity in the extrapolation of the modeled system responses to the full system depth.

1.3.3 SCALE AND TRUNCATION FACTOR IN MODEL TESTING

An important issue in model testing using equivalent mooring systems is "scaling effects". Satisfying the non-dimensional numbers (Reynolds', Froude's and Strouhal's) simultaneously at model and prototype scales is practically impossible. This implies that dimensional similitude often times cannot be achieved, and that the ratios between the forces acting on the floater-mooring system will be different at model and prototype scale. Scaling effects refer to the differences that arise between forces on or motion of the model system, and the corresponding forces or motions of the prototype system.

Effects of drag forces on slender cylindrical members are generally considered the most critical scaling effects in model testing. Mooring lines are important cylindrical members of floating production systems, along with risers. These drag forces generally depend on Reynolds' number and the surface roughness of the cylinder. On the other hand, Froude's number is considered the most important dimensionless number in model testing involving gravity waves and is used as the basis for scaling such model tests. The application of Froude's number introduces scale effects as it has no compliance with Reynolds' and Strouhal's numbers.

To address scaling effects in a way that reduces its complexity, choices must be made based on the relative importance of the forces applicable to the project under consideration. The designer has to determine which dimensionless number will control the scaling of the model tests. Hydrodynamic design will

most often require the application of Froude's number, as wave and current forces are the most prevalent forces that drive the design. This may not necessarily be the case for the static design of the floater-mooring system. In general, with respect to the choice of scale the following apply:

- An increase in the scale allows the designer to model the interactions between the free (water) surface and the floating structure better.
- As the truncation factor increases, it becomes more difficult to achieve acceptable equivalence between the full depth system and the truncated system.
- Additionally, as the scale is increased (i.e. scale factor is reduced) the truncation factor increases. A schematic illustration of how the uncertainty of the verification process depends on the model scale as well as the degree of truncation is shown in fig 1.5.

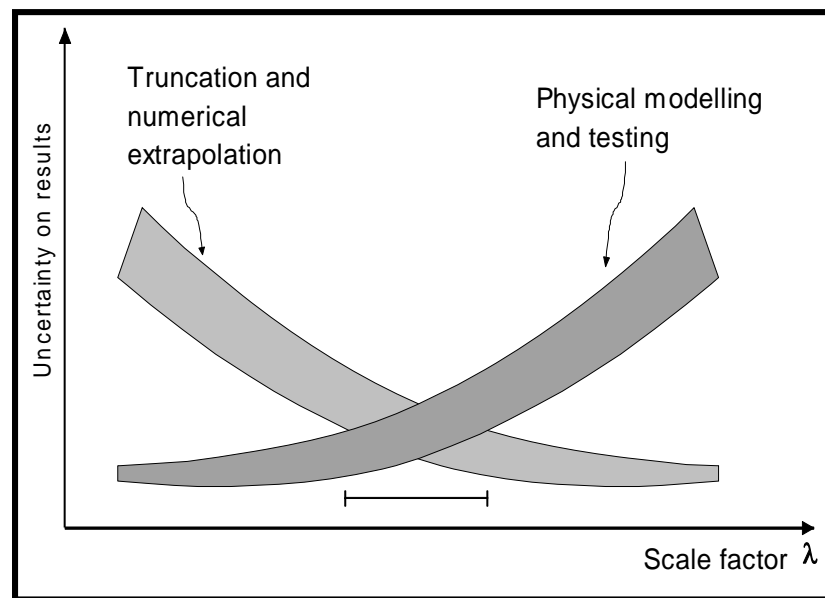


Fig. 1.5: Dependence of uncertainties on model scale
Source: Stansberg [1]

The figure describes qualitatively how a large scale model can lead to large uncertainties due to truncation, and how a small scale can lead to uncertainties

due to small models. It is therefore important to operate within an optimal scale range where the total uncertainties are minimal. In the verification process discussed in earlier sections, the numerical tools which are part of the hybrid approach can curb the risk of these uncertainties on the design results, provided that such tools are efficient and accurate in designing the statically equivalent mooring system and modeling the tested floater model. This again emphasizes the need for the use of competent software for such verification processes.

A number of practical issues arise in model testing involving statically equivalent mooring systems with very small scales (in the order of $\lambda > 100$). Most of these effects are related to the dynamics of the system, but in this text emphasis is made only on the issues related to the system statics. A major effect is that small offsets in the force transducers can lead to large apparent static loads. If this occurs, measurements of offsets during testing will hardly be accurate, and it will become necessary to quantify the magnitude of the resulting response due to the apparent static loads.

A typical range of model scales for equivalent mooring systems is 1:50 – 1:70. In most cases, it is preferred that these scales cover the modeling of the complete floater system with moorings and risers. Within this range of scales, scaling effects are reduced and hydrodynamic effects are modeled more accurately. Some hold that studies done on certain types of platforms show that model testing in ultra small scales down to 1:150 – 1:170 is in fact possible, at least for motions and mooring line forces on such floaters under severe weather conditions. Other experienced model testing engineers have strong doubts about the integrity of tests conducted at such small scales. However, the maximum or minimum scale used in testing will depend on the available basin dimensions, wave and current generation system, among other factors.

1.3.4 PRACTICAL ISSUES IN EQUIVALENT MOORING DESIGN

Another reason for which concise software is needed in the design of statically equivalent mooring systems is that practical limitations are difficult to account for when using complex programs in analysis. The practical limitations of small scale testing must be recognized whenever model testing is done. Even though most tests are directed toward wave-induced effects such as platform motions and sea-keeping characteristics, knowing the static mooring response is also important in design.

One practical problem frequently encountered when modeling the static response of a vessel is the mismatch in model and prototype static responses, generated by the rapid change in model mooring line departure angle, compared to the prototype, for a comparable scaled displacement. For an equivalent mooring system similar to that shown in fig. 1.6, one cause of this mismatch could be the closeness of the line-turning pulley to the platform, compared to the bottom connection point of the prototype system. This problem could very well occur even if the scaled spring rates were matched for the equilibrium position (the position of the vessel with no environmental forces present). A schematic depicting the practical arrangement of this problem is shown in fig 1.6. The mismatch is illustrated in fig. 1.7 where the total mooring reaction has been resolved into horizontal surge and sway reactions and a vertical reaction.

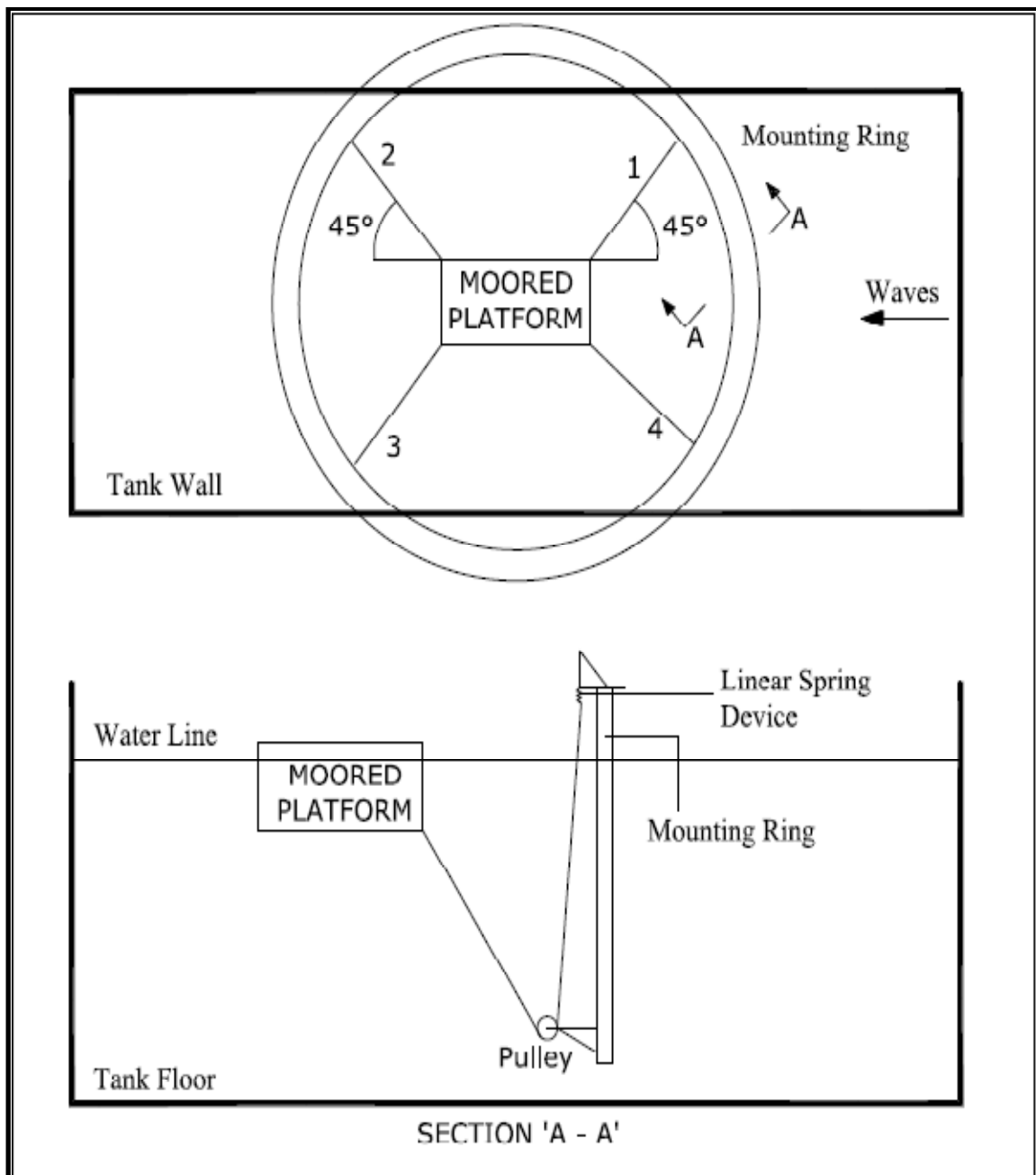


Fig. 1.6: Model tank station-keeping equipment
Source: McNatt [3]

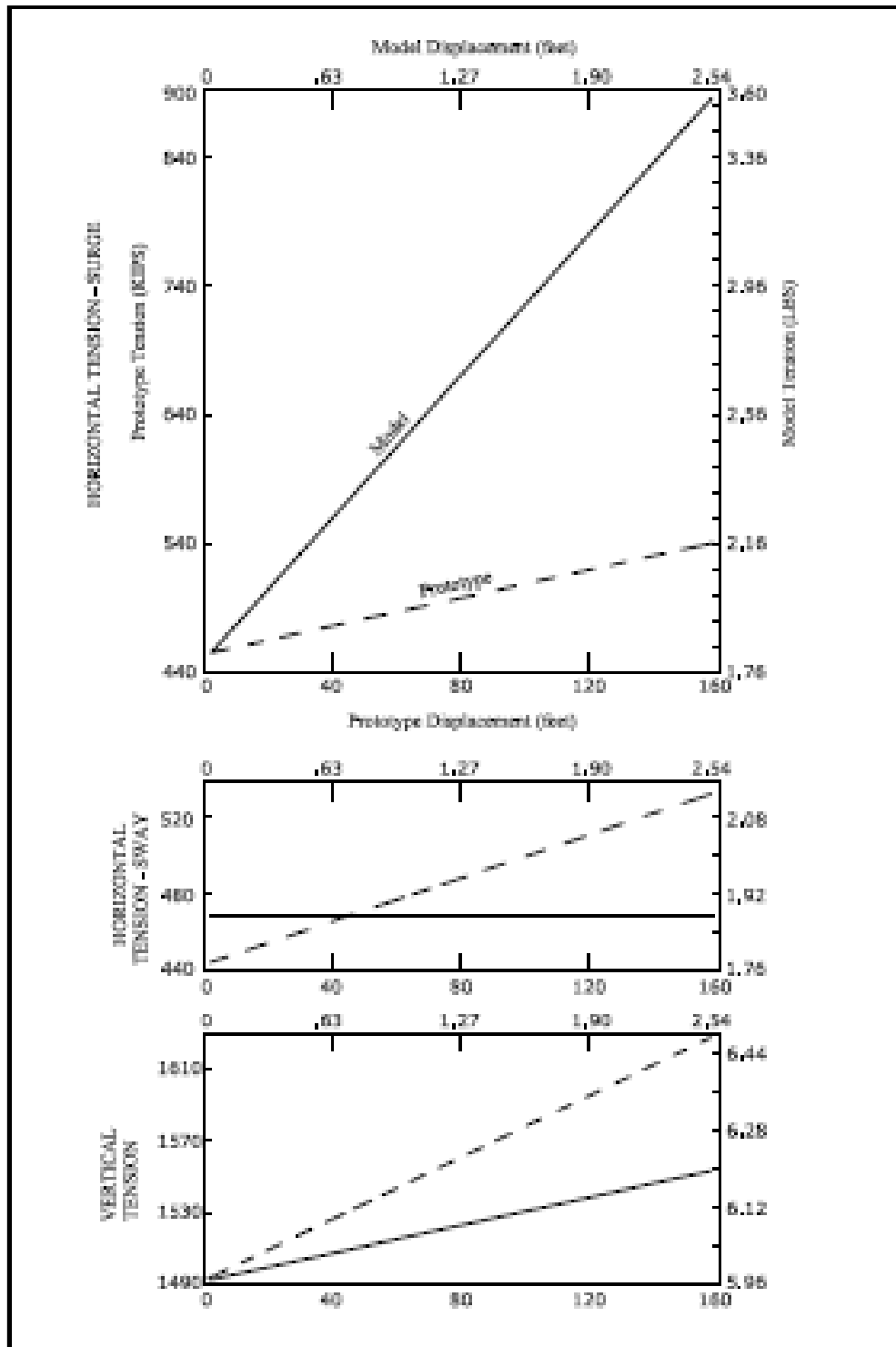


Fig. 1.7: Static mooring line responses - prototype versus model
Source: McNatt [3]

Another issue is the use of point masses to obtain sufficiently large vertical top forces, especially with large truncation factors. If point masses are used, the possible additional dynamic effects need to be checked. Figure 1.8 shows an example of the use of point masses for a CALM buoy.

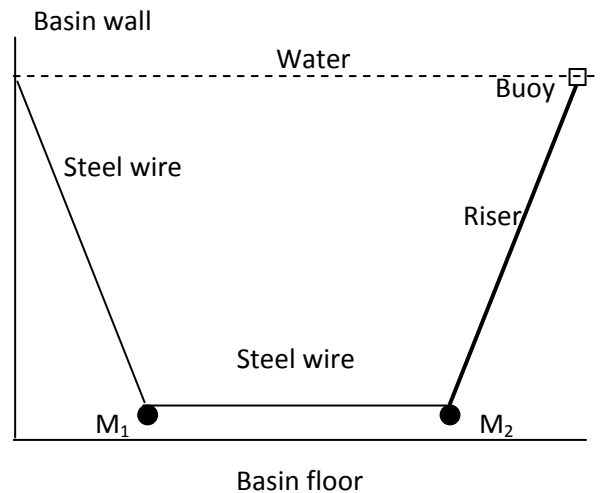


Fig. 1.8: A sketch showing the use of point masses in truncated systems

In the system shown in fig. 1.8 the mooring lines and risers are truncated just above the basin floor such that the characteristics of the truncated system are as close as possible to those of the full-depth system. However, only a short stretch of the lines can be modeled with this arrangement. This results in a pretension that is too low because not all of the weight is accounted for. To correct this problem the location of the point masses could be adjusted to obtain the correct pretensions, but this is not applicable to systems with large truncation factors. For large truncation factors, the geometrical stiffness will be too high if the top tension is maintained. One option which could be used to obviate this problem for systems with large truncation factors is to insert a coil spring between the masses (M_1 and M_2) to obtain a sufficiently low horizontal stiffness.

In the design of equivalent mooring systems it is necessary to ensure that physical characteristics of the prototype mooring system are reproduced in that of the model, such that the effects of the components in both systems are similar. Physical properties such as submerged unit weight (w), buoyancy and stiffness (EA_0) of chain, wire rope etc. are important in the validation of the numerical simulation, and so must be chosen such that extrapolation to the full depth system is easier and more accurate. In many robust / sophisticated numerical simulation codes the major focus is dynamic analyses and so the programs are generally geared for such. As a result, model assembly and interpretation of results for simple static analyses is often unnecessarily cumbersome when using such programs. Therefore more concise programs with which these variables can be flexibly altered in design and verification processes, are worth developing.

1.4 SCOPE OF RESEARCH PROJECT

This research project involves the formulation of a simple, efficient, fit-for-purpose designer-friendly program for the determination of static responses of moored floating structures, moored with spread mooring systems. The software produced is aimed at affording design engineers some flexibility in investigating the static response of equivalent mooring systems under different design conditions. Programs are compiled for the analysis of single-segment, two-segment, and three-segment mooring systems to verify the approach to be used in formulating the software. It is important to consider up to three-segments of mooring lines when working with equivalent systems, because this ensures the flexibility of using different line types in an effort to obtain the desired overall behavior or property of the lines. Considering spatial constraints in wave basins, it would be impossible to use just one line type that would satisfy the requirements of all testing projects.

To ensure that the user has the opportunity to view static responses during design on the same interface, the software is formulated using Microsoft Excel Visual Basic. The package provides the capability to work with spreadsheets and user-friendly controls used in the execution of the program. Test cases are considered for single line mooring analysis and global analysis of spread mooring systems. The results from the program produced through this research are compared to those from existing programs (LINANL [4], MOORANL [5] and Orcaflex [6]) with similar capabilities. An equivalent mooring design for a representative structure that could be tested in the Offshore Technology Research Center (OTRC) at Texas A&M University is then performed using the software. The design outputs are compared to those of the prototype system. Future modifications to the program produced through this research are discussed as its current limitations are also highlighted.

1.5 MOORING LINES AND COMPONENTS OF MOORING SYSTEMS

Discussions on mooring lines and mooring components are introduced here to offer the reader some understanding of their specific applications and engineering behaviors under various operating conditions. It is important to relate strongly the engineering properties of various mooring lines and components to the performance of the mooring systems which they constitute. Some components of mooring systems find better use under certain conditions than others.

The factors which determine the types of mooring lines and components to use in a prototype system include durability, compatibility with the global system, cost, and functionality under the environmental conditions which they will be operating. However, these factors are not essentially applicable in the selection of mooring components for equivalent mooring design. Rather, the selection of the components which constitute the statically equivalent mooring system will

depend on the engineering properties required of the mooring lines to attain the global match in static properties of the model system when compared to that of the prototype. Design engineers require a broad knowledge of the properties of these mooring components, to aid the explanation of design results and decision making.



Fig. 1.9: Stainless steel cable
Source: WebRiggingSupply.com

The mooring lines considered for discussion include steel cable (or wire rope), chain, synthetic fiber (nylon and polyester) rope and springs. Typically, these are the mooring line types deployed in model testing of deepwater floating structures. Other mooring components include different types of anchors and connectors. At model test scales, it may be difficult to appreciate the features of these mooring components, and so most of the figures presented in this section are those of prototype systems, but their engineering properties as associated with both systems are discussed.

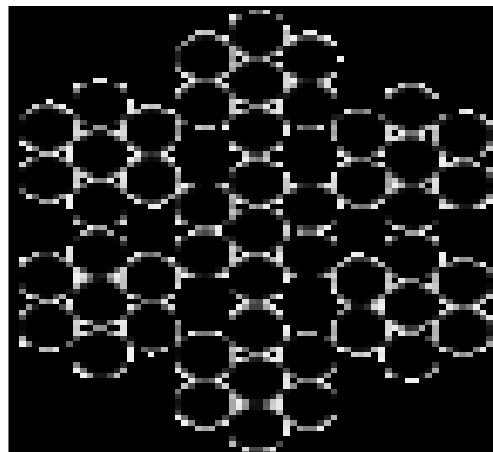
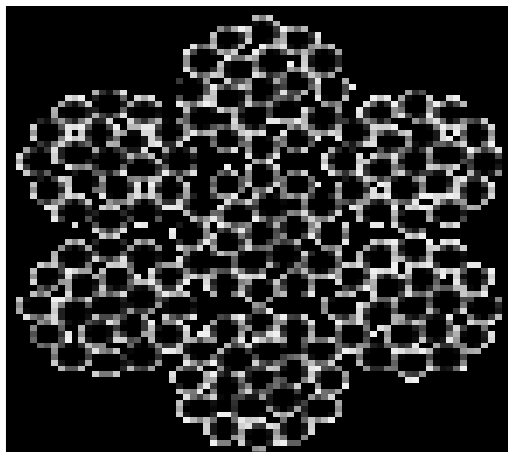


Fig. 1.10a: Very flexible steel cable

Fig. 1.10b: Flexible steel cable

Source: WebRiggingSupply.com

Steel cables or wire ropes could be made out of carbon steel or stainless steel. They find extensive application in deepwater operations due to their high strength-to-size ratios. Examples of steel cables with different internal structures are shown in figs. 1.9, 1.10a and 1.10b. Their flexibility is proportional to the cross-sectional matrix of the internal strands. This type of material can resist attacks from aquatic inhabitants, thereby reducing risks of physically-induced failure. Also, steel is a known material with simple properties, making its effect easy to account for when interpreting results. However, corrosion becomes an issue in the use of wire ropes after some time, and this reduces the life span of the mooring line. If large vessel excursions are envisaged for a given project, then wire ropes may not be the best choice for such cases, as they only elongate under very high tensions. In the use of wire ropes for equivalent mooring, corrosion is not an issue, since the testing projects do not last long enough for such effects to be at play.

Chains are also used in statically equivalent mooring systems, and their unique characteristic is providing catenary effects in the mooring lines. Chains find extensive use in shallow and sometimes intermediate-water depth applications. In deepwater, the weight of chain required for vessel mooring is enormous and

expensive constituting the primary reasons for which its application in deepwater is highly limited. However, wave tanks are typically not that deep; and in general material costs for model mooring systems are very modest.

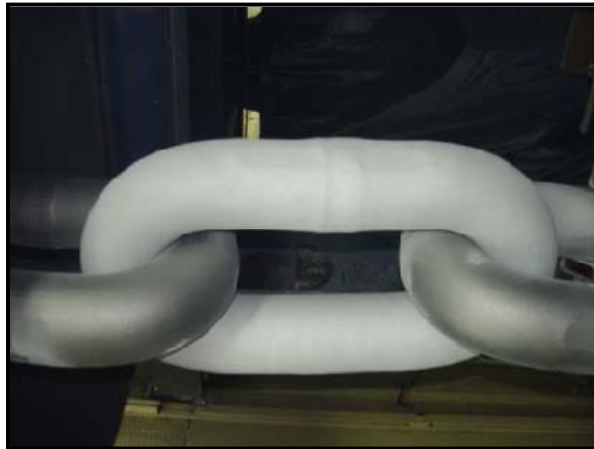


Fig. 1.11: Studless mooring chain

Source: TEKNA conference on DP and Mooring of Floating Offshore Units, 2008 [7]

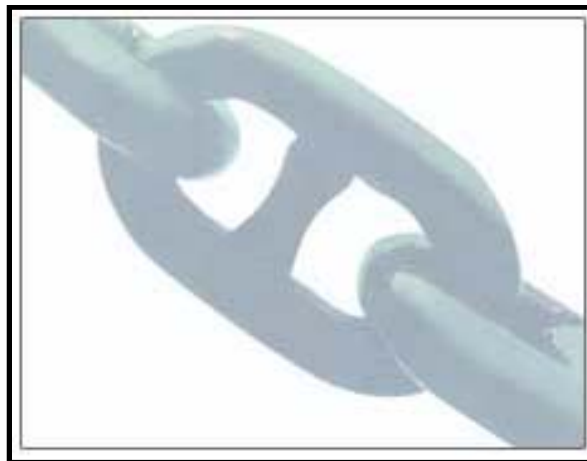


Fig. 1.12: Stud-linked mooring chain

Source: www.cmic.cc

The use of chain however ensures a greater life span for prototype mooring systems and increases strength and abrasion resistance. In addition, due to their weight, chains increase the resistance to anchor pull, giving the floating unit

more stability over the station under extreme weather conditions. Chains could either be studless or stud-linked (figs. 1.11 and 1.12 respectively) chains. The former is usually deployed in permanent moorings, while the stud-linked chains are used in mooring lines which have to be replaced at intervals during the life span of the facility. For floating structures at full depth, applications of chains as part of the mooring lines will mostly favor the use of studless chains because of the uncertainties associated with the performance of stud-linked chains when they are twisted while carrying axial loads – especially when the stud links are welded. A discontinuity at the welded joint could cause failure, and many consider the use of studless chains to be of lower risk. However, the physical and mechanical properties of such studless chains must satisfy strength requirements and further requirements against corrosion. Stud-linked chains on the other hand may be used in model testing without threat.

Synthetic fiber ropes are highly applicable in offshore mooring systems. These ropes essentially find greater applicability in deepwater above chains and wire ropes because they are much lighter in weight, and possess very good strength-to-submerged weight ratios. The major materials in synthetic ropes are polyester and nylon. Numerous yarns are combined in diverse cross-sectional matrices to produce synthetic ropes of various strengths and elasticity.



Fig. 1.13: Synthetic fiber rope
Source: 7th International Rope Technology Workshop, 2007 [8]

Synthetic ropes (fig. 1.13) overcome the problem of corrosion in mooring lines, but they are also susceptible to fish bites and plastic flow at high stresses. In addition, due to their light weight, numerous lines are usually required to achieve stability in floating structures because large excursions will be experienced. This compliant behavior could be to the advantage of the structure during extreme offshore weather conditions, as the elasticity of the lines will reduce the pull on the anchors thereby mitigating the pull-out failure and snapping (breaking) of the mooring lines. Other issues with synthetic lines used in full depth systems have been the infiltration of water and particle ingress between the yarns, causing an increase in friction and eventually a reduction in axial strength. Considering the length of time for which model tests run, and the fact that there are no threats from aquatic inhabitants, the above mentioned factors do not influence the selection of synthetic ropes as components of equivalent mooring systems. Also, springs are frequently used in model testing to replace synthetic ropes because they obviously possess the elastic property required of synthetic ropes. To represent prototype mooring systems which use fiber ropes, the equivalent mooring system is sometimes modeled with the use of thin steel wires inside flexible hoses, with springs attached at the ends. The approach obviates the situation of having to account for the engineering behaviors of small diameter synthetic ropes. The stiffness and drag effects of the mooring lines are preserved using this approach.

Anchors are used in equivalent mooring systems (just as in full-depth systems) to restrain the mooring lines at the basin floor thereby resisting the vertical and horizontal components of tension. In the design of equivalent mooring systems, the tensions at the anchors in the prototype system need not be matched by those of the equivalent mooring system, and the resistance to pull can be provided using much smaller anchors installed at the bed of the wave tank. Owing to the fact that the mooring lines are typically very small in size at model scale, and considering that the model excursions are not very large, the anchors

do not necessarily require embedment at the bottom of the wave tank. Anchors of adequate weight with the provisions to fasten the mooring lines, such as shown in figs. 1.14 and 1.15 are appropriate for model testing purposes. Figure 1.14 shows a lead brick of sufficient weight sitting on a metal plate which holds the line-clamping device. Additional weights may be used but typically the pull on the anchor is relatively low enough for one or two lead bricks to support.

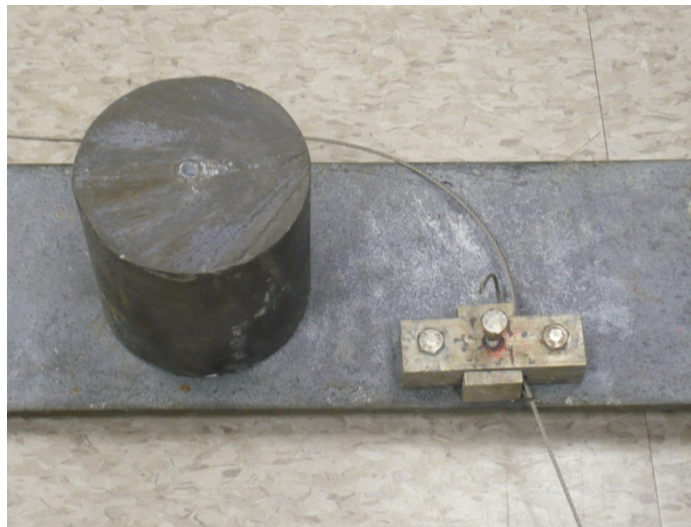


Fig. 1.14: Anchor set-up for basin scale mooring



Fig. 1.15: Clamping device for basin scale mooring line

A side view of the clamping device is shown on fig. 1.15. The bolt on the device is screwed to hold the wire rope tight in place. If any adjustments to the line length are required, the bolt is loosened and the rope is pulled in the desired direction.

Connectors or links such as shown in fig 1.16 could be components of an equivalent mooring system. Links enable the combination of different mooring line components having varying properties. The links are tension members, which in some cases have provision for the installation of floatation to increase buoyancy effects in the mooring line. Connectors provide an efficient way to manage the properties of different mooring components such as springs, chain, cable, etc. while not compromising the integrity of the mooring system. Figure 1.16 shows a connecting link (left) which can be used to connect two line components of different types (say chain and polyester). The coupled set-up (right) shows the connection of a wire rope to a screw which may be used at the terminal point of the line.

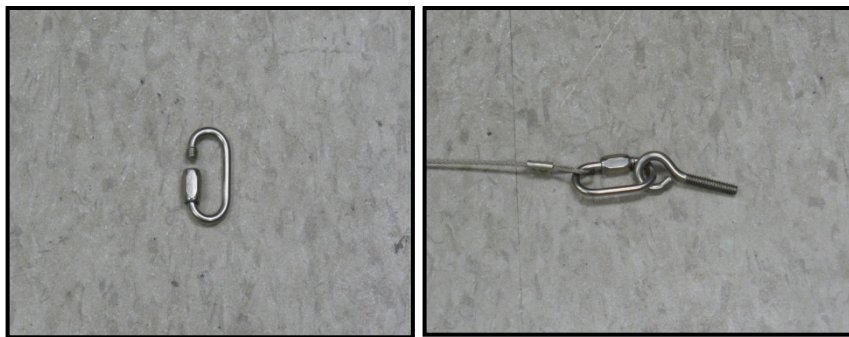


Fig. 1.16: Connectors for model scale mooring

Fairleads are important components of mooring systems, provided to guide mooring lines around the floating structure. In some cases, the floater's hull could be built in such a way that the fairleads are holes within the hull, while in other cases they could be separate pieces of hardware attached to the vessel's hull. The bending shoe fairleads (fig 1.17) are simple and less expensive

compared to the rotary sheave type, but they also have adverse effects on the chains when the chains are tensioned. Under this condition, the lying links of the bending shoe fairlead will be subjected to bending moments; this effect is not imminent with the rotary type (fig 1.17). At model scale, small sizes of fairlead types similar to those discussed here may or may not be used. Similar devices such as pad-eyes and turning rings could also be fabricated during model building to perform similar tasks as the fairleads, and this is more likely than the installation of well finished fairleads. The pad-eye screw shown in figure 1.18 is driven into the hull of the model to serve as the fairlead and the mooring line is attached to it as in fig 1.16.

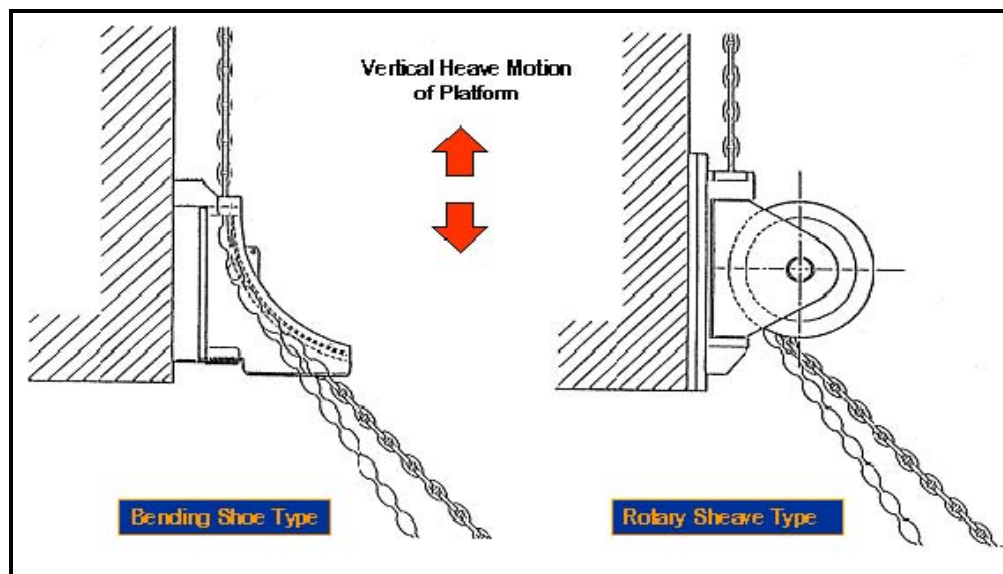


Fig. 1.17: Bending shoe and Rotary sheave fairleads
Source: Texas A&M Ocean Engineering Seminar [9]



Fig. 1.18: Pad-eye screw

It is worthy of mention that the mooring components discussed in this text are only a few of the existing types used in the model testing processes. Specialized projects or tasks may warrant the use of unique mooring components which are peculiar to such projects. Various industries also have patents in manufacturing specialized equipment for offshore mooring projects, so readers interested in more elaborate information on a wide range of equivalent deepwater mooring components should search beyond this text.

1.6 OFFSHORE MOORING SYSTEMS

A coupling of the required mooring components (lines, connectors and anchors) to the floating structure can be considered a mooring system. This research focuses on spread mooring systems only, and they can be classified as shown in fig. 1.19.

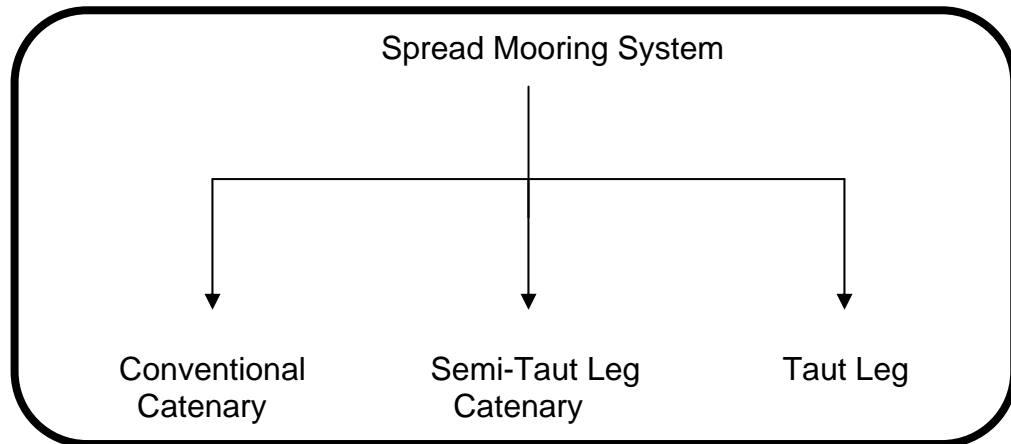


Fig. 1.19: Classification of spread mooring systems

One common capability of systems in fig. 1.19 is that they are all applicable to deepwater projects. The choice of one over the other in any application depends on the factors discussed in the introductory section of this chapter. Figure 1.20 illustrates the different types of mooring systems.

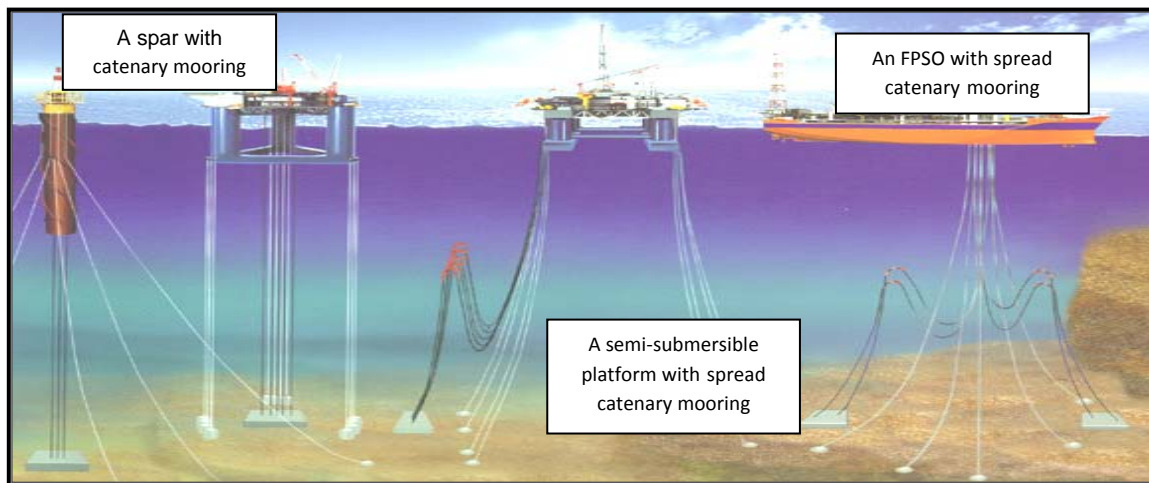


Fig. 1.20: Spread mooring systems

Source: Texas A&M Ocean Engineering Seminar [9]

Although tendon systems are of great application to some floating structures (such as TLPs), this research focuses on spread mooring systems which are applicable to other floater types such as semi-submersible platforms, spars and FPSOs. Spread mooring systems simply have multiple mooring lines and other

corresponding mooring components necessary for vessel stability. Even though pre-tensioning individual mooring lines of such systems correctly is fairly challenging, the vessel excursions are significantly reduced. Practical issues with spread mooring systems have to do with the entanglement of one line against another in the event of failure under extreme weather, and the alignment of the floating structure with the weather.

The conventional catenary system is used in analysis to allow for flexibility in choice of mooring line properties. With the catenary formulations, the designer could choose to stiffen or increase the stretch in the mooring lines by altering the line properties towards the static configurations that correspond to those of the prototype system. Providing an efficient algorithm to obtain the static equilibrium solutions for single mooring and spread mooring analysis becomes the next major concern.

CHAPTER II

DESIGN-RELATED LIMITATIONS OF EXISTING MOORING METHODOLOGIES

Quite a number of works have been documented on approaches for design of equivalent mooring systems and static analysis of spread mooring systems, some tailored to suit specific cases and others more general. Most of the existing approaches aim for the same outputs but there may be variations in methodology (computation techniques) due to efforts made to control computation durations, increase accuracy of results and / or obtain unique information from the analysis. From a designer's perspective, these various interests are important and the preferred methodology would be one which is robust enough to capture relevant information on the mechanics of the mooring system in performance, with a high degree of accuracy and optimum computation duration.

Given that attaining the objective of this research requires adherence to acceptable approaches used in model testing as well as mooring line analysis, the reviews presented in this report can be considered under these two perspectives. Works related to the present challenges in model testing using equivalent mooring systems are reviewed first, after which some methodologies used in mooring analysis are considered. The essence of these reviews is to justify the need for this research project, and to establish the suitability of the method used over some of the existing methodologies.

2.1 CHALLENGES IN DEEPWATER MODEL TESTING USING EQUIVALENT MOORING SYSTEMS

In a study by Kim [10] at the OTRC, FPSO responses in hurricane seas predicted by a vessel-mooring-riser coupled dynamic analysis program were

compared to wave tank measurements. A tanker-based turret-moored FPSO moored by 12 chain-polyester-chain taut lines in 6,000 ft of water was studied. A series of model tests (of scale 1:60) were conducted in the OTRC's wave basin at Texas A&M University with a statically-equivalent mooring system to assess its performance in the hurricane condition. In the 1:60-scale OTRC experiment shown in fig. 2.1, the water depth could not be proportionally scaled as a tank depth of 100 feet would be required. Therefore, an equivalent mooring system was developed using steel wires, springs, clump weights, and buoys to represent the static surge stiffness of the prototype mooring design as closely as possible. Figure 2.2 (a) shows the mooring system of the prototype system, while fig. 2.2 (b) shows the equivalent mooring system of the OTRC experiment.

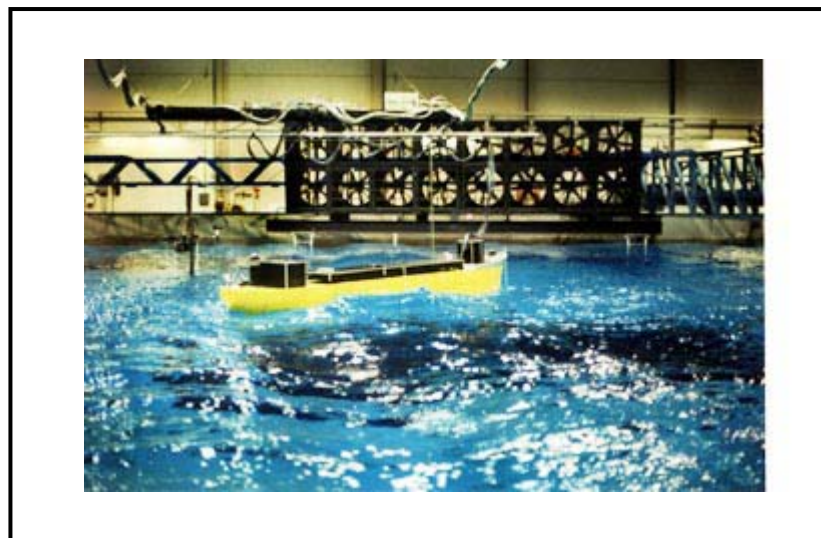


Fig. 2.1: OTRC wave basin and FPSO model
Source: Kim [10]

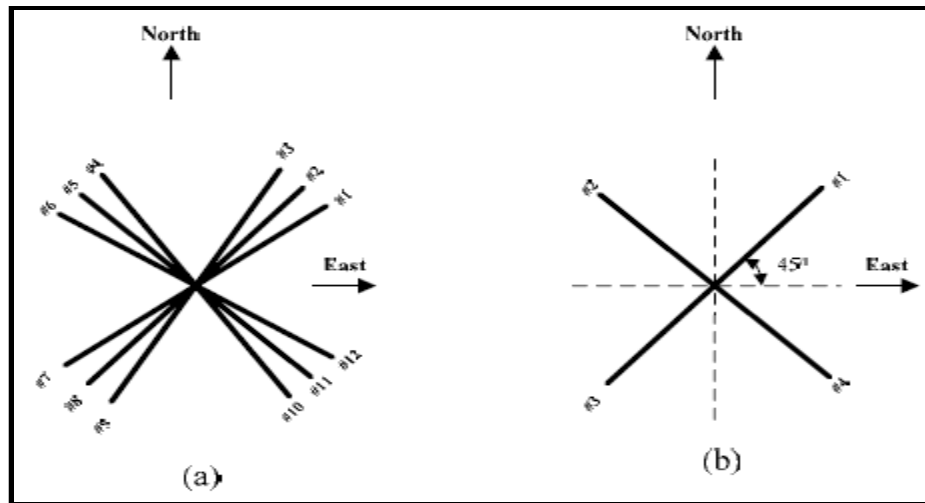


Fig. 2.2: Prototype (a) and Equivalent (b) mooring system layouts
 Source: Kim [10]

Due to its complexity, direct numerical modeling of the equivalent mooring system was not attempted in this project, even though acceptable experimental results were obtained. The conclusions made in this study include the facts that the differences between measured and predicted results can be attributed to the uncertainties related to viscous effects, wind force generation, the current profile and its unsteadiness, the mooring line truncation, and the usage of springs, buoys and clump weights in the equivalent mooring lines. It is believed that numerical modeling of the equivalent mooring system would have been more feasible if the equivalent system was less complex (i.e. without clump weights and buoys etc.); such a relatively simpler set-up could easily embrace the use of a fit-for-purpose software for direct numerical modeling of a statically equivalent mooring system, thereby reducing the uncertainties related to mooring line truncation.

A review of model testing procedures for global analysis verification of floating production systems in ultra deepwaters is given in the work of Stansbeg, Karlsen, Ward, Wichers and Irani [1]. Their work suggests guidelines to this verification process, with the philosophy that a numerical model of the equivalent

set-up is validated against the tests, and the resulting calibration information is then applied in full-depth verification simulations. Principles for design of equivalent systems are also discussed. The concerns expressed in their work include the challenges in model testing, the greatest of all being spatial limitations in wave tanks. They recommend the hybrid method in which numerical models are used in the design of statically equivalent mooring systems and discuss a procedure based on guidelines worked out for DeepStar as a part of a more general guideline study on global analysis of deepwater floating production systems [11].

Their recommended guidelines reflect important issues to consider in model testing using equivalent systems, including the following:

- The most critical response parameters for the floater being tested (e.g. static or dynamic responses, horizontal or vertical responses etc.)
- When to choose an equivalent system
- Selection of criteria for system truncation
- Degree of system truncation in relation to coupling effects of floater and underwater systems
- Possibility of equivalent riser modeling
- Response data needed in verifying numerical model, such as slow drift information (excitation and damping).

Obviously, some considerations in their guidelines pertain to statically equivalent systems, while others are associated with dynamic equivalence. As such one may consider their guidelines to be more general. Stansberg and others [1] also state that the design of an equivalent mooring system should strive to obtain the same responses of the floater that would result from the full-depth mooring, in order to reduce the uncertainties related to extrapolation of test results from equivalent to full-depth systems. Issues further acknowledged

include the fact that equivalent mooring systems with more continuously distributed properties tend to perform better and are easier to analyze.

A truncation case study example is given in their work, where a semi-submersible platform with 12 catenary mooring lines and 8 risers was tested at a scale of 1:55 with a full-depth system in 335m depth (fig. 2.3) as well as with an equivalent system in 167.5m depth (fig. 2.4) of water. It is noted that the actual water depth in this case is not representative of deepwater, but the idea was to verify the hybrid approach with equivalent versus full-depth tests, with both depths included in conventional scale. The statically equivalent mooring system was selected from static mooring analysis using the computer program MIMOSA on the basis of comparison of the horizontal restoring force and single line characteristics versus full-depth. The full-depth lines were of steel wire with chain segments at the upper and lower parts, while the truncated lines were all chain. Results presented in fig. 2.5 show a close match in total restoring forces for the full-depth and equivalent system.

Stansberg and others bolster most of the arguments which form the basis for this research as discussed in chapter I. However, they offer few leads that suggest the need for further research on the verification of prototype floater design using statically equivalent mooring systems. The authors mention the importance of a good numerical tool for such designs and that such tools must offer flexible optimization capabilities. Even though the results from MIMOSA presented can be considered accurate, there is no mention of the efficiency of the software in the design process. Either way, the authors support the formulation of flexible design tools that can mimic the full-depth system as closely as possible, with the argument that such tools would reduce the uncertainties in the design process.

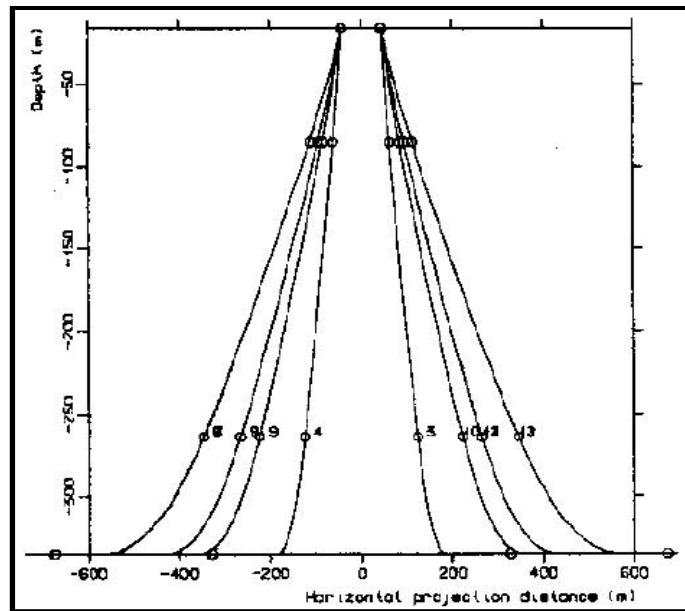


Fig. 2.3: Vertical profile of catenary mooring system – full depth system
Source: Stansberg and others [1]

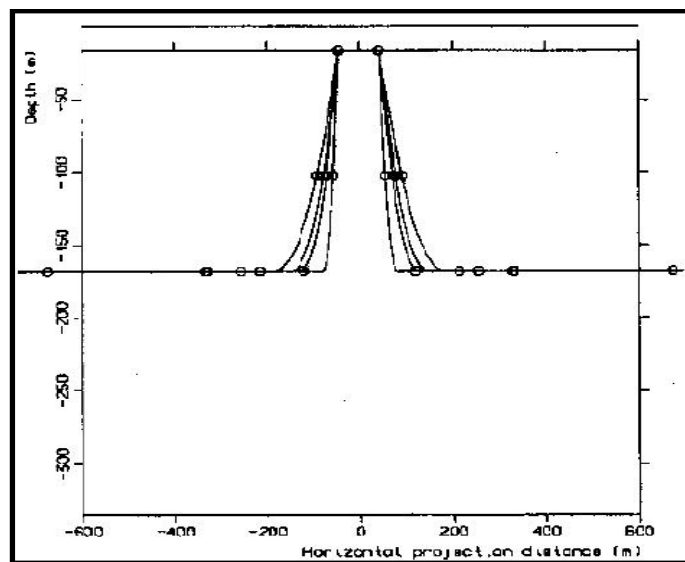


Fig. 2.4: Vertical profile of equivalent system
Source: Stansberg and others [1]

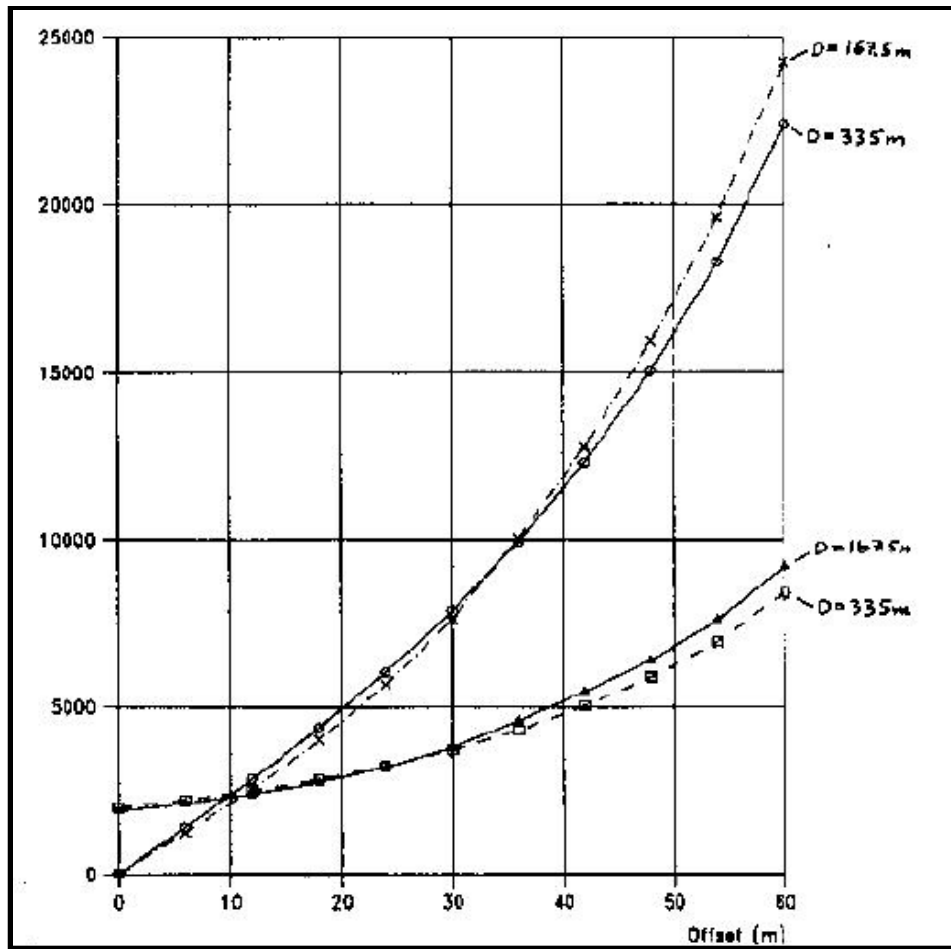


Fig. 2.5: Total restoring force (in kN) and single line static characteristics of systems – full depth system versus equivalent
Source: Stansberg and others [1]

In an earlier study by Stansberg, Ormberg and Oritsland [12] on the challenges in deep water experiments, the use of the hybrid method to obviate some of the uncertainties in the design of statically equivalent mooring systems is explicitly presented. It is no surprise that the background information in this work is similar to that of Stansberg and others [1]. They suggest the following rules to be followed in the design of test set-ups involving statically equivalent mooring systems:

- Model the correct total, horizontal restoring force characteristic

- Model the correct quasi-static coupling between vessel responses (for example, between surge and pitch for a moored semisubmersible)
- Model a representative level of mooring and riser system current force
- Model the representative single line tension characteristics (at least quasi-static)

For equivalent mooring systems, modeling the line tension characteristics is not generally necessary, but it could be useful in confirming that the numerical tool is producing correct results. The philosophy behind this recommended process is that the numerical simulations in the modeling process shall take care of the deviations between the full-depth and equivalent system.

Amongst the enumerated challenges in their work is the need for an efficient methodology in the design of equivalent mooring systems, such as the application of an optimization technique to establish the equivalent system with the required system properties. They also identify that faster and more efficient algorithms are needed, amongst other numerical challenges.

Fylling and Stansberg [13] used a non – linear optimization code to reduce the manual iteration work in designing statically equivalent mooring systems. They explain explicitly that the hydrodynamic loads on a floating structure are not directly influenced by the mooring systems, and therefore tests on smaller water depths can be used for obtaining hydrodynamic characteristics of the floating structure. Their work sought to reproduce the environmental loads and the most important part of the forces from moorings and risers by reproducing the quasi-static force vectors from individual lines and risers. They emphasize that contrary to quasi-static characteristics considered, line dynamics are generally difficult or even impossible to reproduce by truncated models, and must in all cases be finally verified by a full-depth numerical model. The hybrid verification method is used in their work. Design requirements for equivalent mooring

systems are also stated, much the same as in the work of Stansberg and others [1, 12].

Formulating the mooring line equivalence as an optimization problem, Fylling and Stansberg define the objective function to be a weighted difference of the restoring forces between the full-depth and the equivalent lines calculated at a number of offset points. The design requirements that are translated to constraints are as follows:

- Horizontal stiffness
- Vertical stiffness
- Horizontal pre-tension force
- Vertical pre-tension force
- Horizontal distance from fairlead to anchor
- Length of line on sea-bed
- Capacity of mooring lines

It is important to mention that even though Fylling and Stansberg list the horizontal distance from fairlead to anchor and the length of line on the sea-bed as constraints, these parameters are actually alterable in the design of equivalent mooring systems, though there will be limits to the values that can be assigned to them. They apply a gradient search method which considers only continuous variables. Using this approach, three types of optimization variables may be specified:

- Line variable, pretension or distance to anchor.
- Segment variables comprising segment lengths and one to four cross-section parameters, depending on segment type.
- In the case of discrete buoyancy or clump weight modules, the net submerged weight can be specified as a variable.

A program called MOOROPT_Trunc was used in solving an example model test problem at a 1:70 scale. The full-depth semi-submersible is moored in a water depth of 1500m with polyester lines, while the basin depth is 6.43m with the model carrying wires, springs, dyneema lines, chains and a buoy. The authors report a close-to-perfect correspondence of the restoring forces and stiffness between the full-depth and equivalent test set-ups.

Ormberg, Stansberg and Yttervik [14] worked on integrated vessel motion and mooring analysis in hybrid model testing. They describe a computer program (RIFLEX-C) for coupled numerical analysis of moored vessels, where the vessel is integrated as part of a finite element model of the complete mooring / riser system. Experimental verification of the program is carried out by detailed numerical reconstructions of time series from model tests with a semi-submersible floater. Ultimately the program is used in a model test case study with equivalent moorings. The authors identify that the essential difference between running RIFLEX-C and a more conventional stationkeeping program with a quasi-static mooring line tension model is that dynamic tensions can be simulated by RIFLEX-C whereas a quasi-static model cannot perform such analyses. In their application of this program to a model test project, it is noted amongst other conclusions that the total hybrid testing technique with coupled analysis is quite complex and time-consuming due to finite element computations and several steps in the computation procedure. This approach is however reported to produce simulated line tensions, including low-frequency as well as nonlinear dynamical components that compare reasonably well with model test measurements. With the constraints mentioned by the authors, the use of the coupled numerical analysis tool in the design of statically equivalent mooring systems would seem to be working-too-hard to get the task done. A review such as this is included here to support the fact that it is time consuming and unnecessary to consider dynamic computations when the target in design is static equivalence.

In the final report and recommendations to the 22nd ITTC [15], the specialist committee on deep water mooring emphasizes the need for the improvement of numerical modeling techniques for model testing. While the committee appreciates the notion that model testing of moored floating offshore vessels in waves can be carried out successfully at a scale ratio of 1:170, it is expected that at such scales practical problems rather than scaling effects seem to be the limiting factor in testing. Once again, the hybrid method is believed to offer an interesting solution to the well known scaling law conflict. The committee suggests that if parts of the mooring system that are most troubled by the scale effects are replaced by actuators coupled to on-line computational models with full scale properties, the complete system can to some extent be free from scale effects. Recommendations to future work include further pursuance of verification and validation of physical and numerical models, and enhancement of the hybrid model testing procedure.

The reviewed literature portrays many common facts, all of which directly imply the need for more research in the model testing procedures and tools using equivalent mooring systems. In response to this need, the formulation of tools to obviate the inherent uncertainties in the verification-of-design process while ensuring that such tools are designer-friendly is to do the least. A convenient position would be being able to optimize the requirements of a statically equivalent mooring system, by doing the least amount of work. Much is involved in achieving such tools, and it is necessary to approach such a goal from a realistic point of view. "Realistic" because formulating a tool for the design of dynamically equivalent systems is extremely challenging and the efforts might outweigh the benefits. On the other hand, with diligent considerations of acceptable methods with a view to producing accurate designs through an efficient algorithm and process, formulating a tool for the design of statically equivalent mooring systems is doable.

2.2 SUITABILITY OF EXISTING APPROACHES FOR MOORING LINE ANALYSIS

Amongst the many analytical and numerical approaches used in solving mooring line problems, this research considers just one approach. It certainly is worth questioning why this particular approach is favored above others. To address the suitability of existing approaches for mooring line analysis, some works are reviewed here with the intention of examining how applicable their approaches might be in the static analysis of spread mooring systems as related to statically equivalent mooring design.

Smith and MacFarlane [16] present four methods to solve catenary equations for a three-component mooring system, made up of two line segments connected at a buoy or sinker. The different methods presented are peculiar to specific configurations of the system. Their analysis assumes that the water depth and fairlead tensions are given.

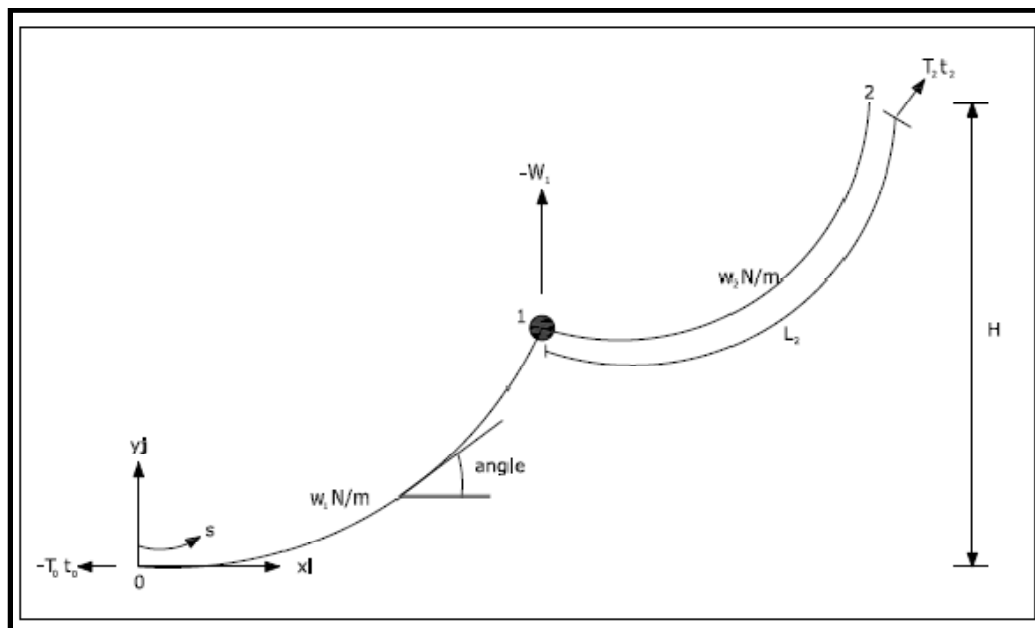


Fig. 2.6: Free body diagram of considered mooring system
Source: Smith and MacFarlane [16]

For the configuration shown in fig 2.6 the static equilibrium between the touchdown point at the origin of the axes x and y , and the distance s along the mooring is given by the summation of forces presented as:

$$-T_0\hat{t}_0 + \int_0^s f d\tau + T(s)\hat{t}(s) = 0 \quad (2.1)$$

where \hat{t} is the unit tangent in the direction of increasing s , f is the external load distribution and T is the tension. The external load is given by:

$$f = w_1 + W_1\delta(s - s_1) + (w_2 - w_1)H(s - s_1) \quad (2.2)$$

where w_1 and w_2 are uniform immersed line weights per unit length, W_1 is a concentrated load at the connection point 1, while δ and H are Dirac impulse and Heaviside step functions. Equations (2.1) and (2.2) are resolved in the x and y directions (i.e. in the plane of the mooring line) and the resulting equations are manipulated to obtain the classical catenary equations:

$$\frac{dy}{dx} = (\sinh w_i x / T_0 + \alpha_i)$$

$$y = T_0 / w_i \cosh(w_i x / T_0 + \alpha_i) + \beta_i \quad (2.3)$$

$$s = T_0 / w_i \sinh(w_i x / T_0 + \alpha_i) + \gamma_i \quad (2.4)$$

$$T = w_i(y - \beta_i) \quad (2.5)$$

where the subscript “ i ” equals 1, 2 for the mooring lines on the intervals $0 = s_0 \leq s < s_1$, $s_1 \leq s \leq s_2$ and α_i, β_i and γ_i are integration constants to be determined from boundary conditions. In their work, the elongation of the line was included by way of uncertainty in the weight per unit length.

The first method reduces boundary conditions to a system of five equations which depend on the line properties (length and weights per unit length), the load at the connection point, as well as H and T . On prescribing these properties, t is found by iterating through the reduced boundary conditions.

A second method is presented, with a specified condition $w_2 \neq w_1$. It considers no buoy between the lines and is only for a mooring configuration which has only two component lines with different weights per unit length. The derivations under this assumption yield a quartic equation in t , with roots that have a closed form solution. It is emphasized that this method offers no practical advantage over Laguerre's iteration which is applied in the third method.

This third method is an extension of the preceding one, with the inclusion of a buoy or sinker between the lines, and yields a polynomial equation in $1/T_0$ of degree eight. The roots of the polynomial are obtained by Laguerre's iteration which is considered efficient and rapidly convergent in evaluating the roots of a polynomial. The fourth method is only an alternative solution sequence to the third method, with the primary aim of verifying the symbolic equivalence between the polynomial coefficients using numerical tests.

In the cases examined by Smith and MacFarlane the numerical equations are derived based on the given configurations. Even though the numerical schemes used guarantee accurate results, the iteration yields the solution for the derived equations only. Analyzing say, a two segment line with equal weights per unit length would require the mathematical derivations of the boundary conditions, and then the application of the numerical scheme to obtain the solutions. In addition, the effect of line elongation is an external computation, rather than an in-built property of the mooring lines. Considering the stiffness of the mooring lines while developing the equations for analysis would be a more efficient approach to reduce computation times and errors. Line stiffness is one of the important parameters which should be available for adjustments to the designer of an equivalent mooring system. Therefore from a design standpoint, these methodologies neglect a key instrument that enhances the process of seeking a match between static design specifications of the prototype and that of the equivalent mooring system.

Carbono, Menezes and Martha [17] present a steady-state genetic algorithm to solve mooring pattern optimization problems, owing to the fact that traditional optimization methods fail to efficiently provide reliable results. They describe the term “genetic algorithm” to refer to any population-based model that uses several operators (e.g. selection, crossover and mutation) to evolve. Their work holds that because the distribution of mooring lines is one of the factors directly affecting the excursions experienced by floating units, the determination of an optimum mooring pattern results in an optimization problem, whose ultimate goal is to minimize the displacements of the floating units.

The specific aspects in which genetic algorithms differ from the most common mathematical programming techniques, they explain, are:

- Genetic algorithms use a population of individuals or solutions instead of a single design point.
- They work on a codification of the possible solutions instead of the solutions themselves.
- These algorithms use probabilistic transition rules instead of deterministic operators.
- Genetic algorithms handle continuous, discrete or mixed optimization problems, with minor modifications without requiring further information such as the gradient of the objective function.

Their formulation of the optimization problem expresses the optimum mooring pattern as an unconstrained continuous optimization problem, shown as:

$$\text{Minimize} : \sum_{i=1}^m \Delta_i^2(\alpha) = \sum_{i=1}^m [\Delta x_i^2(\alpha) + \Delta y_i^2(\alpha)] \quad (2.6)$$

$$\text{Subject to} : \alpha_{i \min} \leq \alpha_i \leq \alpha_{i \max}, i = 1 \dots n \quad (2.7)$$

where $\alpha = (\alpha_1, \alpha_2, \dots, \alpha_n)$ is a vector holding the design variables (e.g. the azimuth of each mooring line); $\Delta_i(\alpha)$ is the resulting floating-unit displacement

(which can be decomposed into the components $\Delta x_i(\alpha)$ and $\Delta y_i(\alpha)$) for a given set of environmental conditions; n is the number of independent design variables; m is the number of sets of environmental conditions; and the inequalities shown in Eq. (2.7) are the side constraints (where a side constraint is an upper or lower bound of a design variable). Equations (2.6) and (2.7) represent a typical unconstrained optimization problem.

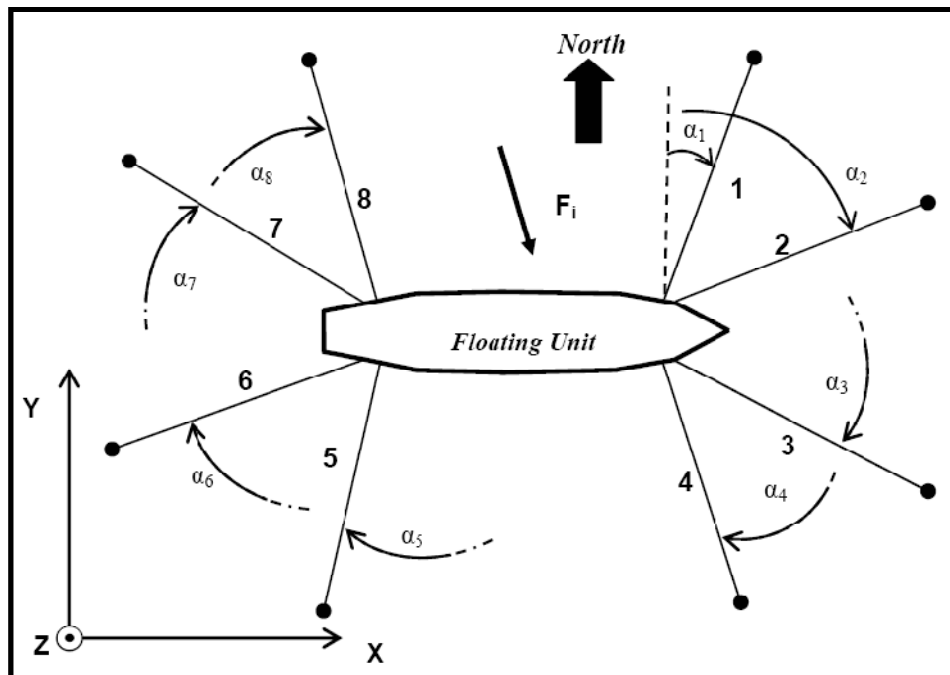


Fig. 2.7: Representation of floating unit with eight mooring lines
Source: Carbono, Menezes and Martha [17]

The optimization problem is used to analyze the floating unit shown on fig 2.7. The implementation of the algorithm involved coding the design variable using a fixed-length binary digit string representation, constructed with the binary alphabet $\{0,1\}$ and concatenated head-to-tail to form one long string, and this concatenated structure represents the chromosome (every chromosome contains all design variables). To obtain the real values of the design variables in the domain region, computations are performed to decode each chromosome.

In computing the static offsets, the environmental loads are transformed into an equivalent external static force (F_i) acting on the floating structure. The mooring lines are modeled as non-linear springs that impose restoring forces on the structure. The restoring forces are obtained through the restoring curves (fig. 2.8) for each mooring line, which are generated using the catenary equation. A new static equilibrium position is computed (after the out-of-balance forces are obtained) by solving the following system of non-linear equations:

$$Kd = F_i - R_{int} \quad (2.8)$$

where K is the global stiffness matrix; d is the unknown displacement vector; F_i corresponds to the external forces due to each set of environmental conditions; and R_{int} is the resultant of the internal (restoring) forces, taking all the mooring lines into consideration.

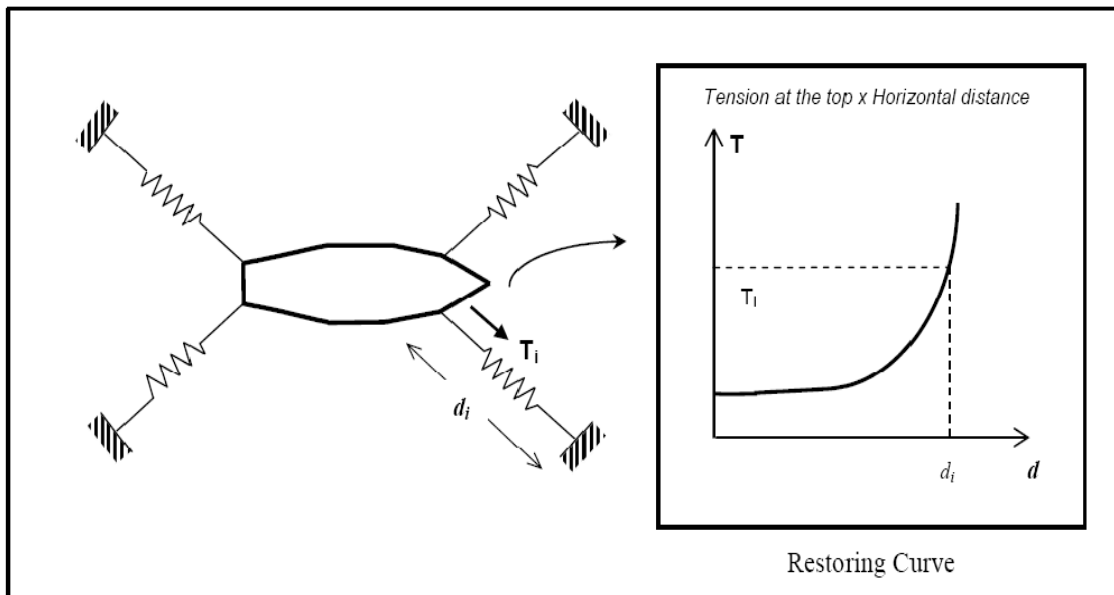


Fig. 2.8: Representation of mooring lines by means of non-linear springs
Source: Carbono, Menezes and Martha [17]

Evaluating Eq. (2.8) yields a new offset for the floating structure. At this point in the algorithm the computation is repeated until the resultant of the computed

displacements is lower than a specified tolerance – signifying the final static equilibrium position of the structure. The entire algorithm proposed in their work is summarized in the following outline.

1. Start
 - Initialize parameters
2. Seeding
 - Initial population is generated randomly
 - Initial population is decoded
 - Fitness values of each individual are computed by applying fitness function
3. Reproduction
 - Two chromosomes are selected as parents
 - Application of the crossover operator
 - Application of the mutation operator
4. Updating
 - The two new offspring chromosomes substitute the two worst chromosomes of the current population
5. Evaluation
 - The two chromosomes are decoded
 - Fitness of the two new chromosomes is computed
6. Stopping criterion satisfied
 - If so, then go to step 7; else go back to step 3
7. Report
8. End

This algorithm has been applied to optimize the mooring pattern of a floating unit, anchored at eighteen (18) different points. Each mooring line is said to be composed of three different materials, and the authors report that the algorithm proved to be robust and effective in analyzing this system. Figures (2.9a) and

(2.9b) show the initial and final mooring patterns of the analyzed system, respectively.

One may agree that the terminologies in this approach are unique, and the application of this method to regular problems requires an in-depth knowledge of genetic algorithms. In addition, because the principles of evolutionary computations are based on the concepts of Darwin's evolutionary theory and genetics, a good background in this area may be very helpful in formulating analysis and design tools based on this approach.

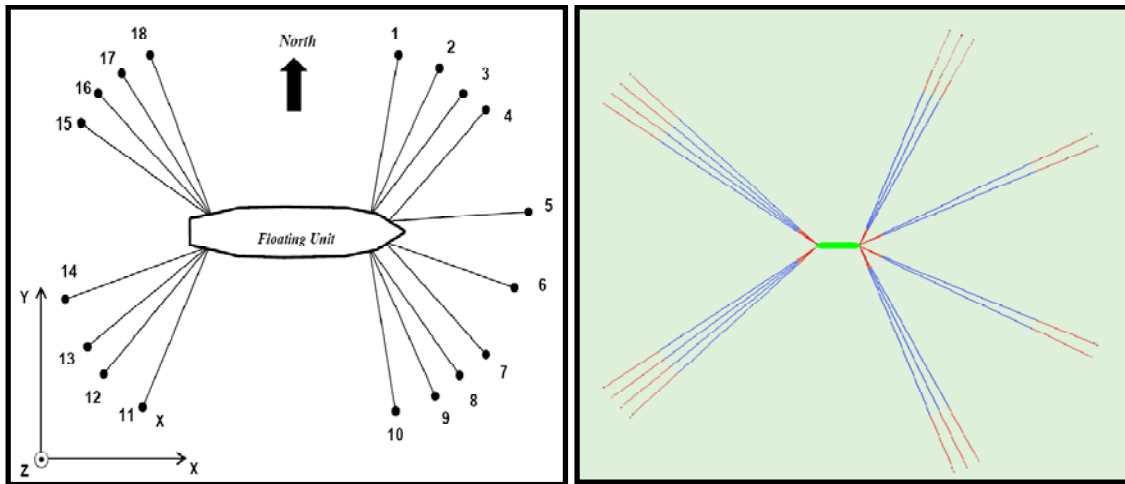


Fig. 2.9a: Initial mooring pattern Fig. 2.9b: Final mooring pattern
Source: Carbono, Menezes and Martha [17]

As confirmed by the authors of this work, with the genetic algorithm presented the design of spread mooring systems can be done to acceptable accuracies, though with heavy computational costs. The computational procedure offers limited options in the form of inputs into the process. Design variables are coded using specific methods (binary-digit strings, floating-point representations, etc.), which in turn necessitate decoding of the design variables. In addition to these challenges, using this method to design an equivalent mooring system would require a robust objective function given the multiple objectives in the design process. This could be quite a complexity in the design of equivalent mooring

systems, where the design variables are altered continuously to replicate the static results of the prototype system.

It is important to emphasize the difference between optimizing (or altering) design variables (or mooring system properties), and numerically searching for equilibrium using derived equilibrium equations. In the design of equivalent mooring systems, both optimization of the design parameters and numerical analysis of the system are inevitable. Selection of mooring system properties precedes the numerical iterations, but the designer of an equivalent mooring system is most comfortable with an algorithm which allows swift and repetitive alternation between these two stages in design. Therefore with the unavoidable computational complexities in genetic algorithms (which even yield accurate results), the challenge posed to the equivalent mooring designer is not made any easier.

The analysis methodology for integrated mooring and riser design was explored by Connaire, Kavanagh, Ahilan and Goodwin [18]. Their work holds that the justification for integrated design methods lies in the importance of hydrodynamic loads, stiffness, damping, added mass and potential compliant effects of risers as part of a moored system, and also in the need to recognize the precise station keeping requirements. They developed and investigated alternative riser and mooring analysis methodologies for five selected floating production systems, and evaluated the design approaches – this is backed by the consideration that integrated design of deepwater risers and moorings has the potential to bring substantial benefits in terms of system response, cost and safety. Design methods considered in their research represent increasing levels of complexity and integration of mooring and riser design.

A Central North Sea (CNS) FPSO in 150 meters of water depth, a West of Shetland (WOS) FPSO in 400 meters of water depth, a Northern North Sea (NNS) semi-submersible located at 350 meters of water depth, a Brazilian FPSO

in 1000 meters of water depth and a generic Gulf of Mexico floating production unit in 1700 meters of water depth constitute the five vessels used in their investigation. The first method considered (for each vessel) is a simplified method which assumes that risers and mooring lines may be represented by an equivalent vertical cylinder of height equal to the clearance under the keel and drag diameter equal to that of the actual moorings and risers. Their major remark about this method is that it is considered appropriate for systems having negligible riser stiffness, added mass and damping contributions. A second method, one considered to be of intermediate complexity, considers the integration of riser stiffness contribution to the overall stiffness of the system. It involves the calculation of loads on the vessel due to current acting on risers and mooring lines, and finite element modeling of the risers and moorings to obtain vessel reaction forces, which are then used to represent the mean vessel load contribution due to current on the risers and moorings. After explicit modeling (among other calculations performed) of risers and mooring lines, taking into account their catenary shape and all inherent material and structural nonlinearities, the riser restoring forces as a function of the position of the riser top are computed. The horizontal reactions at the top connection opposing the direction of the applied vessel excursion are evaluated against offset, and the horizontal reaction versus offset relationship for each riser is then incorporated in the mooring system. Lastly, their work discusses a final methodology involving the analysis of a fully integrated three-dimensional, finite element time domain dynamic riser and mooring system. It is reported that this method implicitly accounts for all contributions from the risers and mooring lines to the behavior and response of the entire system.

The reader may have observed that the second method in the work of Connaire and others is elaborated in this text somewhat more than the first and last methods. Amongst the three methods, the second method is the recommended algorithm in their work, and thus the extra attention to the details. Issues

acknowledged include the contribution to system stiffness, by considering the contribution to reduction in vessel excursion for a given static load. Reductions in static offset due to riser stiffness are presented in Table (2.1) while the mooring stiffness curve for the Brazilian FPSO is shown on fig. 2.10.

Table 2.1: Comparison of effective system stiffness contribution due to presence of risers

Vessel	Percentage Reduction in Static Offset due to Riser Stiffness
CNS FPSO	<1%
WOS FPSO	<2%
NNS Semi-submersible	Up to 18% in a Single Direction
Brazilian FPSO	Approximately 10% in all Directions
GOM FPU	35%

Source: Connaire, Kavanagh, Ahilan and Goodwin [18]

These selected results are included in this text to further expose the capability of their second algorithm in producing accurate results; therefore lack of accuracy is not the limitation of this algorithm, in view of using it as a tool in the design of statically equivalent mooring systems. Figure 2.10 depicts the accuracy of the algorithm as the analytical results for static offsets produced using the intermediate (recommended) method match those of model tests with and without risers.

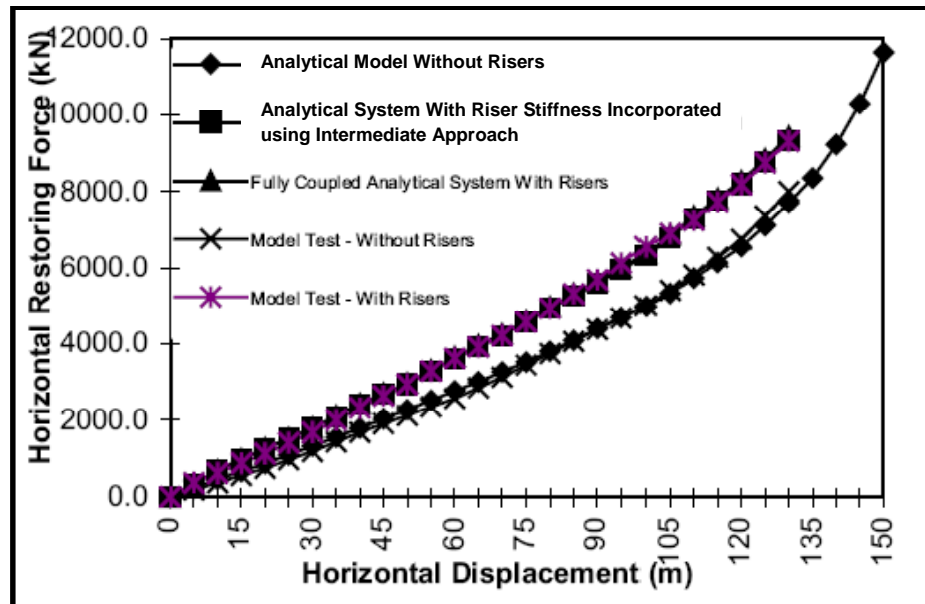


Fig. 2.10: Mooring stiffness curves for the Brazilian FPSO
Source: Connaire, Kavanagh, Ahilan and Goodwin [18]

A significant observation in the recommended algorithm is that the computation procedure flows from the calculation of vessel loads due to dynamic effects, to the calculation of riser stiffness and other relevant parameters, and finally the static offsets via mooring analysis, with the inclusion of the effects from all risers in the system. The authors acknowledge that due to the incorporation of the risers, there is an influence on the equilibrium of the entire system. Adjustments to the mooring line pretensions are therefore necessary in order to maintain the static equilibrium of the vessel, and this adjustment could be critical in terms of overall restoring force and susceptibility to line dynamic tension amplification.

Considering the use of this algorithm for equivalent mooring design implies the tedious task of adjusting mooring line tensions to restore the system equilibrium, for every alternative design configuration (or set of system properties) used to search for an agreement in design outputs between the model to be tested and the prototype mooring system. With risers incorporated in the system, the overall static response depends on more design parameters than if the risers were left

out. Consequently, isolating the static response of the vessel based on the mooring system only would be a lot more demanding.

Russell and Lardner [19] performed a statics experiment on an elastic catenary. Their work is expressed as a variation of the experiments discussed in Irvine [20] where the change in profile of the catenary line is measured for a small horizontal cable as additional weights are added at the center and in Irvine and Sinclair [21] where the weights are added at quarter points. It is highlighted that the effects of elasticity were negligible in the experiments conducted by Irvine, and this forms the basis for their experiments to verify the accuracy of the predictions of the equations of an elastic catenary for a guy wire in which elasticity is important.

With respect to fig. 2.11 the equations of an elastic catenary (which can also be found in Irvine [20]) as given in Russell and Lardner are eqns. 2.9 to 2.13.

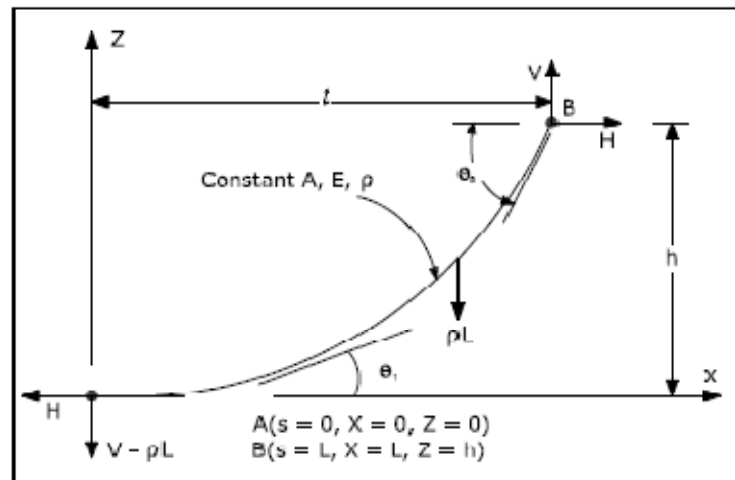


Fig. 2.11: Free body diagram of elastic cable connecting points A and B
Source: Russell and Lardner [19]

In this set-up, the vertical and horizontal distances between the end points of the cable are l and h respectively. The initial unstrained cable length is L , the Lagrangian coordinate along the unstrained cable measured from the bottom is

s , the horizontal component of the tension H is constant throughout, and the vertical component of tension at $s = L$ is V . The elastic modulus and unstrained cross-sectional area are E and A respectively, while ρ is the weight per unit length. The cable tension at any point s is given by:

$$T(s) = \sqrt{H^2 + [V - \rho(L - s)]^2} \quad (2.9)$$

The horizontal and vertical coordinates as a function of s are:

$$X(s) = \frac{Hs}{EA} + \frac{H}{\rho} \left[\sinh^{-1} \left(\frac{V - \rho(L - s)}{H} \right) - \sinh^{-1} \left(\frac{V - \rho L}{H} \right) \right] \quad (2.10)$$

and

$$Z(s) = \frac{s}{EA} \left[V - \rho \left(L - \frac{s}{2} \right) \right] + \frac{H}{\rho} \left\{ \sqrt{\left[\frac{V - \rho(L - s)}{H} \right]^2 + 1} - \sqrt{\left(\frac{V - \rho L}{H} \right)^2 + 1} \right\} \quad (2.11)$$

respectively.

Applying the boundary conditions $X(s = L) = l$ and $Z(s = L) = H$ to equations (2.10 and 2.11) we obtain:

$$l = \frac{LH}{EA} + \frac{H}{\rho} \left[\sinh^{-1} \left(\frac{V}{H} \right) - \sinh^{-1} \left(\frac{V - \rho L}{H} \right) \right] \quad (2.12)$$

$$h = \frac{L}{EA} \left(V - \frac{\rho L}{2} \right) + \frac{H}{\rho} \left[\sqrt{\left(\frac{V}{H} \right)^2 + 1} - \sqrt{\left(\frac{V - \rho L}{H} \right)^2 + 1} \right] \quad (2.13)$$

Numerical techniques can be used to obtain solutions for equations (2.10) to (2.13). The authors compare the numerical predictions from the equations of the elastic catenary with experiments from the guy wire with special interest in the

values of tension at the base of the cable for different values of the horizontal span l . For both horizontal and vertical components, the measured tensions at the base of the guy wire are reported to be an average of 2.5% lower than the theoretical values predicted using the elastic catenary equations. It is concluded that on a scale-model guy wire, the base tensions can be measured to within 5% accuracy when compared to the predictions from the governing equations.

One interesting characteristic of the elastic catenary equations is the inherent consideration of line stretch. The effect of EA can easily be controlled as an input into the equations, rather than an external computation. Additionally, the simplicity of the equations allows users to control numerical iterations by setting a known quantity as a boundary condition. These equations deal strictly with the statics of the system and they offer accurate solutions even at model scale, as in the case of Russell and Lardner. The parameters do not in any way depend on the dynamics of the system, and in effect these line properties constitute the design parameters of interest in statically equivalent mooring systems. Considering these features of the elastic catenary equations, as long as the numerical scheme is efficient, it is encouraging to simulate the static performance of single-segment, two-segment and three-segment mooring systems with confidence that the results will be accurate as well. It is possible to code these equations independent of parameters from other submerged structures connected to the floater (e.g. risers). For these reasons at the least, the elastic catenary equations are used in the analysis of spread mooring systems, as applied to this research.

2.3 ENGINEERING BEHAVIOR AND MODES OF FAILURE OF MOORING LINES

Different mooring lines respond differently to a diverse range of loading conditions. The properties which they exhibit and the factors surrounding such

behavior must be identified and understood by the designer. To satisfy station-keeping requirements in a full-scale system, the properties that are required for the design of mooring lines include breaking strength, endurance under cyclic loading (tension-tension fatigue), durability, dimensions and load-elongation characteristics. For a clear understanding of the behavior of mooring lines under varying load conditions, rope testing must be done and the results analyzed. However, according to Francois [22], whilst some essential tests (such as breaking strength tests) are usually performed on full size prototypes, other tests may be omitted when the test results are available from previously qualified ropes (i.e. ropes which have gone through a full rope qualification process by the Classification Society).

In model test projects for floating structures, rope testing is not usually an integral part of the scheme. The selection of mooring lines used in the wave basin is based on an understanding of the engineering properties of the lines used in the prototype system, combined with sound engineering judgment. Components such as springs may be used as equivalent replacement for the elastic components of the prototype system, while ensuring that the static outputs of both systems are essentially the same. The performance of mooring lines at very small scales may vary slightly or significantly from those at large scales, depending on loading conditions. Such disparities if overlooked may result in greater challenges during the selection of equivalent mooring components for design. The notion here is that the more different the engineering properties of the full scale components are from those of the equivalent system, the clumsier the optimization process will be in design, or the more likely that obtaining a good match will be more challenging.

2.3.1 ENGINEERING PROPERTIES OF FIBER ROPES

The required minimum breaking strength of a rope is one of the principal parameters considered in design. Many other parameters used in the design of station-keeping systems are a function of the breaking strength of the line. For fiber ropes, at least three samples of rope are tested, and a quantifiable margin is verified if the breaking strengths of all three samples are above a specified minimum. A limitation in the 3-tests approach is that the tests will not provide accurate enough information to adjust the breaking strength from the test results upward or downward in case of a (marginally) failed test [22]. The breaking strength should be considered as the basis for a viable check in the performance of mooring lines even at model scale. Satisfying such conditions will only add to the integrity of the equivalent mooring design.

Cyclic loading endurance is an important dynamic property of a mooring line, which offers insight on its response to cyclic tension. Fiber ropes used in deep water will experience random-amplitude tensions primarily due to wave forces acting on the floating structure. The endurance of typical polyester ropes has been quantified for station-keeping, using extensive cyclic loading tests (up to 40 million cycles endurance) performed within the “Rope Durability” project [23], and found to be far above that of a steel wire rope of the same size. For a properly designed and manufactured fiber rope, tests indicate that the prevailing failure mode under such cyclic loading tests is internal abrasion. Other potential failure mechanisms identified include compression fatigue in synthetic fibers, slippage in terminations and back-of-the-eye failure. Compression fatigue however has been found with tests down to 1% minimum loads not to be an issue [22].

Assessing the durability of any fiber rope involves accounting for all physical impacts including chaffing, cutting, and internal abrasion by ingress of foreign materials, which could occur right at the installation phase of the mooring

system. The durability of the ropes is directly related to the damages incurred during the in-service stage. Most cuts (by passing vessels or loose steel wire ropes) on the fiber ropes are partial; therefore the time to failure is prolonged, and failure occurs when the load in the line finally exceeds its residual strength. Assessments made on dropped ropes show that penetration of particles into fiber ropes is site dependent, and that it is difficult to predict the level of ingress across the entire length of the rope. The worst case scenario of course, is when the line is touching the sea floor. Marine growth inside the rope is also strongly enhanced in such regions while the durability of the rope is reduced.

Francois [22] defines a process called “Bedding-in” as the modification of the properties of a rope during the first loading(s) and during the early stage of rope service, pointing out that this behavior is specific to fiber ropes. Bedding-in is understood to result in the accumulation of permanent elongation and stabilization of load-elongation properties which are not recoverable unless the rope is returned to loose (no load) condition for a substantial amount of time. Francois and Davis [24] proposed a model derived from the results of creep and recovery tests, to compute the permanent elongation of such ropes as:

$$u_f = u_p + s_p \cdot PT \quad (2.14)$$

where PT is the mean (permanent) tension, s_p is a flexibility for the long term elongation ($s_p = 1/10$ is suggested, and PT is in % of the rope MBS), and the term u_p is to be obtained from testing.

The static stiffness of a fiber rope under varying loading conditions depicts the effect of mean load variations under fluctuating environmental forces. Such loads may be due to a continuous increase and decrease in a storm or the existence of loop currents at the station-keeping site. Bureau Veritas [25] describe a static stiffness test which is depicted in fig 2.12. After a proper

bedding-in, the rope is cycled between two tension levels with each half cycle consisting of a load change (higher or lower) between the two levels. At each load level there is also a loading plateau during which creep recovery is measured. The broken red lines in fig 2.12 show the creep deformation stages of the rope at each loading level. Ultimately, from this test and equations obtained from the works of Francois and Davies, a prediction can be made of the elongation over a longer duration of each 1/2 cycle; more representative of events intended to be modeled.

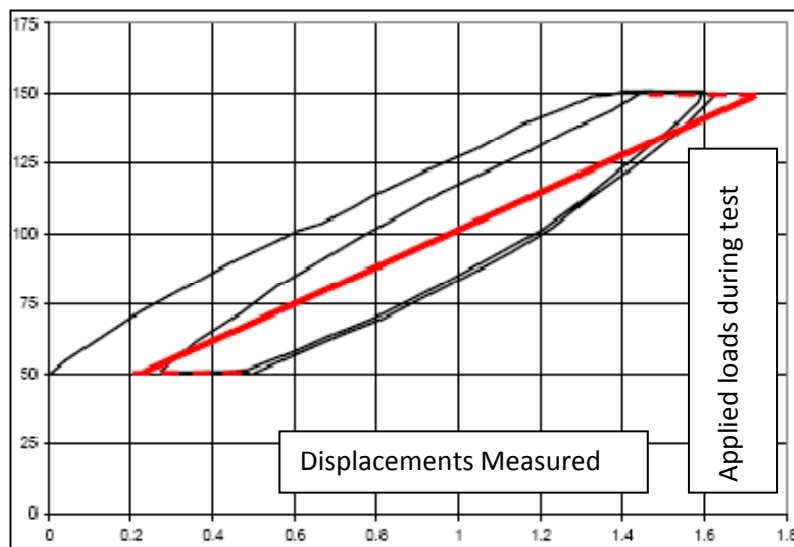


Fig. 2.12: Static stiffness test
Source: Francois [22]

Testing for the dynamic stiffness of fiber ropes involves harmonic loading at constant amplitude of either load or elongation, about a given mean load. Francois [22] explains further that testing conditions should include proper control and measurement of tension using load cells and elongation using gauge length extensometers. Casey and Banfield [26] have performed long duration tests and found that the dynamic stiffness in fiber ropes rapidly increases at the beginning of the run, and then tends to stabilize. They hold however that without

prior bedding-in, the stiffness continues to increase over durations of hundreds of thousands of cycles.

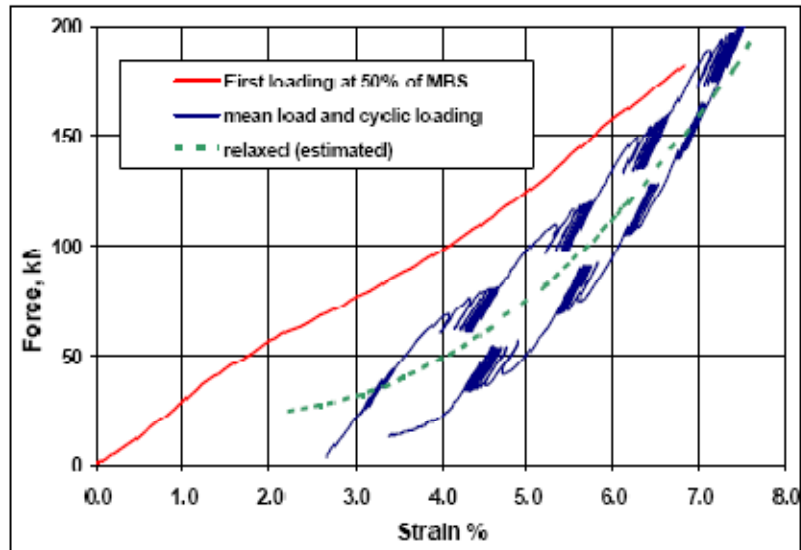


Fig. 2.13: Mean load steps and cycling tests
Source: Francois [22]

A similar test called the “mean load steps in cycling” test is also discussed in their work. The loading and unloading sequence for this test is said to be a single mean-loading cycle consisting of several steps (fig 2.13). The authors compare the force-strain trend from the “mean load” test to that obtained by loading the rope at 50% of the minimum breaking strength and to that obtained from estimates. Details on how the estimated trend is obtained are not provided in their work and specifics on the loading sequences are also not provided. However, they observe that there is a relationship between the stiffness increase and the level of stabilization of the rope, be it creep or recovery, and that in these tests a complete stabilization is never achieved.

2.3.2 PERFORMANCE OF MOORING CHAINS

Mooring systems involving the use of chains show the major loading mechanisms to be twist (on the vessel attachment), bending (within the fairlead), highest tensions (just below, or at the fairlead) fatigue (within the arc length of the line) and wear (towards the end of the line), as illustrated in fig. 2.14.

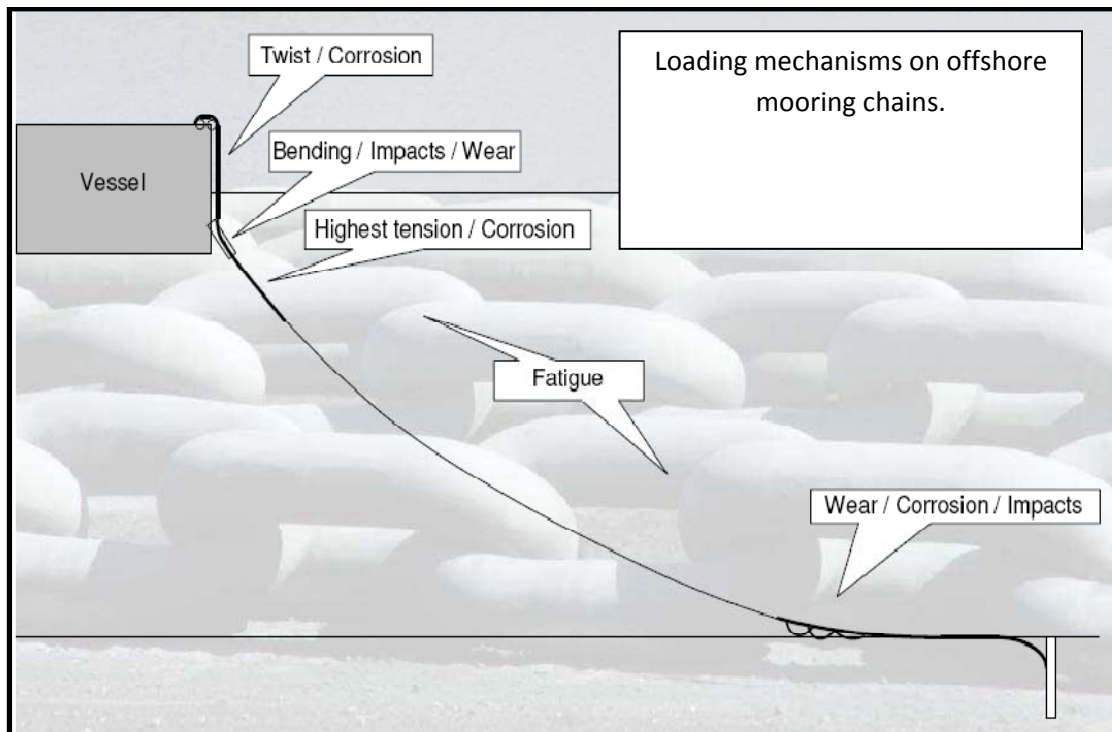


Fig. 2.14: Loading mechanisms on offshore mooring chains

Source: TEKNA Conference on DP and Mooring of Floating Offshore Units [7]

Like any other mooring line type used in offshore operations, chains experience a range of cyclic tension variations which induce tension fatigue. Figure 2.15 shows examples of chain fatigue. The relationship between the stress range associated with chains and the number of loading cycles to failure is depicted in fig 2.16.



Fig. 2.15: Fatigued sections of a mooring chain
Source: TEKNA Conference on DP and Mooring of Floating Offshore Units [7]

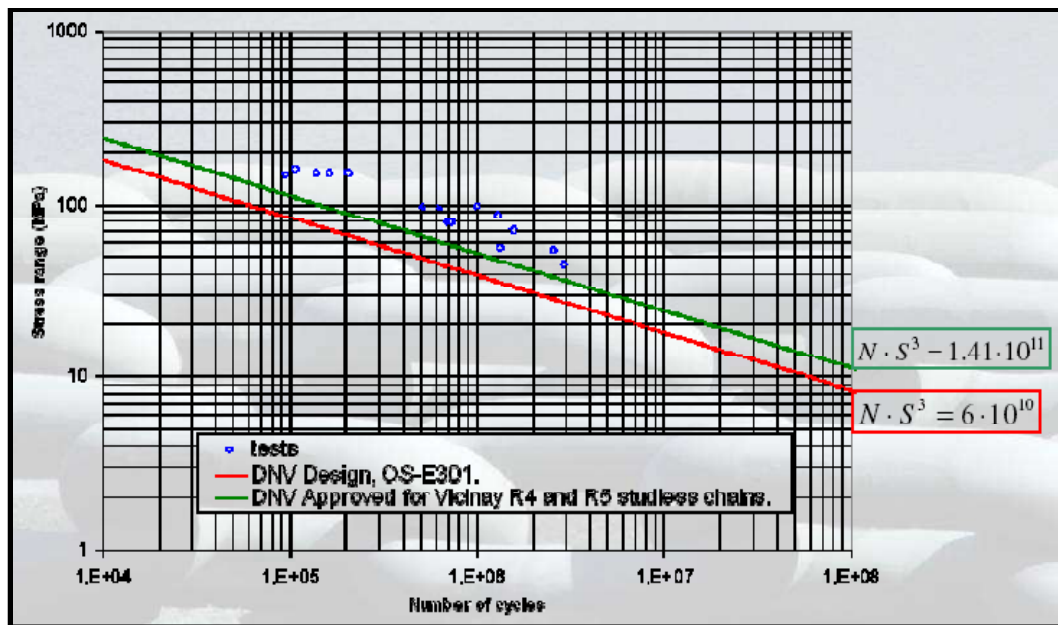


Fig. 2.16: Stress range - No. of cycles relationship
Source: TEKNA Conference on DP and Mooring of Floating Offshore Units [7]

Comparing results from fatigue tests, those obtained from DNV design (OS-E301) and the DNV-Vicinay approved method for estimating the stress range for chains as a function of number of cycles, the relationship between the two parameters follows similar trends. The big picture portrays a reduction in the

number of loading cycles until failure as the stress range increases, even though the DNV-Vicinay method has slightly higher magnitudes for the stress ranges.

2.3.3 BEHAVIOR OF SMALL WIRES

A possible deviation of stretched wires from the simple 2-dimensional catenary form was investigated by Bowden [27]. His research holds that for real wires, stretch and bending stiffness modify the catenary form, even for thin wires. The main effect of stretching, without surprise, is seen to be a reduction in the weight per unit length. This reduces the wire sag. Bowden gives an expression for the parabolic approximation for the mid span sag of a stretchable wire as:

$$y\left(\frac{l}{2}\right) = -\frac{1}{8} \left(\frac{1}{1+\varepsilon} \right) \frac{w_0}{T} l^2 \quad (2.15)$$

and the reduced weight per unit length after stretch is given as:

$$w = w_0 / (1 + \varepsilon) \quad (2.16)$$

where $y\left(\frac{l}{2}\right)$ is the deflection at mid span, w is the initial weight per unit length, T is the horizontal component of tension in the wire (which is uniform throughout its length), l is the length of the wire and ε is the strain on the wire. In an experiment using a 100 meter 0.5 mm diameter wire with Young's modulus $E = 2.1 * 10^3 \text{ kg/mm}^2 (207 \text{ GPa})$, tensioned to 14kg, the wire is found to stretch by $\varepsilon = 0.003$ or 0.3m. This strain reduces the deflection by about 0.5mm, an effect considered to be measurable. At larger scales, similar effects can be expected in wire ropes used in equivalent moorings for model tests. An understanding of the behavior of these lines is important in the interpretation of statics results. It makes it easier to decipher when the outputs are completely different from what the designer intuitively expects, if such intuition is based on a well informed perspective regarding the potential behavior of the mooring system components.

CHAPTER III

FORMULATION OF STAMOORSYS

With a clear focus on the objectives discussed in earlier chapters, STAMOORSYS is formulated using governing principles of static analysis of spread mooring systems. The algorithm applied to obtain the desired results is concise and easy to comprehend. The software is formulated to allow the combination of mooring lines of different properties in the mooring system. This is important in model testing, as the designer may desire to model or represent the prototype mooring lines with a combination of devices that increase the tendency of obtaining a match in the static parameters of interest. STAMOORSYS allows the use of up to 8 mooring lines, all of which can be 3-segment lines. Modifying the code to accept a different number of lines or a different number of segments will require a substantial amount of work, as the user interface will need modification, leading to alterations in almost all cell references (in Microsoft Excel).

The codes for STAMOORSYS are written using Visual Basic macros in Microsoft Excel 2007 version. Using this package makes it easy to create an efficient interface between the codes and the user while retaining the ability to view results instantly at the end of each analysis. Alternating between different windows during the design of statically equivalent mooring systems is completely ruled out, as the design interface is formulated to be self-sufficient regarding required inputs and desired outputs. By creating the program in Microsoft Excel, there is the added advantage available to the user to apply the tools originally embedded in Excel for any desired post-processing analysis possible with such tools. One of such tools (particularly useful during the design process) is the 'scenario manager' in Excel. The scenario manager is extremely useful in saving design scenarios for future use. Such tools will also substantially

reduce the time required to enter input data for design. It is also possible to save the spreadsheet and rename it for archival purposes after each design project.

3.1 GENERAL PRINCIPLES IN STATIC ANALYSIS OF SPREAD CATENARY MOORING SYSTEMS

Given that a spread mooring system comprises several individual catenary mooring lines, the procedure used in the analysis of a single line forms the basis for resolving the static parameters of the spread mooring system. The fundamental principles of system equilibrium apply, and can be expressed in the following equations:

$$\sum F_x = 0 \quad (3.1)$$

$$\sum F_y = 0 \quad (3.2)$$

$$\sum F_z = 0 \quad (3.3)$$

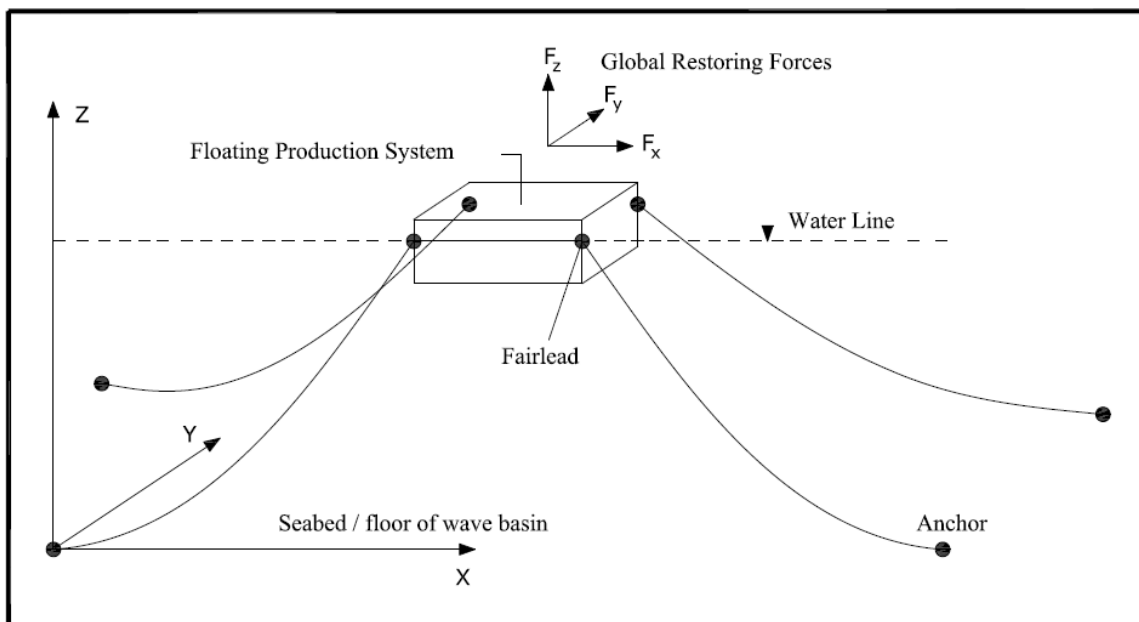


Fig. 3.1: Sketch of spread mooring system with 4 mooring lines in elevation

Considering fig. 3.1, eqns. (3.1) to (3.3) are the only equilibrium equations of interest regarding the static equivalence under discussion. Although additional static equilibrium equations ($\sum M_x = 0, \sum M_y = 0, \sum M_z = 0$) could be considered, the floater is assumed (at the moment) not to rotate, hence moment equilibrium is not considered. The primary target is to ensure that the static global horizontal forces and stiffness on the floating vessel in the equivalent system are close enough to those of the prototype system.

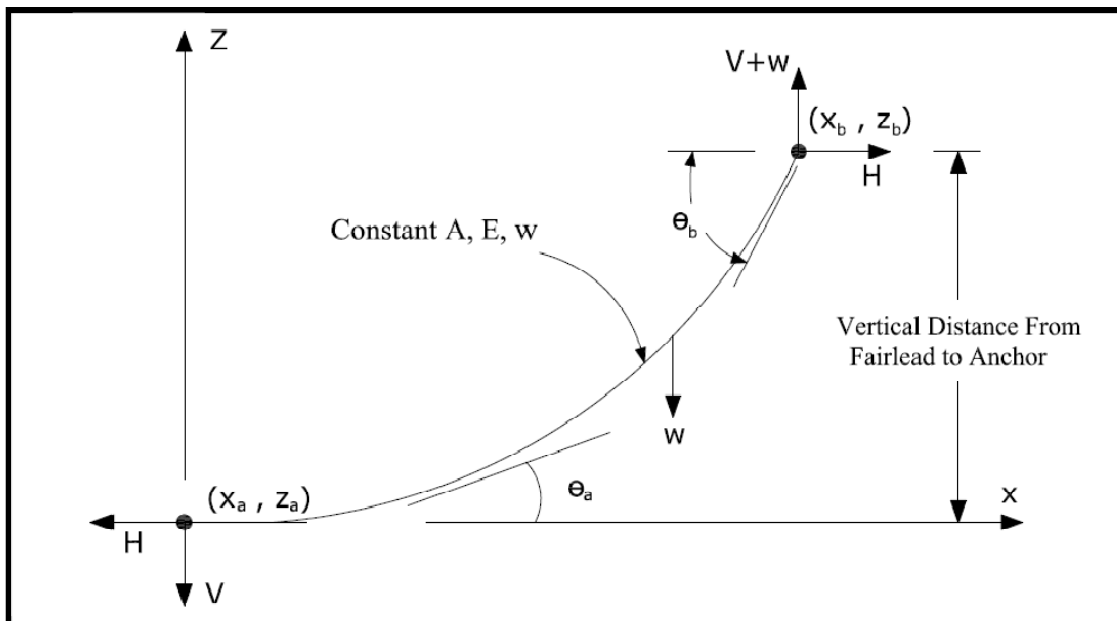


Fig. 3.2: Single-segment mooring

For a single segment mooring under equilibrium conditions such as that shown in fig. 3.2, the equilibrium equations for static analysis can be derived as shown in eqns. (3.4) through (3.37). The configuration in fig. 3.2 and the subsequently derived equations are specifically for the case where the point “a” (the left end of the line) corresponds to the catenary touch-down point or to a point where there is a vertical uplift component to the tension. It is assumed that the water is calm, that is, it does not exert a force on the cable (other than buoyancy). The submerged unit weight of the cable is w (weight per unit length).

Considering an isolated elemental length ds of the line in fig. 3.2, the free body diagram can be drawn as shown in fig 3.3. The tension T at the left end of the section is replaced by its vertical and horizontal components V and H respectively, and the submerged weight per unit length is w .

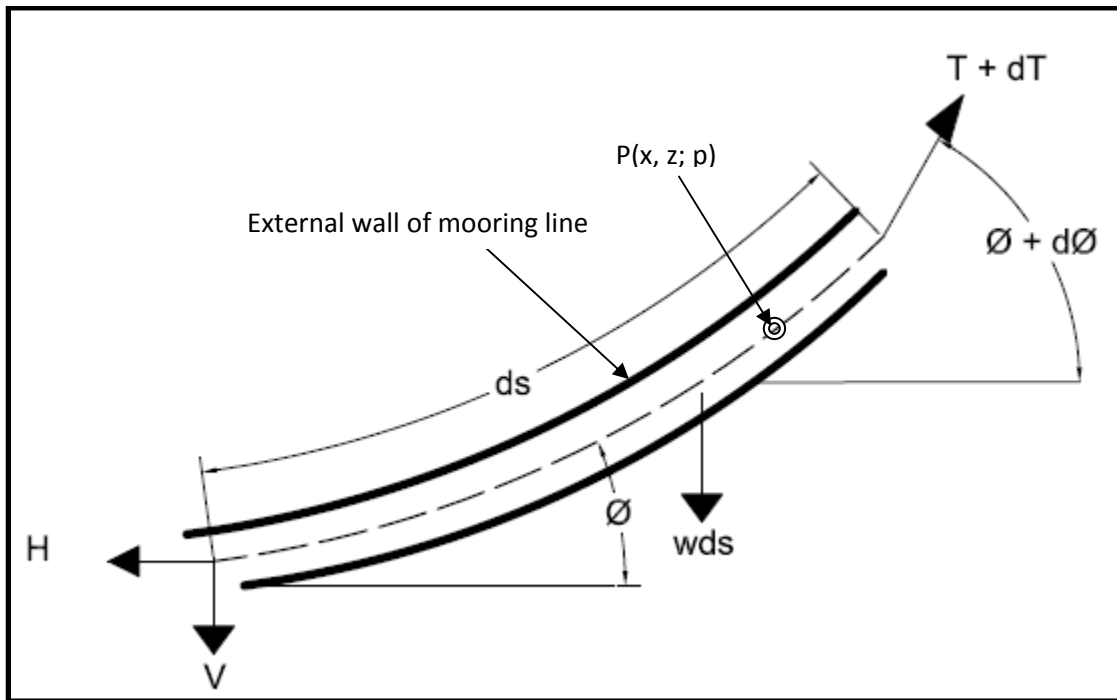


Fig. 3.3: Free body diagram of elemental section

Taking summation of forces in the horizontal axis in fig. 3.3:

$$\sum F_x = 0$$

$$-H + (T + dT)\cos(\phi + d\phi) = 0 \quad (3.4)$$

Using the identity:

$$\cos(\phi + d\phi) = \cos\phi\cos d\phi - \sin\phi\sin d\phi$$

Equation (3.4) can be written as:

$$-H + (T + dT) \cdot [\cos\phi \cos d\phi - \sin\phi \sin d\phi] = 0$$

$$-H + (T + dT) \cos\phi \cos d\phi - (T + dT) \sin\phi \sin d\phi = 0$$

If we assume that $d\phi$ is small, then $\cos d\phi \approx 1$ and $\sin d\phi \approx d\phi$

$$-H + (T + dT) \cos\phi - (T + dT) \sin\phi d\phi = 0$$

$$-H + T \cos\phi + dT \cos\phi - T \sin\phi d\phi - dT \sin\phi d\phi = 0$$

Since $H = T \cos\phi$,

$$dT \cos\phi - T \sin\phi d\phi - dT \sin\phi d\phi = 0$$

We can consider the third term on the left hand side to be very small relative to other terms; hence we neglect it to obtain:

$$dT \cos\phi - T \sin\phi d\phi = 0 \tag{3.5}$$

from which:

$$\frac{dT}{T} = \tan\phi d\phi \tag{3.6}$$

Similarly we take the summation of forces in the vertical axis in fig. 3.3:

$$\sum F_z = 0$$

$$-V - wds + (T + dT) \sin(\phi + d\phi) = 0 \tag{3.7}$$

$$-V - wds + (T + dT) \cdot [\sin\phi \cos d\phi + \sin d\phi \cos\phi] = 0$$

Again if we assume that $d\phi$ is small, then $\cos d\phi \approx 1$ and $\sin d\phi \approx d\phi$

$$T \cos \phi d\phi + dT \sin \phi = w ds \quad (3.8)$$

Substituting eqn. (3.6) into eqn. (3.8)

$$T(\cos \phi d\phi + \tan \phi d\phi \sin \phi) = w ds$$

If we substitute $T = \frac{H}{\cos \phi}$ and $\tan^2 \phi = \sec^2 \phi - 1$

we obtain:

$$\frac{H}{\cos^2 \phi} d\phi = w ds$$

Integrating both sides, we have:

$$H \int \frac{1}{\cos^2 \phi} d\phi = w \int ds$$

$$\frac{w}{H} s = \tan \phi + C \quad (3.9)$$

At $s = 0$, $\phi = \phi_a$ and therefore $C = -\tan \phi_a$

Therefore eqn. (3.9) can be written as:

$$ws = H \tan \phi - H \tan \phi_a \quad (3.10)$$

which can also be written as:

$$V = ws + H \tan \phi_a \quad (3.11)$$

The magnitude of the tension in the mooring line at point “a” can be expressed as:

$$T = \sqrt{H^2 + V^2}$$

Therefore along the mooring line, the tension as a function of arc length can be expressed in terms of eqn. (3.11) as:

$$T(s) = \sqrt{H^2 + (ws + H \tan \phi_a)^2} \quad (3.12)$$

or

$$T(s) = H \sqrt{1 + \left(\frac{ws}{H} + \tan \phi_a \right)^2} \quad (3.13)$$

Equation (3.12) or (3.13) gives the tension distribution along the mooring line.

As in Irvine [28], let s be the Lagrangian coordinate of the un-stretched mooring line. We can define a point P along this s coordinate. However, under the self weight of the line (or external loads) the point P moves to occupy a new position in the stretched configuration of the mooring line described by Cartesian coordinates x, z and Lagrangian coordinate p . With respect to point P we can write:

$$\cos \phi = \frac{dx}{dp} \quad (3.14)$$

and

$$\sin \phi = \frac{dz}{dp} \quad (3.15)$$

So we can write the horizontal component of the tension at point P as:

$$H = T \frac{dx}{dp} \quad (3.16)$$

It is assumed that the elasticity of the mooring line can be modeled by Hooke's law as:

$$\frac{\Delta L}{L_0} = \frac{T}{EA_0} \quad (3.17)$$

where L_0 is the un-stretched length of the line (under no tension), E is the Young's modulus of the mooring line and A_0 is the effective cross-sectional area of the mooring line. The ratio of change in length to the original length can also be expressed as:

$$\frac{\Delta L}{L_0} = \frac{dp}{ds} - \frac{ds}{ds} = \frac{dp}{ds} - 1 \quad (3.18)$$

So from eqns. (3.17) and (3.18)

$$T = \left(\frac{dp}{ds} - 1 \right) EA_0$$

$$\frac{dp}{ds} = \frac{T}{EA_0} + 1 \quad (3.19)$$

The change along the x coordinate with respect to the Lagrangian coordinate s can be expressed as:

$$\frac{dx}{ds} = \frac{dx}{dp} \cdot \frac{dp}{ds} \quad (3.20)$$

From eqn. (3.16):

$$\frac{dx}{dp} = \frac{H}{T} \quad (3.21)$$

Therefore substituting eqns. (3.19) and (3.21) into (3.20), we have:

$$\frac{dx}{ds} = \frac{H}{T} \left(\frac{T}{EA_0} + 1 \right) = \frac{H}{EA_0} + \frac{H}{T} \quad (3.22)$$

Substituting eqn. (3.12) in eqn. (3.22), we have:

$$dx = \frac{H}{EA_0} ds + \frac{H}{\sqrt{H^2 + (V + ws)^2}} ds \quad (3.23)$$

Recalling that the integral of the form $\int \frac{1}{\sqrt{a^2 + x^2}} dx = \sinh^{-1} \left(\frac{x}{a} \right)$

On integration, eqn. (3.23) becomes:

$$x(s) = \frac{Hs}{EA_0} + H \left\{ \frac{1}{w} \left(\sinh^{-1} \left(\frac{V + ws}{H} \right) \right) \right\} + C \quad (3.24)$$

At $s = 0, x(0) = 0$, so

$$C = -\frac{H}{w} \left\{ \sinh^{-1} \left(\frac{V}{H} \right) \right\}$$

and therefore

$$x(s) = \frac{Hs}{EA_0} + \frac{H}{w} \left\{ \sinh^{-1} \left(\frac{V + ws}{H} \right) - \sinh^{-1} \left(\frac{V}{H} \right) \right\} \quad (3.25a)$$

Equation (3.25a) gives the x coordinate of the mooring line as a function of s .

For an inextensible mooring line $EA_0 \rightarrow \infty$ and eqn. (3.25a) reduces to (3.25b):

$$x(s) = \frac{H}{w} \left\{ \sinh^{-1} \left(\frac{V + ws}{H} \right) - \sinh^{-1} \left(\frac{V}{H} \right) \right\} \quad (3.25b)$$

Similar to eqn. (3.20), with respect to the z axis:

$$\frac{dz}{ds} = \frac{dz}{dp} \cdot \frac{dp}{ds} \quad (3.26)$$

Recall from eqn. (3.19) that: $\frac{dp}{ds} = \frac{T}{EA_0} + 1$

From eqn. (3.15):

$$\sin \phi = \frac{dz}{dp} = \frac{V}{T}$$

Substituting into eqn. (3.26)

$$dz = \frac{V}{EA_0} ds + \frac{V}{T} ds \quad (3.27)$$

Now with respect to eqn. (3.11), we can write eqn. (3.27) as:

$$dz = \frac{ws + H \tan \phi_a}{EA_0} ds + \frac{ws + H \tan \phi_a}{\sqrt{H^2 + (V + ws)^2}} ds \quad (3.28)$$

The integration of eqn. (3.28), where the second term is integrated by substitution method, yields:

$$z(s) = \frac{ws^2}{2EA_0} + \frac{Hs \tan \phi_a}{EA_0} + \frac{H}{w} \left[1 + \left(\frac{ws}{H} + \tan \phi_a \right)^2 \right]^{\frac{1}{2}} + C \quad (3.29)$$

At $s = 0$, $z(0) = 0$, so

$$\frac{H}{w} \left[1 + \tan^2 \phi_a \right]^{1/2} + C = 0$$

Therefore $C = -\frac{H}{w} \sec \phi_a$

Equation (3.29) can now be written as:

$$z(s) = \frac{ws^2}{2EA_0} + \frac{Hs \tan \phi_a}{EA_0} + \frac{H}{w} \left[1 + \left(\frac{ws}{H} + \tan \phi_a \right)^2 \right]^{1/2} - \frac{H}{w} \sec \phi_a \quad (3.30)$$

Therefore the z coordinate of the mooring line as a function of s is given by eqn. (3.30). For an inextensible mooring line $EA_0 \rightarrow \infty$ and eqn. (3.30) reduces to:

$$z(s) = \frac{H}{w} \left\{ \left[1 + \left(\frac{ws}{H} + \tan \phi_a \right)^2 \right]^{1/2} - \sec \phi_a \right\} \quad (3.31)$$

We can derive an expression for the arc length s of the mooring line as a function of the x coordinate, using the governing differential equation of the catenary. Recalling eqn. (3.10):

$$ws = H \tan \phi - H \tan \phi_a$$

$$\frac{ws}{H} = \frac{dz}{dx} - \tan \phi_a \quad (3.32)$$

Differentiating both sides with respect to x :

$$\frac{d}{dx} \left(\frac{ws}{H} \right) = \frac{d^2z}{dx^2} \quad (3.33)$$

Equation (3.33) is the governing differential equation of the catenary line.

Since $(ds)^2 = (dx)^2 + (dz)^2$, we can write

$$\frac{ds}{dx} = [1 + z'^2]^{\frac{1}{2}} \quad (3.34)$$

$$\text{where } z' = \frac{dz}{dx} . \quad (3.35)$$

Substituting eqn. (3.34) into eqn. (3.33)

$$H \frac{d^2z}{dx^2} = w [1 + z'^2]^{\frac{1}{2}}$$

$$\frac{w}{H} = \frac{\frac{d^2z}{dx^2}}{[1 + z'^2]^{\frac{1}{2}}}$$

$$\int \frac{w}{H} dx = \int \frac{1}{[1 + z'^2]^{\frac{1}{2}}} dz'$$

$$\frac{w}{H} x = \sinh^{-1} z' + C_1$$

$$z' = \sinh \left(\frac{w}{H} x - C_1 \right)$$

$$z = \int \sinh \left(\frac{w}{H} x - C_1 \right) = \frac{H}{w} \cosh \left(\frac{w}{H} x - C_1 \right) + C_2$$

At $x = 0, z' = \tan \phi_a$, therefore

$$C_1 = -\sinh^{-1}(\tan \phi_a)$$

At $x = 0, z = 0$, therefore

$$C_2 = -\frac{H}{w} \cosh(\sinh^{-1}(\tan \phi_a))$$

Therefore;

$$z(x) = \frac{H}{w} \left[\cosh\left(\frac{w}{H}x + \sinh^{-1}(\tan \phi_a)\right) - \cosh(\sinh^{-1}(\tan \phi_a)) \right] \quad (3.36)$$

Equation (3.36) gives the vertical coordinate of a mooring line as a function of x , the horizontal coordinate.

From equation (3.32);

$$s(x) = \frac{H}{w} \left(\frac{dz}{dx} - \tan \phi_a \right) = \frac{H}{w} \left\{ \sinh\left[\frac{wx}{H} + \sinh^{-1}(\tan \phi_a)\right] - \tan \phi_a \right\} \quad (3.37)$$

Equation 3.37 gives the arc length of the mooring line as a function of the horizontal coordinate x . A summary of the major equations used in obtaining equilibrium solutions for single segment mooring is presented in Table 3.1.

Other equations such as those for $s(x)$ and $z(x)$ may also be used in determining static equilibrium, but this will depend on the numerical strategy adopted for the iteration process. To obtain static solutions using the equations shown in Table 3.1, the following information must be provided:

- The elevation of the top end of the mooring line segment, relative to the bottom end
- Line weight per unit length w , line length L , axial stiffness EA_0

- Horizontal component of tension in the line (H), or known horizontal offset position of the top end of the line relative to the bottom end.

Table 3.1: Summary of major equations used in obtaining static equilibrium solutions

EQUATION	PURPOSE
$z(s) = \frac{ws^2}{2EA_0} + \frac{Hs \tan \phi_a}{EA_0} + \frac{H}{w} \left[1 + \left(\frac{ws}{H} + \tan \phi_a \right)^2 \right]^{1/2} - \frac{H}{w} \sec \phi_a$	<p>Computes the vertical coordinate of the top attachment point of the mooring line, relative to the anchor point.</p>
$x(s) = \frac{Hs}{EA_0} + \frac{H}{w} \left\{ \sinh^{-1} \left(\frac{V + ws}{H} \right) - \sinh^{-1} \left(\frac{V}{H} \right) \right\}$	<p>Computes the horizontal coordinate of the top attachment point of the mooring line, relative to the anchor point.</p>
$T(s) = H \sqrt{1 + \left(\frac{ws}{H} + \tan \phi_a \right)^2}$	<p>Computes tension as a function of arc length, along the mooring line.</p>

The primary condition which must be satisfied (as applied in this research) to obtain correct static equilibrium solutions is that the computed vertical coordinate of the top attachment point of the line $z(s)$ must be close enough (or equal) to the specified fairlead elevation relative to the anchor point. It may be possible to control the numerical iteration using some other known constant parameter, but

the condition stated above is the only one used in this work at this point. Only after this condition has been satisfied is the horizontal coordinate of the line computed. In the iteration procedure the angle of the line at the bottom end (ϕ_a) or the length of the line on seafloor is adjusted until static equilibrium is reached.

For three segment lines, three vertical coordinates are used in the computations. If the described equilibrium condition is not satisfied after the first vertical coordinate $z_3(s_3)$ (for the third segment) has been computed, then the second vertical coordinate $z_2(s_2)$ is computed and a summation of both first and second vertical coordinates are compared to the “iteration parameter”, in this case the fairlead elevation. A summation of all three vertical coordinates is computed and compared to the iteration parameter, if the condition is not satisfied after the second comparison. This process is explicitly explained in the following section and with the aid of a detailed flow chart.

3.2 ALGORITHM USED IN STAMOORSYS FOR THE DESIGN OF STATICALLY EQUIVALENT SPREAD MOORING SYSTEMS

With the elastic catenary equations and the principles of static equilibrium, designing the equivalent mooring system requires efficient algorithm that produces the static solutions efficiently and with high accuracy. Whether the mooring system is a single component (or single-segment) system or a multi-segment system, a direct solution cannot be obtained as the problem is highly nonlinear. The solutions have to be obtained iteratively, using a known quantity to control the iteration process.

The primary requirement of the design process is to match the global restoring force versus offset, and the global stiffness versus offset curves for a range of offsets specified by the user. A combination of line properties selected by the designer will produce a unique result. If there is no match between the obtained

results and the target curves, the designer will have to continue optimizing the selected components and configurations of the mooring line, in search of a satisfactory match. It is therefore necessary that the mechanism of computation be such that results are returned quickly, to allow the efficient management of the optimization processes by the designer.

Overall, the algorithm used in STAMOORSYS to analyze and design a statically equivalent spread catenary mooring system is summarized as follows:

- Read input data – anchor and fairlead coordinates, vessel offsets, line properties, minimum and maximum preliminary restoring forces, numerical increment value to be used in iteration (i.e. quantity by which angle at the bottom end of line or length of line on seafloor will be adjusted numerically) for analysis of all lines (1 to 8).
- For each given offset (as in fig. 3.4) compute the departures (horizontal distance from anchor to fairlead) in each line, in the plane of the line.

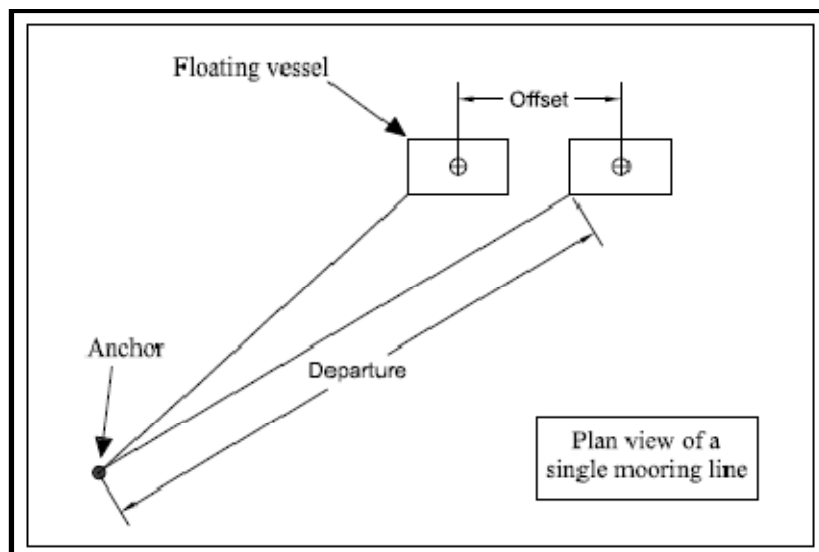


Fig. 3.4: Sketch of single line mooring showing offset and departure

- Given the range of preliminary restoring forces (minimum, maximum and number of points), compute preliminary departures in the plane of one

line using the same line properties to be used in design. The departures are calculated using an iterative process, which uses the vertical distance between fairlead and seabed as the conditional parameter.

- Using the known departures in the planes of the respective lines for each offset, interpolate within the preliminary departures to find the corresponding restoring forces in the plane of each line.
- Resolve the forces into the Cartesian planes, and apply equilibrium equations to obtain the static global forces on the vessel.
- Compute the global stiffness in the respective Cartesian planes

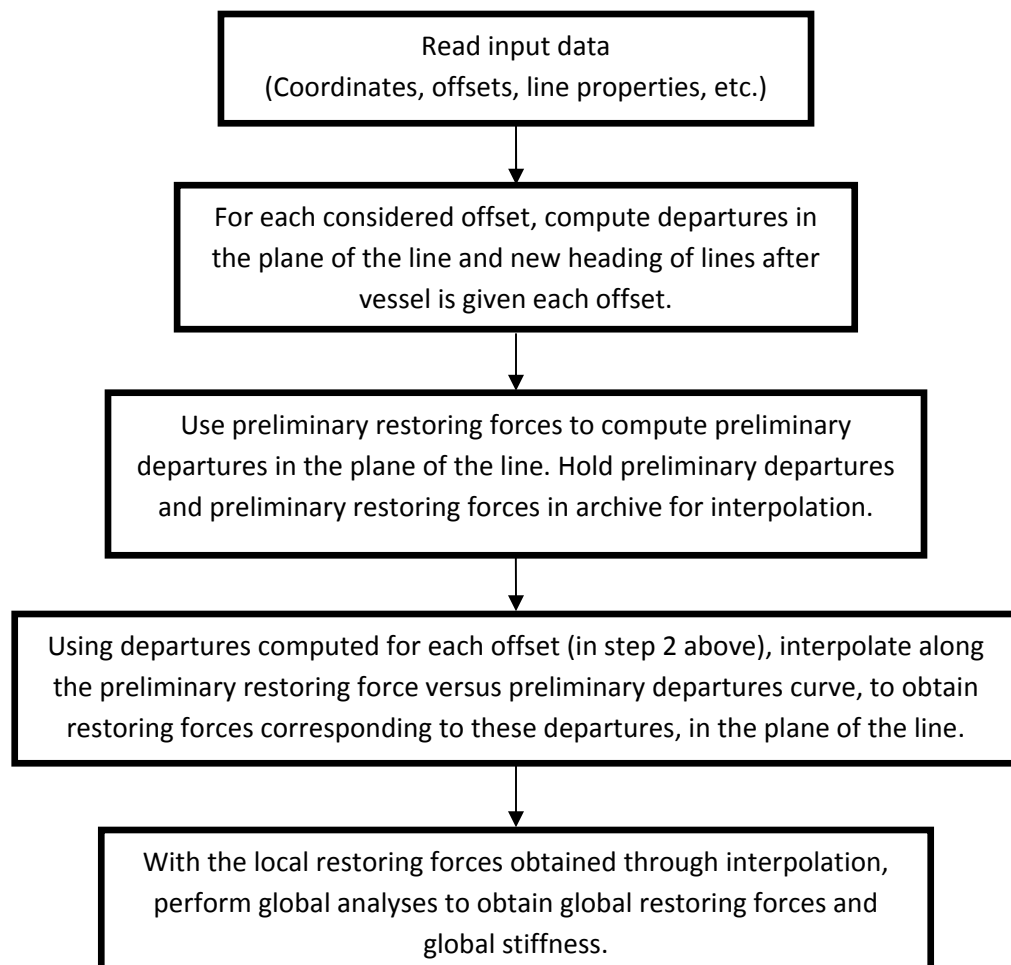


Fig. 3.5: A summary of the computation procedure in STAMOORSYS

The computation procedure just described is depicted in fig. 3.5. It is important to explore each step in the algorithm in detail, beginning with the reading of input data. Given that the user interface for STAMOORSYS is hosted in a spreadsheet, input data is entered into the spreadsheet cells in an orderly array. On execution of the static analysis using the controls on the user interface, the Visual Basic macros in Excel call-in the input data from the spreadsheet, and perform the coded operations.

To calculate the departures in the plane of the lines for each given offset, several offset cases are considered. STAMOORSYS considers a total of 4 different cases, each of which typically differs in coordinates from the other. STAMOORSYS regards the center of the platform at the zero-offset position of the vessel as the origin of the global coordinate system, and all coordinate inputs are in Cartesian coordinates. A parallel body-fixed coordinate system has its origin at the center of the platform. In general, the expression for calculating the departure of the i^{th} mooring line is:

$$D_i = \sqrt{\left(X_i \pm X_{off} \pm X_{fp_i}\right)^2 + \left(Y_i \pm Y_{off} \pm Y_{fp_i}\right)^2} \quad (3.38)$$

In eqn. (3.38) X_i is the x-coordinate of the anchor relative to the global coordinate system, X_{off} is the x-coordinate of the given offset on the vessel relative to the global coordinate system, and X_{fp_i} is the x-coordinate of the fairlead relative to the body-fixed coordinate system at the center of the platform. The subscript “ i ” is the line number index. It is clear from eqn. (3.38) that the magnitude and direction of the given offsets affect the resulting departure. The different offset cases considered are given in the following bullets, and case 1 is illustrated in fig. 3.6.

- Case 1: $X_{off} = 0, Y_{off} = 0$

- Case 2: $X_{off} = 0, Y_{off} > 0$
- Case 3: $X_{off} > 0, Y_{off} = 0$
- Case 4: $X_{off} > 0, Y_{off} > 0$

STAMOORSYS has no restrictions on the locations of lines 1 through 8. However, the program assumes that all fairleads have the same elevation and that all anchor points have the same depth. An additional restriction is that for any line which has one of its anchor coordinates as zero, STAMOORSYS assumes the corresponding fairlead coordinate in that direction to be zero, for that line. So for line 2 for instance in the 8-line set-up shown on the right of fig. 3.6, because the x-coordinate of the anchor relative to the center of the platform is $X_2 = 0$, STAMOORSYS will assume that its fairlead attachment point will be $X_{fp_2} = 0$.

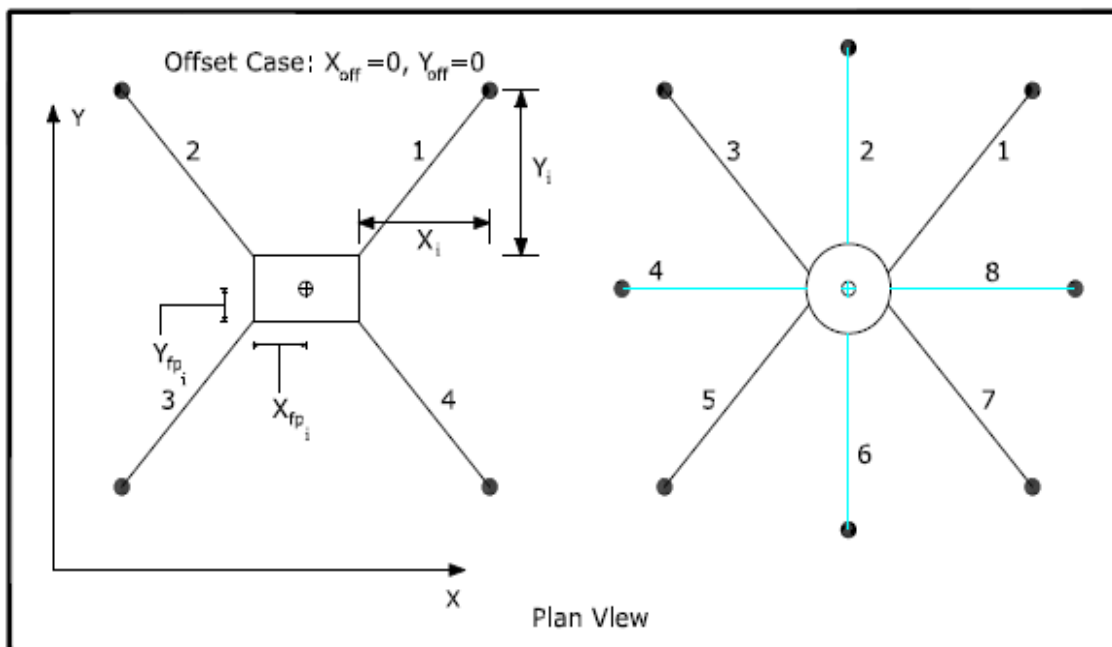


Fig. 3.6: Sample layout of 4-line and 8-line system for zero offset case

As mentioned earlier, computing the preliminary departures to be used in interpolation for restoring forces is an iterative process. For STAMOORSYS the numerical iteration process (fig. 3.7) depends on the fairlead elevation as the specified known quantity. It is important to emphasize the distinction between adjustable parameters in the numerical analysis and the adjustable design parameters used to optimize the design. The numerical computation uses the most sensitive parameters of the quasi-static simulation to adjust the configuration of the mooring lines, in search for the equilibrium configuration. These sensitive parameters are the length of line on the seafloor or the angle which the mooring line makes as it comes in contact with the seafloor. Adjusting either of these parameters by small amounts until the computed fairlead elevation is close enough to the given fairlead elevation is the major numerical strategy.

On the other hand, to optimize the design of the statically equivalent mooring system, one must consider the physical properties (submerged weight per unit length, length, and axial stiffness) of the mooring line segments and the coordinates of the anchor relative to the center of the platform. However, different combinations of design parameters may increase or reduce computation times, depending on the probability of attaining static equilibrium with the selected properties.

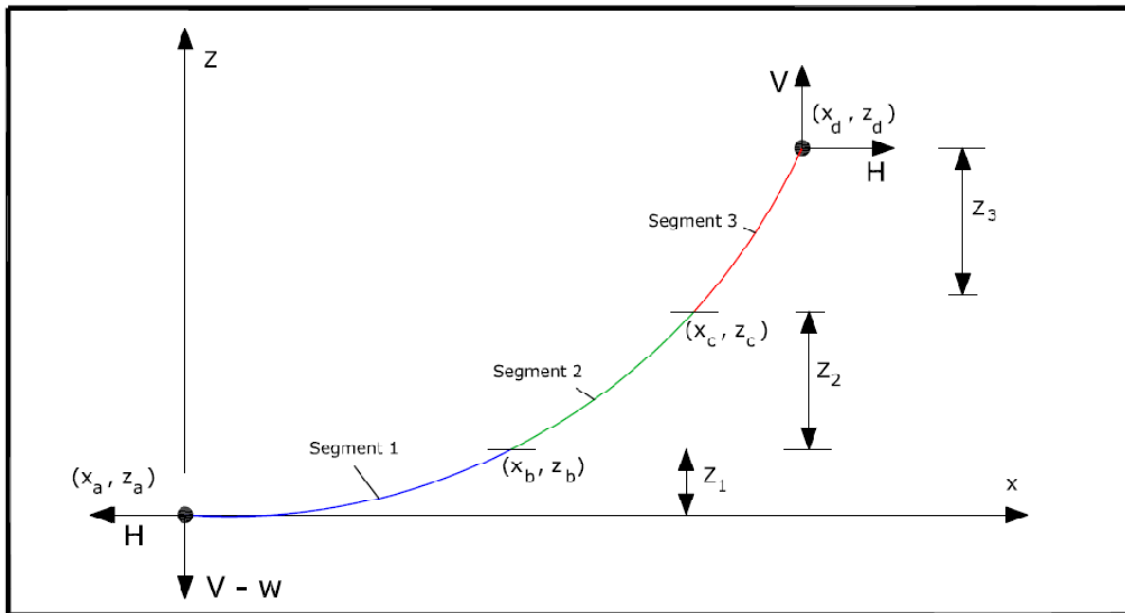


Fig. 3.8: Simple sketch of 3-segment mooring line

A sketch of a 3-segment mooring line is shown in fig. 3.8. Limiting configurations of a three-segment single line mooring system are shown on figs. 3.9 through 3.14. The conditional statements depicted in fig. 3.7 are written to search through the configurations displayed in figs. 3.9 through 3.14 for a coinciding scenario, within which the sensitive parameters of the quasi-static simulation are adjusted.

In the STAMOORSYS set-up and design pages, the parameter labeled 'numerical increment value in iteration' is the amount by which either the length of line on the sea floor or the angle which the line makes with the sea floor will be adjusted in the search for the equilibrium configuration. A value of 0.01 (feet or meter, or radian) is the recommended default value for analysis in STAMOORSYS. A value smaller than the recommended value will yield more accurate results but at the cost of simulation time.

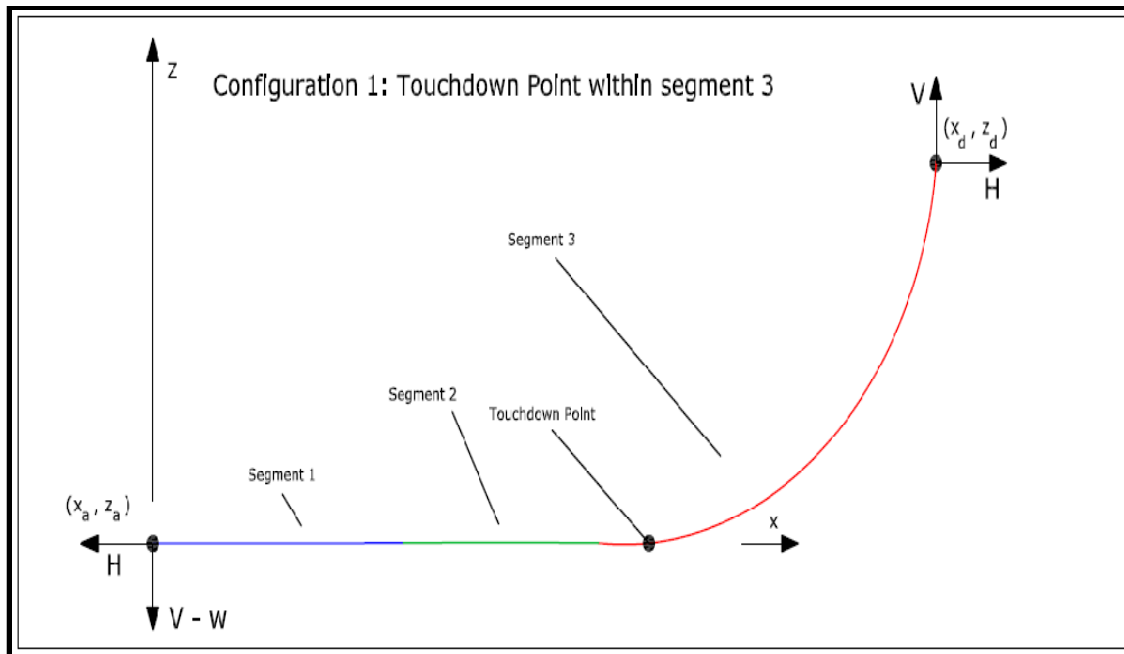


Fig. 3.9: Equilibrium configuration found with touchdown point within segment 3

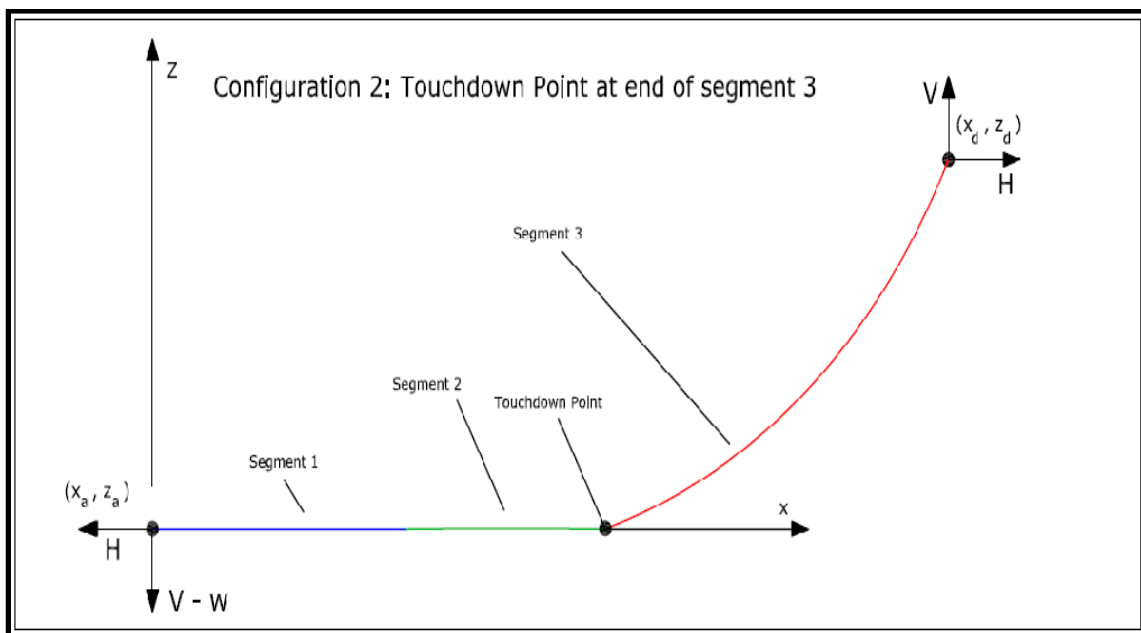


Fig. 3.10: Equilibrium configuration with touchdown point at end of segment 3

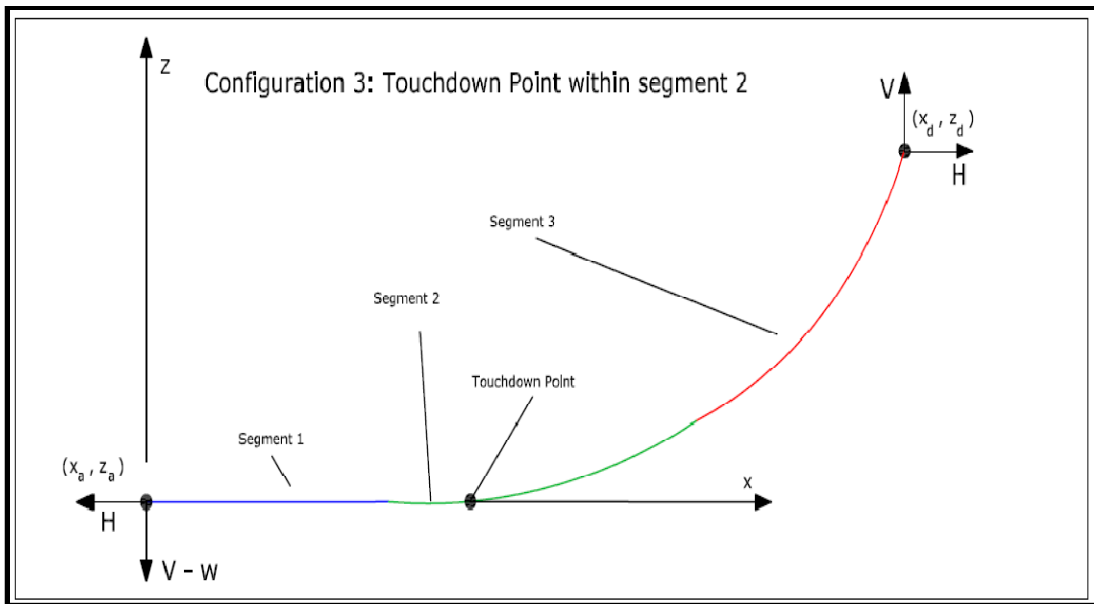


Fig. 3.11: Equilibrium configuration found with touchdown point within segment 2

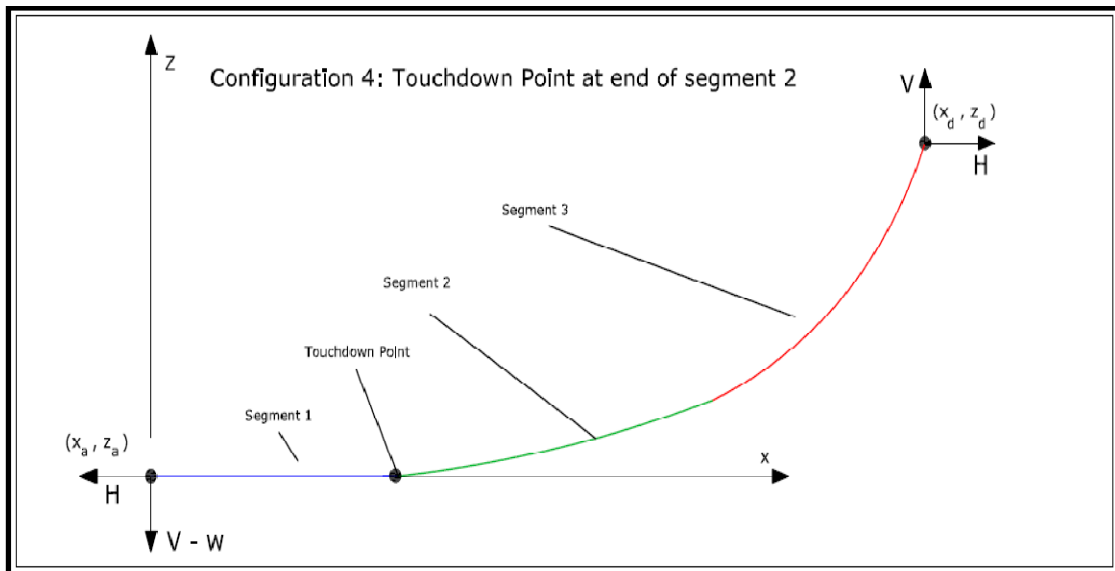


Fig. 3.12: Equilibrium configuration with touchdown point at end of segment 2

It is important to mention that figs. 3.9 to 3.14 are mildly exaggerated. For more of the mooring line to be suspended, the floating vessel must move through some offset distance. These figures are only directed at illustrating the

configuration of the mooring line when the touchdown point is at different locations.

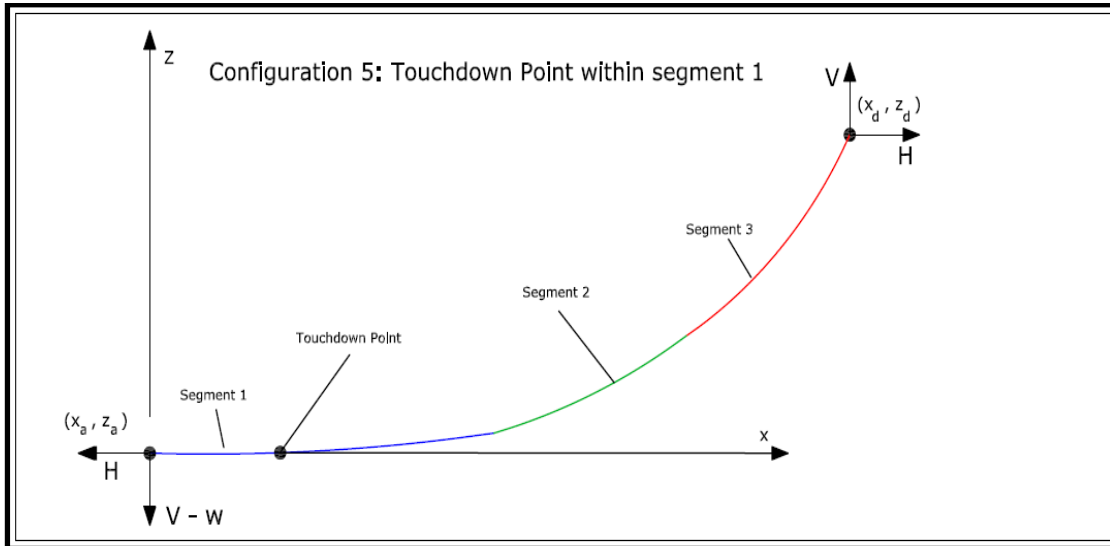


Fig. 3.13: Equilibrium configuration found with touchdown point within segment 1

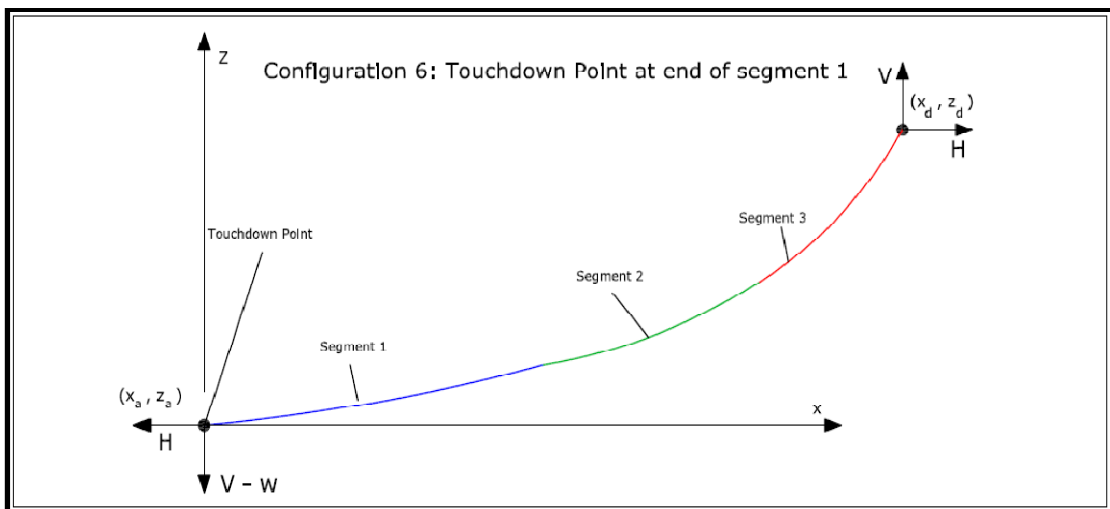


Fig. 3.14: Equilibrium configuration with touchdown point at end of segment 1

Obtaining the restoring forces in the plane of each line is done with linear interpolation. At this point, one may question the use of linear interpolation on a curve that may in some cases be of a different (higher) order. In the formulation

of STAMOORSYS, one approach which was contemplated in an effort to overcome this problem is the use of regression analysis on each resulting curve, to obtain the equation relating plotted parameters. The challenge in using this approach is to justify the order of the polynomial used in the regression analysis. For a given resulting curve, if the variables are related by a polynomial of higher degree than that used in the regression analysis, then the errors which will be incurred will most likely be significant. A safer (i.e. one with lower possibility of large errors) approach would be to assume the continuous curve to be a piecewise continuous function. Discretizing the function into very small linear functions validates linear interpolations between the end points of each small segment. Although greater interpolation accuracy can be achieved by fitting a polynomial through these very close points (especially along the steep section of the restoring force versus departure curve), wrong interpolated values can be obtained along the flat section of the curve as illustrated in fig. 3.15. It then follows that the greater the number of small discrete linear functions, the greater the accuracy of the interpolation process.

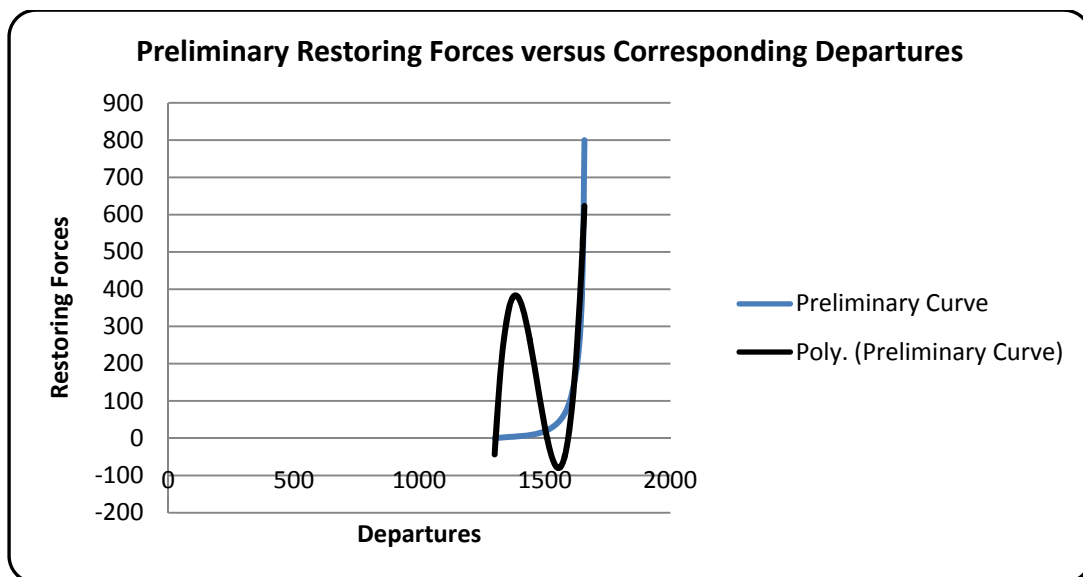


Fig. 3.15: Challenge in using higher order interpolation in STAMOORSYS

To ensure that the linear interpolation process yields accurate results, the error between two values of restoring force obtained for the same departure by using two sets of points is calculated. Figure 3.16 depicts the process of verifying the accuracy of the interpolation. The first set of points (x_1, y_1) and (x_2, y_2) are used to interpolate for y_{i-2} , with a known value of x_i . This interpolation is repeated using (x_3, y_3) and (x_4, y_4) with the same known x_i to obtain y_{i3-4} . The percentage difference between y_{i-2} and y_{i3-4} is computed; a difference of up to 5% indicates that interpolation is inaccurate, otherwise the value of y_{i-2} is adopted as the interpolated restoring force corresponding to a departure of x_i .

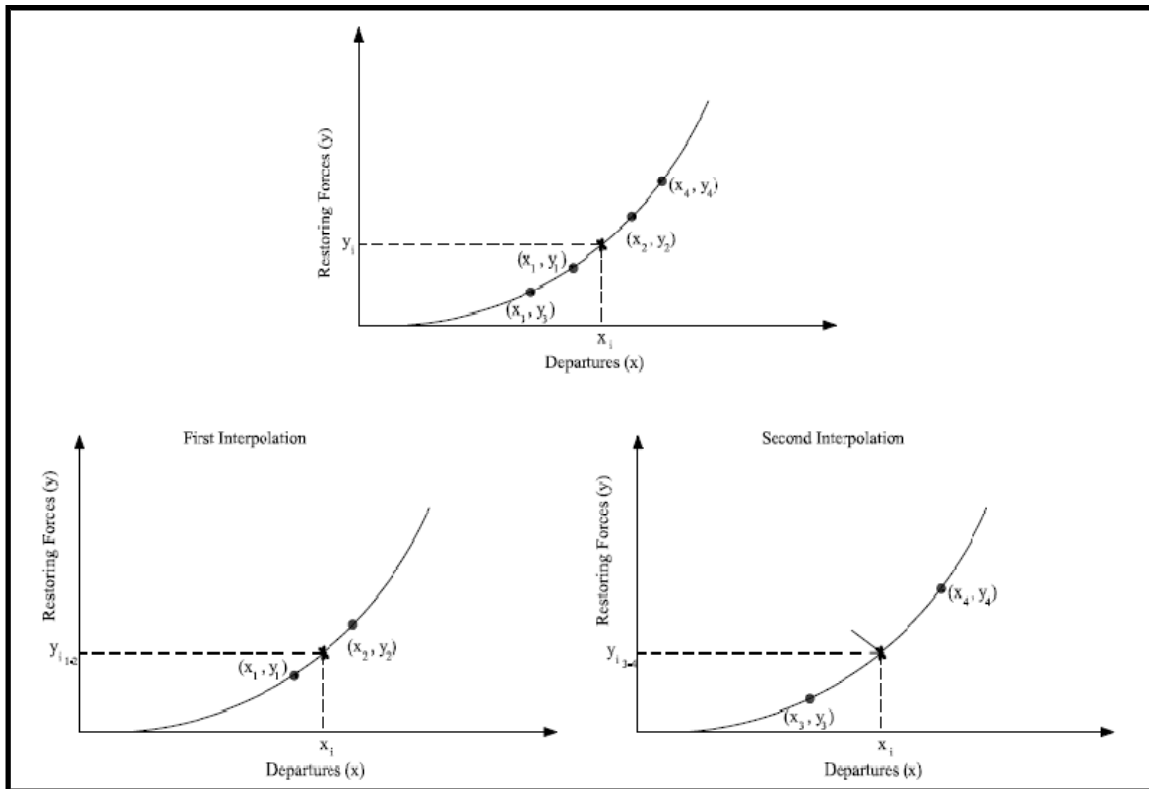


Fig. 3.16: Verification of linear interpolation accuracy

Once the restoring forces in the plane of each line have been obtained through the interpolation process, the principles of statics are applied to resolve the

forces into their different components, and the global forces on the vessel are then computed in each axis. For any arrangement of mooring lines (such as in fig. 3.17), the horizontal global forces on the floating vessel can be computed using eqns. (3.39) and (3.40).

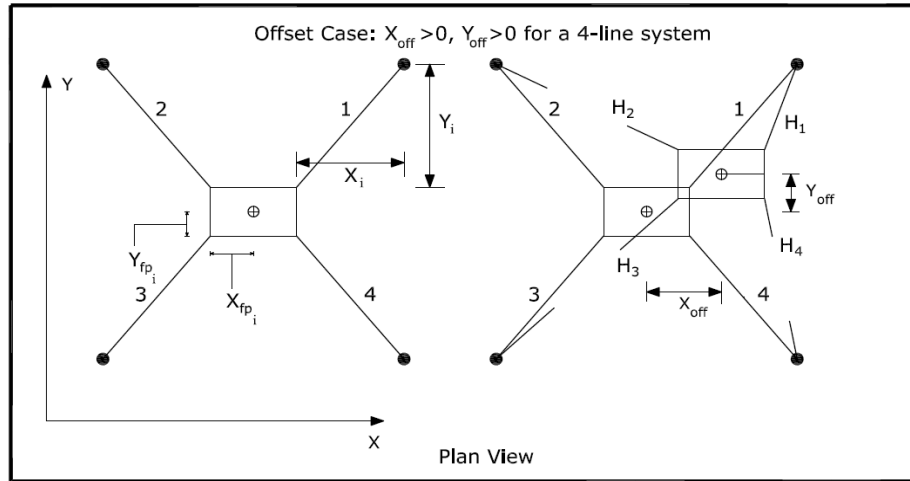


Fig. 3.17: A 4-line mooring system with $X_{off} > 0, Y_{off} > 0$ offset

$$\sum F_x = \sum_{i=1}^n H_i \cos \theta_i \quad (3.39)$$

$$\sum F_y = \sum_{i=1}^n H_i \sin \theta_i \quad (3.40)$$

where $n = 1, 2, \dots, 8$ and $\theta_i = \tan^{-1}\left(\frac{Y_i}{X_i}\right)$ after the vessel has moved to the new offset position.

Each given offset produces corresponding global restoring forces on the vessel. The global stiffness is a measure of the change in the global forces with respect to distance (offset). Considering that the offsets specified by the user may not always be in constant increments or reductions, computing the slopes (stiffness) along the global restoring force versus offset curves requires a scheme that handles unequal offsets effectively. Finite difference expressions presented in

Yang [29] are used in computing the global stiffness. The forward difference formula is applied to the first point, and the backward difference formula is applied to the last point. For intermediate points, the central difference expression is used in computing the stiffness. Denoting the global stiffness by K the global stiffness in the horizontal axes can therefore be written as:

$$K_x = \frac{dF_x}{dx} \quad (3.41)$$

$$K_y = \frac{dF_y}{dy} \quad (3.42)$$

For the first point on the x -axis curve, the forward difference expression is:

$$\frac{dF_x}{dx} = \frac{\Delta x_1^2 [F_{x_{i+1}} - F_{x_{i+2}}] + 2\Delta x_1 \Delta x_2 [F_{x_{i+1}} - F_{x_i}] + \Delta x_2^2 [F_{x_{i+1}} - F_{x_i}]}{\Delta x_1 \Delta x_2 (\Delta x_1 + \Delta x_2)} \quad (3.43)$$

The central difference formula applied to intermediate points on the x -axis curve is:

$$\frac{dF_x}{dx} = \frac{\Delta x_{i-1}^2 [F_{x_{i+1}} - F_{x_i}] + \Delta x_i^2 [F_{x_i} - F_{x_{i-1}}]}{\Delta x_i \Delta x_{i-1} (\Delta x_i + \Delta x_{i-1})} \quad (3.44)$$

The backward difference is computed on the x -axis curve using the formula:

$$\frac{dF_x}{dx} = \frac{\Delta x_8^2 [F_{x_{i-2}} - F_{x_{i-1}}] + 2\Delta x_8 \Delta x_9 [F_{x_i} - F_{x_{i-1}}] + \Delta x_9^2 [F_{x_i} - F_{x_{i-1}}]}{\Delta x_8 \Delta x_9 (\Delta x_8 + \Delta x_9)} \quad (3.45)$$

Equations (3.43) to (3.45) are similarly applied to the y -axis curves to compute the stiffness along the y -axis. In case the reader is pondering why the subscripts in the backward difference expression are “8” and “9”, STAMOORSYS plots the global restoring force versus offset curves using a total of 10 points, which

implies a total of 9 segments between the points. The 8th and 9th segments are used in computing the backward difference for the stiffness at the 10th point.

3.3 A DESCRIPTION OF THE FEATURES IN STAMOORSYS

There are six sheets or pages in STAMOORSYS, and these are:

- Problem Set-Up Page
- Line Response Plot Page
- Restoring Forces Plot Page
- Design Page
- Calculations Page
- Bank Page

PROBLEM SET-UP PAGE

The problem set-up page is the first page to be used in STAMOORSYS for any project. It holds input values of mooring line properties and coordinates of anchors and fairleads. The page also holds the known offsets for which the static responses of the mooring system will be investigated. Only information for the number of lines to be used is required; so for a 4-line analysis only inputs for four lines are needed.

Unacceptable entries into STAMOORSYS will return error messages prompting the user of the acceptable range or formats of inputs. An instance is when the input of an offset is a negative number. The error prompt shown in fig. 3.18 pops-up to inform the user of the acceptable inputs.

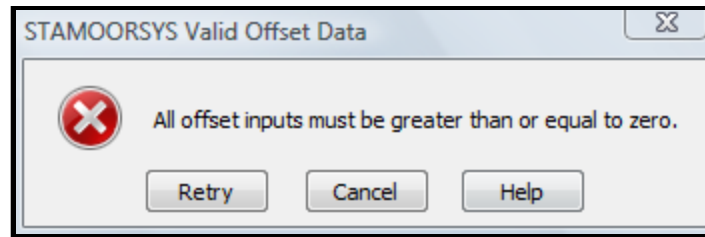


Fig. 3.18: STAMOORSYS offset error prompt

Some other discrepancies may lead to unusual run times, where the simulation just keeps running as though it will never come to an end. In such situations, the user may cancel the run using the escape key on the computer key pad, and check through the inputs for inconsistent entries.

The code execution buttons are arranged in the order of usage during the analysis. Seven (7) code execution controls are available to the user in the set-up page, and these are shown on fig. 3.19. Amongst all seven controls, the last three ('Reset', 'Clear Inputs', and 'Clear Outputs') implement tasks which are less computational compared to the first four controls ('Run Statics', 'Global Forces', 'Update Lines 1 to 4' and 'Update Lines 5 to 8').

A vital component to note is the 'Check!' related to the computed departures and preliminary departures (shown under the code execution buttons). After running statics (by clicking 'Run Statics') this check must read 'Range is ok' before further analysis is continued. Otherwise, the check cell will read 'Extend Range'.

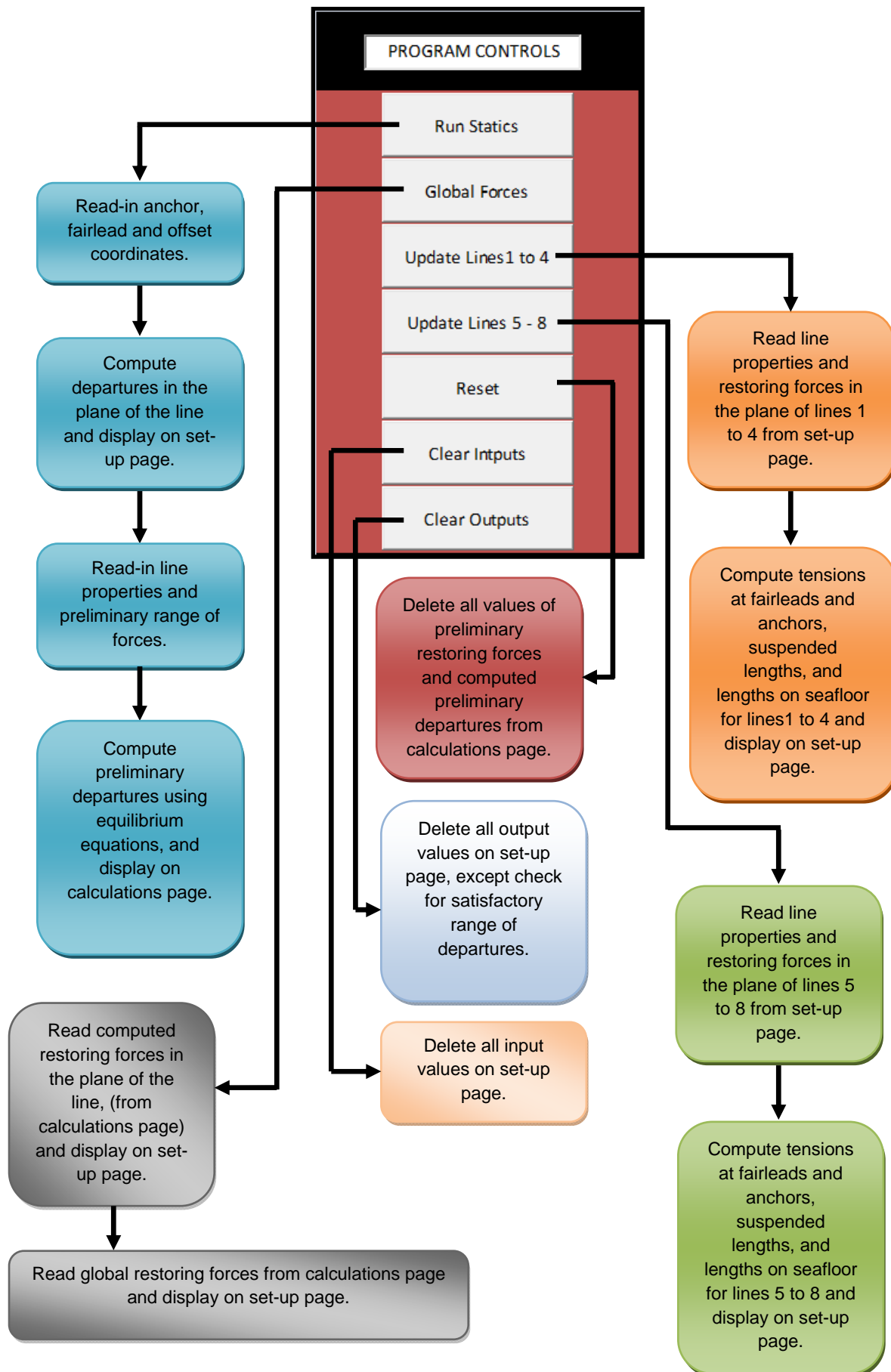


Fig. 3.19: Tasks executed by different user controls in set-up page

Table 3.2: Display of check related to preliminary and computed departures

THIS CHECK MUST BE SATISFIED.		THIS CHECK MUST BE SATISFIED.	
Min. Departure (ft)	2899.23	Min. Departure (ft)	2899.23
Max. Departure (ft)	3878.36	Max. Departure (ft)	3878.36
Min. Prel. Departure (ft)	1552.03	Min. Prel. Departure (ft)	1552.03
Max. Prel. Departure (ft)	4172.14	Max. Prel. Departure (ft)	1919.05
Check!	Range is ok	Check!	Extend Range

} A
} B

Table 3.3: Sample display of check related to grid resolution

THIS CHECK MUST BE SATISFIED.	
Points with \geq 5% Error	0

The 'Extend Range' feedback suggests that the limits of the preliminary restoring forces (in the input section) must be extended. In Table 3.2, the quantities labeled "A" are the minimum and maximum values of the departures computed for all lines used in analysis. That is, all the given offsets have been applied to the lines used in the design simulation and their respective departures are computed. The lowest departure amongst all the lines considering all given offsets displays as the "Min. Departure", while the maximum departure of all the computed departures displays as the "Max. Departure". On the other hand, the set of quantities labeled "B" in Table 3.2 are the minimum and maximum values of all the departures computed from the preliminary range of restoring forces specified by the user. Each restoring force is used in computing a departure; and so for the number of points specified by the user, a set of restoring forces and departures is produced. STAMOORSYS then finds the minimum departure computed using the preliminary restoring forces and displays it as "Min. Prel. Departure" while it displays the maximum value computed as "Max. Prel. Departure".

An additional check to confirm the adequacy of grid (distance between two points along the preliminary restoring force versus preliminary departure curve) resolution is performed by STAMOORSYS. As shown in Table 3.3, if the grid resolution is adequate the program displays “0” for the number of points with $\geq 5\%$ error. Otherwise, the number of points for which the interpolation error is $\geq 5\%$ is reported. If the designer so wishes, the resolution can be increased or reduced by adjusting the value for “number of points” and / or “maximum value of force” in the preliminary range of restoring forces. A full view of the STAMOORSYS problem set-up page can be found in appendix A1 of this document.

LINE RESPONSE PLOTS PAGE

On this page, the static response plots from analysis performed in the problem set-up page are shown. In other words, the static responses on this page will only change automatically when analysis is performed in the problem set-up page. The graphs displayed are suspended line lengths versus departures, lengths of line on sea floor versus departures, tensions at anchor versus departures, and tensions at fairlead versus departures for all lines (1 to 8). Only the plots corresponding to the number of lines for which analysis is performed will be automatically updated.

RESTORING FORCES PAGE

Here the restoring forces in all the lines are plotted against the departures of the lines in their respective planes. These plots are tied to the set-up page only, and as such will only be updated when analysis is performed on the set-up page. Being able to view the plots in the presented array makes it fairly easy to compare the restoring forces in each line. If a symmetric arrangement of mooring lines is used in analysis, similar characteristics should be seen in plots

of corresponding mooring lines separated by the axis of symmetry. With the arrangement of the restoring force plots, any inconsistencies in the plots can be readily observed by the designer.

DESIGN PAGE

In the design page, only the input variables to be varied in the design process are shown. Other input variables such as the vertical distance from fairlead to seabed, coordinates of fairleads, inclination angles and offsets will be pulled from the set-up page while the code is executing. It is therefore necessary to ensure that these input variables are entered adequately in the set-up page to represent the system undergoing design. The primary statics results of interest (global restoring forces and global stiffness), computed departures and the fairlead tensions in all the lines are shown on the same page. Again, the code execution buttons are arranged in the order of analysis. As in the set-up page, after running statics (by clicking 'Run Statics') the check related to the departures must read 'Range is ok' before further analysis is continued. Otherwise, the check cell will read 'Extend Range'. The 'Extend Range' feedback suggests that the limits of the preliminary restoring forces (in the input section) must be extended.

As can be observed in fig. 3.20, the design page is only one user control short compared to the problem set-up page. While striving toward ensuring an efficient design process, it is important that the user controls to be clicked while performing the design is kept at the minimum possible. Unlike in the set-up page, the global restoring forces are computed by the 'Run Statics' control in the design page. Having two separate controls to update statics for the first four lines and the last four lines could be an advantage if the designer is working with four mooring lines or less. This essentially takes away the simulation / run time that would be consumed if all eight lines were used in design.

An additional capability of the design page is to accept and incorporate the target plots of global restoring forces which the designer intends to match as closely as possible. Being able to visually compare equivalent design results with the target (design) outputs from the prototype system is a necessary capability that informs the designer of the proximity of the equivalent mooring system's trend of response to that of the target system. The most appreciable fact about the STAMOORSYS design page is that it is self-contained, such that the designer stays within the same page until the optimally designed statically equivalent mooring system is achieved. Appendix A2 shows the design page.

It is worthy of mention that STAMOORSYS can also be used to determine static horizontal force versus offset curves for prototype mooring systems, if such systems satisfy the constraints embedded in STAMOORSYS (i.e. maximum of eight lines, identical lines with maximum of three segments, equal fairlead elevations and equal anchor depths).

CALCULATIONS PAGE

The calculations page contains raw intermediate results kept within the spreadsheet to relieve the macro codes of some of the burden in the code execution process. Given that the user controls which are hosted by Visual Basic macros in Microsoft Excel have limits to the capacity of procedures (codes) they can execute, there is greater potential of the software 'crashing' or often getting 'stuck' in a 'not responding' mode if the codes embedded are right around the limits of their capacity. Therefore performing some of the computations in the calculations page both reduces the risk of crashing the program, and the computation time required by the macros.

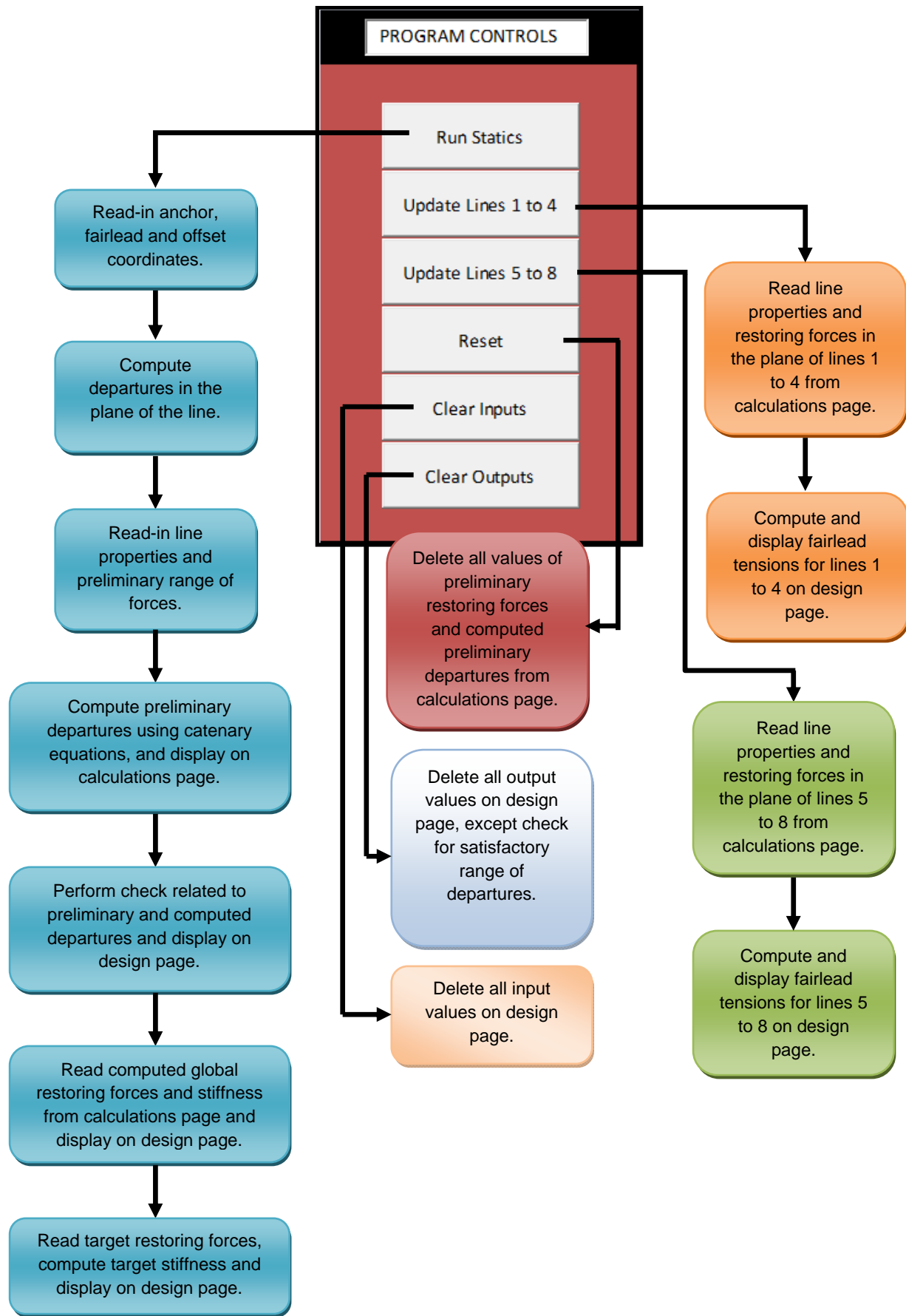


Fig. 3.20: Tasks executed by different user controls in design page

The user does not require any activity in the calculations page. This page only interfaces with the design and problem set-up pages as necessary. No interactive interface exists therein, even though the arrangements of the computation cells are such that the designer / user understands their contents. It is recommended though, that the user makes no attempt to effect any changes in the calculations page, as this may disrupt a routine in STAMOORSYS. The spreadsheet cells in the calculations page contain a lot of formulae, any of which if deleted will adversely affect the working of the program.

BANK PAGE

Within the bank page calculations are performed and computed results are sent to the 'calculations' page. Like the calculations page, no user interface exists in the bank page. The major computations performed are the interpolations to assess the adequacy of the grid resolution used in analysis. Again, performing these calculations in the spreadsheet is intended to reduce the amount of code to be executed by user controls in STAMOORSYS.

A summarized recommended approach to the use of STAMOORSYS is given in fig. 3.21.

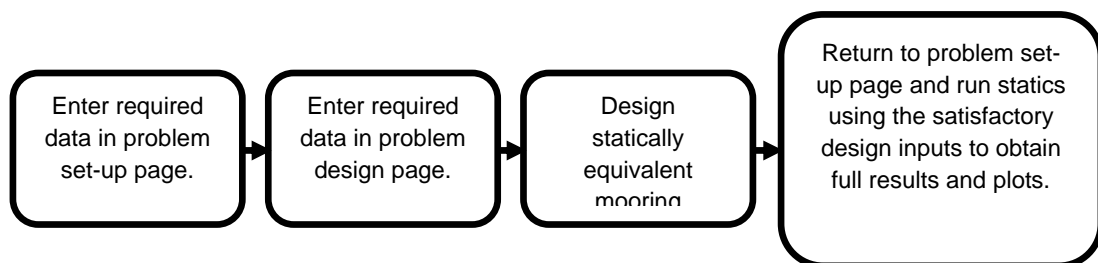


Fig. 3.21: Summary of recommended approach in the use of STAMOORSYS

The additional usefulness of the Set-up, Line Response and Restoring Forces pages is that they make the debugging process for STAMOORSYS a lot easier and they provide additional detailed information for comparison with other codes.

Being able to visualize line configurations for each line used in the simulation offers a good opportunity to verify that the results portray static behaviors that are physically correct.

CHAPTER IV

APPLICATION OF STAMOORSYS IN DESIGN OF STATICALLY EQUIVALENT MOORING SYSTEMS

4.1 ANALYSIS OF SINGLE LINE MOORING SYSTEMS USING STAMOORSYS, Orcaflex AND LINANL

Although the major purpose for STAMOORSYS is the design of statically equivalent spread mooring systems, it is important to demonstrate first that the software analyzes single line mooring systems with acceptable accuracy since the underlying principles used in analyzing spread mooring systems are essentially those of single line systems. LINANL is a static mooring analysis program with the capability of handling multi-component lines. This section discusses three hypothetical cases which are analyzed using STAMOORSYS and LINANL, and one realistic case using Orcaflex, STAMOORSYS and LINANL.

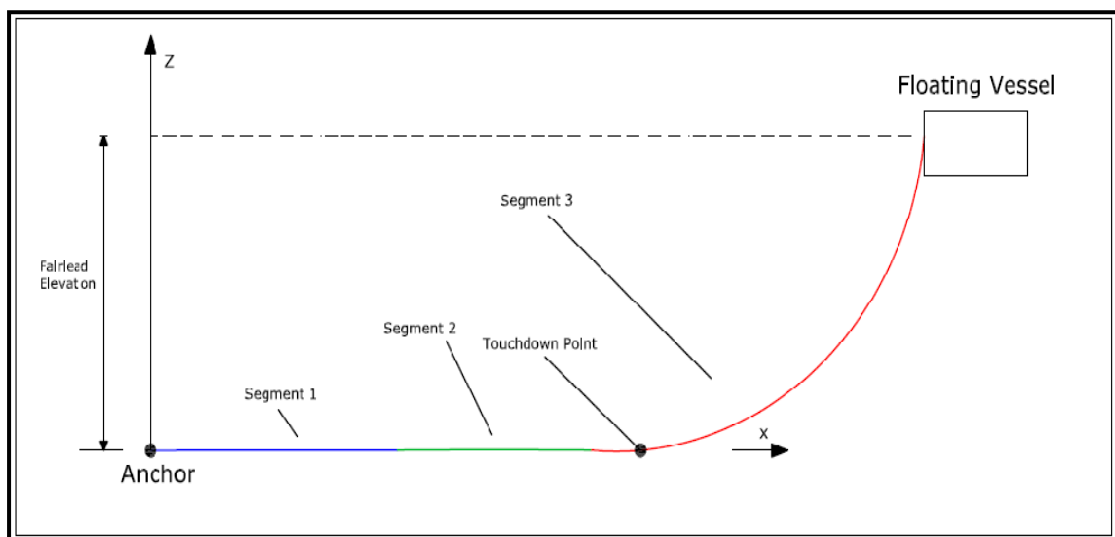


Fig. 4.1: Problem set-up for single line analysis using STAMOORSYS, Orcaflex and LINANL

A floating structure is moored using a 3-segment mooring line as shown in fig. 4.1, with the line properties shown in Table 4.1 for each case of analysis. The

task is to compute the departure of the vessel, under specified values of restoring forces. Tensions at the anchor and fairlead, suspended lengths and lengths on the sea floor computed for each given restoring force are also obtained from both programs and compared. Recalling that the process of computing the departure in STAMOORSYS is numerical, the value of the computed fairlead elevation at convergence (for each applied force) is also obtained and compared to actual fairlead elevation. At least for STAMOORSYS, this comparison (actual versus computed fairlead elevations) in a sense measures the accuracy of the numerical computations. Each test case is a result of varying one or more properties (length, axial stiffness, weight per unit length) of the mooring line. In the first three test cases the fairlead elevation is maintained at a value of 1500 ft above the anchor.

The vessel is subjected to ten different restoring forces ranging from 20000 lbs to 200,000 lbs at increments of 20,000 lbs. Figures 4.2 through 4.6 show the comparison between STAMOORSYS and LINANL for the first case.

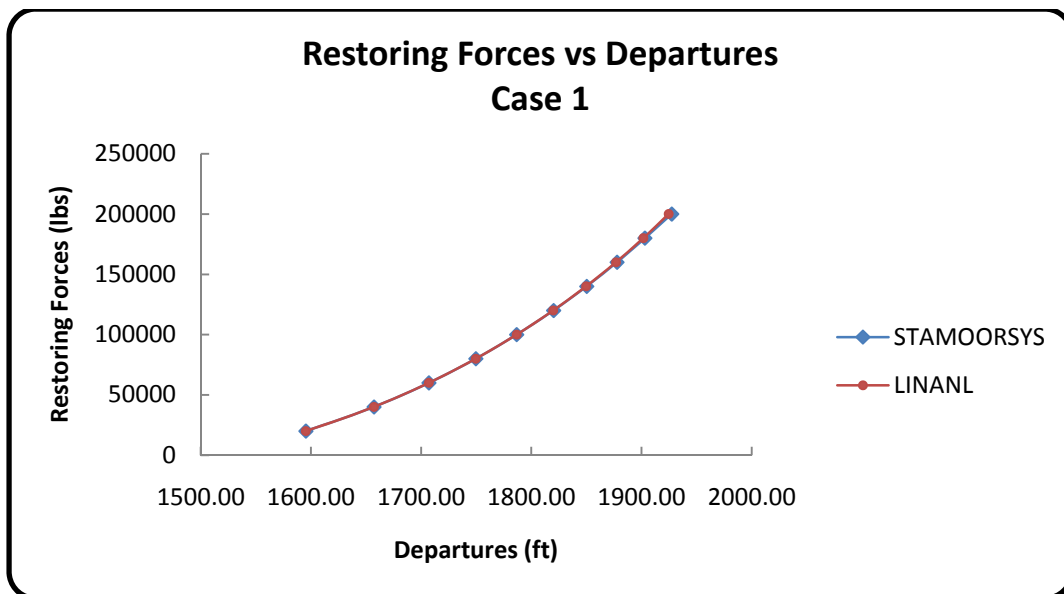


Fig. 4.2: Restoring forces versus departures for Case 1

Table 4.1: Mooring line properties for hypothetical problem

Segment No.	Length (ft)	EA (lbs)	Weight per unit length (lbs/ft)
CASE 1			
1	1000	21E010	800
2	1000	21E010	800
3	1000	21E010	800
CASE 2			
1	1000	21E010	800
2	550	21E010	800
3	650	21E010	800
CASE 3			
1	1000	21E010	800
2	550	205E09	700
3	650	21E010	800

Tables 4.2, 4.3 and 4.4 show the results for the three test cases, respectively. For each case percentage differences between the outputs from LINANL and STAMOORSYS are computed. These differences are very small, indicating a strong agreement between both programs.

Table 4.2: Results for single line analysis, Case 1

Res. Forces (lbs)	Departures (ft)			Fairlead Tensions (lbs)			Tensions at Anchor (lbs)			Suspended lengths (ft)			Lengths on the sea floor (ft)			Fairlead Elevations (ft)		
	STAMOORSYS	LINANL	% Difference	STAMOORSYS	LINANL	% Difference	STAMOORSYS	LINANL	% Difference	STAMOORSYS	LINANL	% Difference	STAMOORSYS	LINANL	% Difference	STAMOORSYS	Actual	% Difference
20000	1595.39	1595.30	0.006	1219923.00	1220000.00	0.006	20000.00	19882.00	0.590	1524.70	1524.79	0.006	1475.30	1475.00	0.020	1499.91	1500.00	0.006
40000	1657.24	1657.10	0.008	1239925.37	1240000.00	0.006	40000.00	39884.00	0.290	1549.10	1549.20	0.006	1450.90	1450.80	0.007	1499.91	1500.00	0.006
60000	1707.08	1707.00	0.005	1259989.39	1260000.00	0.001	60000.00	59886.00	0.190	1573.20	1573.26	0.004	1426.80	1426.70	0.007	1499.99	1500.00	0.001
80000	1749.67	1749.50	0.010	1279942.56	1280100.00	0.012	80000.00	79888.00	0.140	1596.80	1596.99	0.012	1403.20	1403.01	0.014	1499.93	1500.00	0.005
100000	1786.67	1786.70	0.002	1299932.06	1300200.00	0.021	100000.00	99890.00	0.110	1620.10	1620.42	0.020	1379.90	1379.50	0.029	1499.92	1500.00	0.005
120000	1820.24	1819.80	0.024	1319946.09	1320300.00	0.027	120000.00	119890.00	0.092	1643.10	1643.58	0.029	1356.90	1356.42	0.035	1499.94	1500.00	0.004
140000	1850.31	1849.70	0.033	1339973.65	1340500.00	0.039	140000.00	139890.00	0.079	1665.80	1666.49	0.041	1334.20	1333.51	0.052	1499.97	1500.00	0.002
160000	1877.84	1876.90	0.050	1359925.08	1360800.00	0.064	160000.00	159900.00	0.063	1688.10	1689.19	0.065	1311.90	1310.80	0.084	1499.91	1500.00	0.006
180000	1903.09	1901.80	0.068	1379949.92	1381100.00	0.083	180000.00	179900.00	0.056	1710.20	1711.69	0.087	1289.80	1288.31	0.116	1499.94	1500.00	0.004
200000	1927.47	1924.70	0.144	1399959.77	1401600.00	0.117	200000.00	199900.00	0.050	1732.00	1734.03	0.117	1268.00	1256.98	0.869	1499.96	1500.00	0.003

Table 4.3: Results for single line analysis, Case 2

Res. Forces (lbs)	Departures (ft)			Fairlead Tensions (lbs)			Tensions at Anchor (lbs)			Suspended lengths (ft)			Lengths on the sea floor (ft)			Fairlead Elevations (ft)		
	STAMOORSYS	LINANL	% Difference	STAMOORSYS	LINANL	% Difference	STAMOORSYS	LINANL	% Difference	STAMOORSYS	LINANL	% Difference	STAMOORSYS	LINANL	% Difference	STAMOORSYS	Actual	% Difference
20000	795.40	795.53	0.016	1219923.96	1220000.00	0.006	20000.00	19946.00	0.27	1524.70	1524.77	0.005	675.30	675.20	0.015	1499.91	1500.00	0.006
40000	857.24	857.22	0.002	1239925.37	1239900.00	0.002	40000.00	39948.00	0.13	1549.10	1549.12	0.001	650.90	650.88	0.003	1499.91	1500.00	0.006
60000	907.08	907.23	0.017	1259989.39	1259900.00	0.007	60000.00	59950.00	0.08	1573.20	1573.05	0.010	626.80	626.95	0.024	1499.99	1500.00	0.001
80000	949.08	949.87	0.083	1279942.56	1279800.00	0.011	80000.00	79952.00	0.06	1596.80	1596.58	0.014	603.20	603.42	0.036	1499.93	1500.00	0.005
100000	986.97	987.31	0.034	1299932.06	1299600.00	0.026	100000.00	99954.00	0.05	1620.10	1619.74	0.022	579.90	580.26	0.062	1499.92	1500.00	0.005
120000	1020.24	1020.80	0.055	1319946.09	1319500.00	0.034	120000.00	119960.00	0.03	1643.10	1642.53	0.035	556.90	557.47	0.102	1499.94	1500.00	0.004
140000	1050.31	1051.00	0.066	1339973.65	1339300.00	0.050	140000.00	139960.00	0.03	1665.80	1664.97	0.050	534.20	535.03	0.155	1499.97	1500.00	0.002
160000	1077.84	1078.70	0.080	1359925.08	1359100.00	0.061	160000.00	159960.00	0.03	1688.10	1687.09	0.060	511.90	512.92	0.199	1499.91	1500.00	0.006
180000	1103.09	1104.20	0.101	1379949.92	1378900.00	0.076	180000.00	179960.00	0.02	1710.20	1708.88	0.077	489.80	491.12	0.269	1499.94	1500.00	0.004
200000	1126.47	1127.90	0.127	1399959.77	1398700.00	0.090	200000.00	199960.00	0.02	1732.00	1730.39	0.093	468.00	469.62	0.346	1499.96	1500.00	0.003

Table 4.4: Results for single line analysis, Case 3

Res. Forces (lbs)	Departures (ft)			Fairlead Tensions (lbs)			Tensions at Anchor (lbs)			Suspended lengths (ft)			Lengths on the sea floor (ft)			Fairlead Elevations (ft)		
	STAMOORSYS	LINANL	% Difference	STAMOORSYS	LINANL	% Difference	STAMOORSYS	LINANL	% Difference	STAMOORSYS	LINANL	% Difference	STAMOORSYS	LINANL	% Difference	STAMOORSYS	Actual	% Difference
20000	797.39	795.11	0.286	1165011.68	1166900.00	0.162	20000.00	19946.00	0.27	1524.80	1527.11	0.151	675.20	672.89	0.342	1499.94	1500.00	0.004
40000	860.84	856.86	0.462	1185195.19	1188500.00	0.279	40000.00	39948.00	0.13	1549.40	1553.47	0.263	650.60	646.53	0.626	1499.95	1500.00	0.003
60000	912.04	906.79	0.576	1205454.14	1209800.00	0.361	60000.00	59950.00	0.08	1573.70	1579.14	0.346	626.30	620.86	0.869	1499.98	1500.00	0.001
80000	955.69	949.44	0.654	1225693.55	1230900.00	0.425	80000.00	79952.00	0.06	1597.60	1604.15	0.410	602.40	595.85	1.087	1499.91	1500.00	0.006
100000	993.77	986.96	0.685	1246059.13	1251800.00	0.461	100000.00	99954.00	0.05	1621.30	1628.55	0.447	578.70	571.40	1.261	1499.97	1500.00	0.002
120000	1027.77	1020.60	0.698	1266378.33	1272600.00	0.491	120000.00	119960.00	0.03	1644.60	1652.37	0.472	555.40	547.63	1.399	1499.94	1500.00	0.004
140000	1058.44	1051.10	0.693	1286718.95	1293100.00	0.496	140000.00	139960.00	0.03	1667.60	1675.66	0.483	532.40	524.34	1.514	1499.92	1500.00	0.005
160000	1086.28	1079.00	0.670	1307149.26	1313500.00	0.486	160000.00	159960.00	0.03	1690.40	1698.45	0.476	509.60	501.55	1.580	1500.00	1500.00	0.000
180000	1111.92	1104.80	0.640	1327500.00	1333800.00	0.475	180000.00	179960.00	0.02	1712.80	1720.78	0.466	487.20	479.22	1.638	1499.98	1500.00	0.001
200000	1135.63	1128.80	0.601	1347841.14	1354000.00	0.457	200000.00	199960.00	0.02	1734.90	1742.69	0.449	465.10	457.31	1.675	1499.95	1500.00	0.003

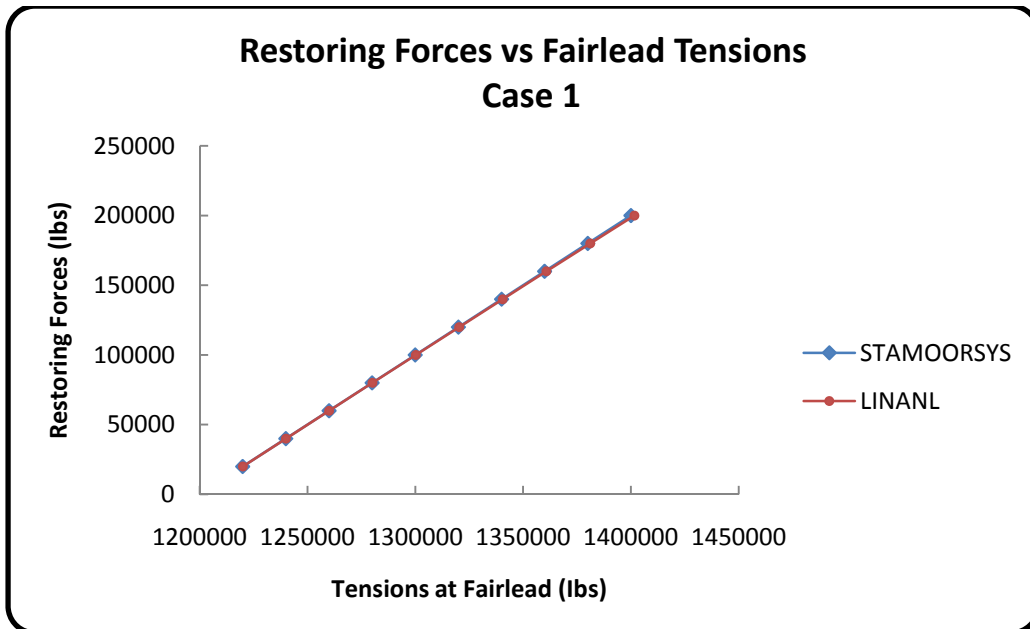


Fig. 4.3: Restoring forces versus fairlead tensions for Case 1

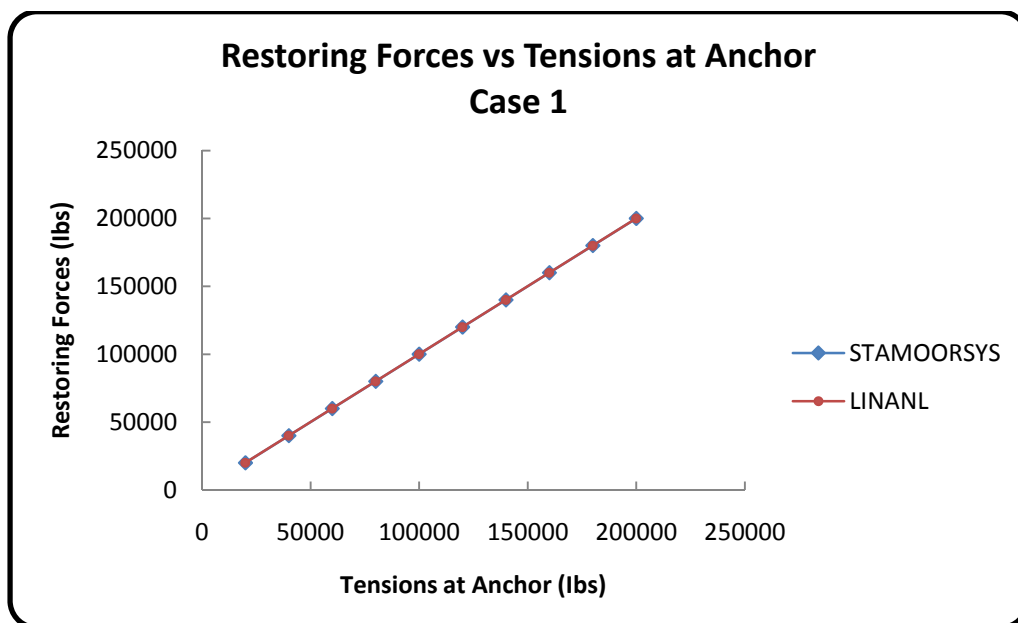


Fig. 4.4: Restoring forces versus tensions at the anchor for Case 1

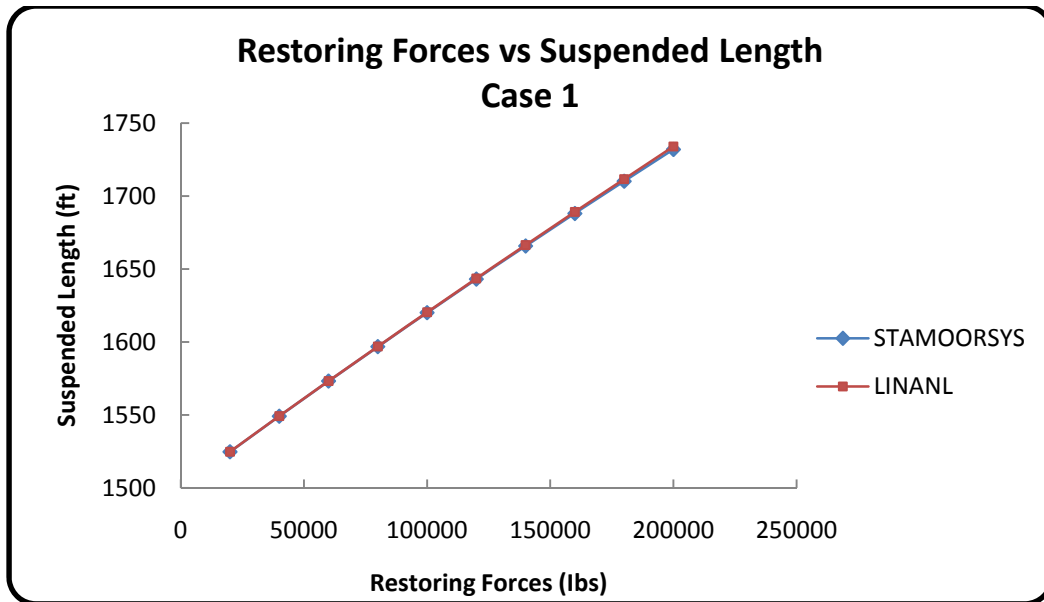


Fig. 4.5: Suspended lengths versus restoring forces for Case 1

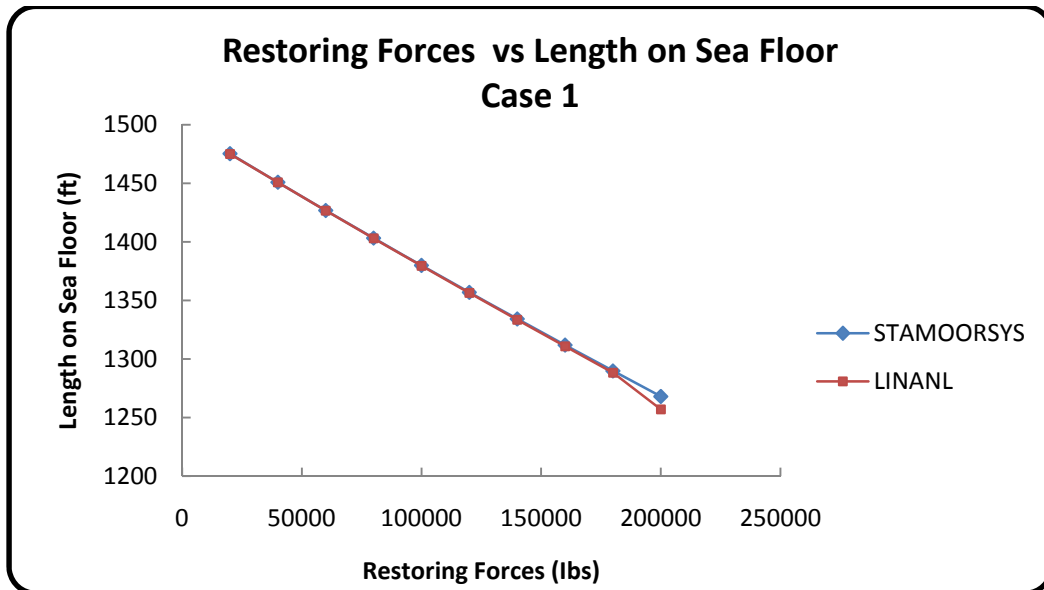


Fig. 4.6: Lengths on the sea floor versus restoring forces for Case 1

In fig. 4.6 a significant deviation is observed between LINANL and STAMOORSYS for the largest restoring force applied (200,000 lbs). A difference of 0.869% is calculated between both programs. The abrupt shift in the trend of

the LINANL curve suggests that the value computed for the force of 200,000 lbs is not indicative of equilibrium. Perhaps the iterative process in LINANL reached convergence with some significant error. It is important to mention that LINANL is coded to reach numerical convergence when the difference between the actual and computed fairlead elevations is within a specified error limit (such as $\leq 5\%$ of the actual fairlead elevation). Unfortunately, the user has no opportunity to select a convenient error limit for analysis while making inputs to LINANL. However, the differences in computed departures and tensions for both programs are very small.

Comparisons made between both programs for the second case are depicted in figs. 4.7 through 4.11. Computed departures, tensions and line configurations at equilibrium agree very strongly. The suspended lengths and lengths on sea floor computed by both programs show the results to be physically correct.

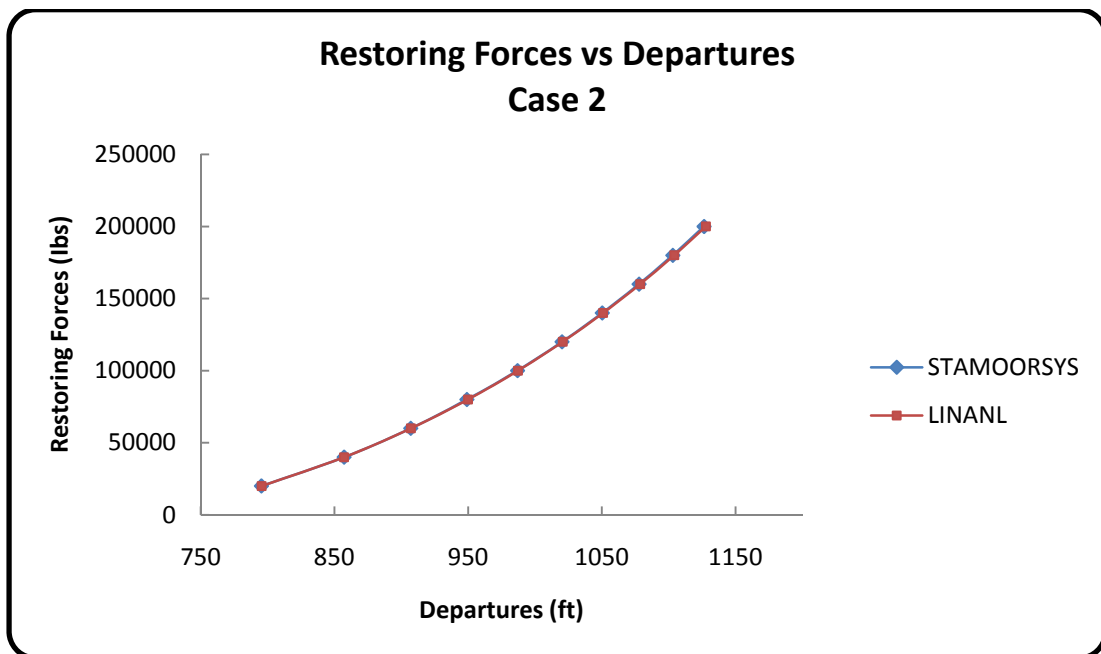


Fig. 4.7: Restoring forces versus departures for Case 2

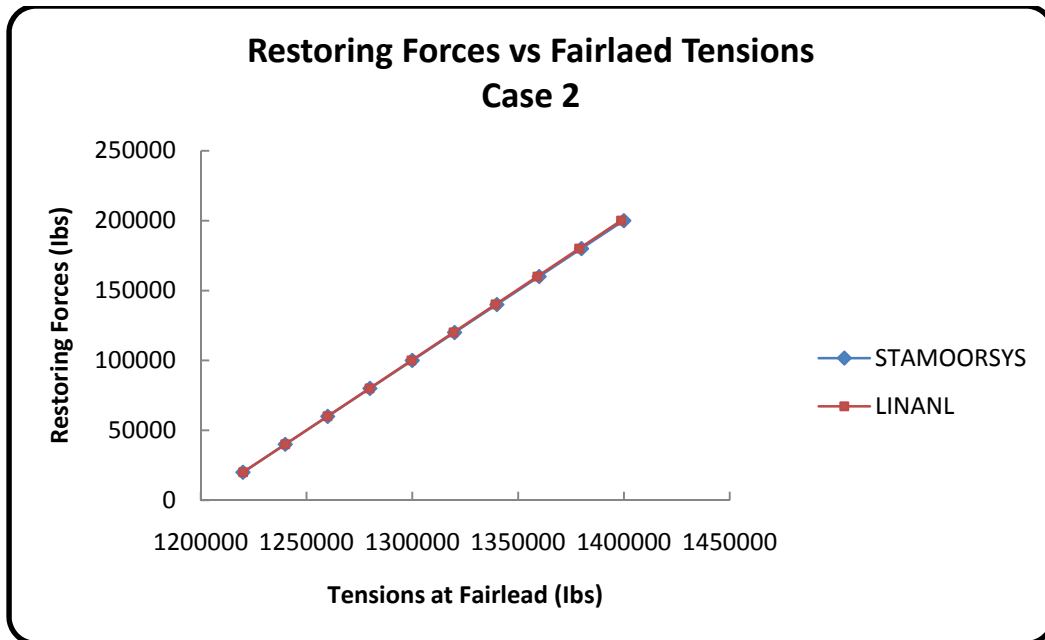


Fig. 4.8: Restoring forces versus fairlead tensions for Case 2

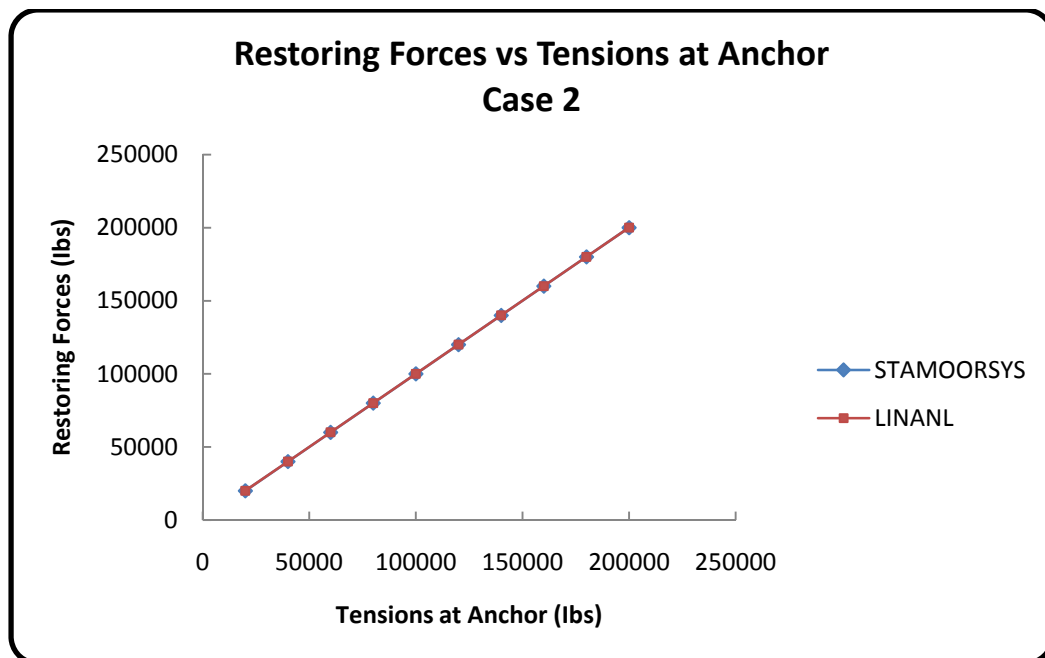


Fig. 4.9: Restoring forces versus tensions at the anchor for Case 2

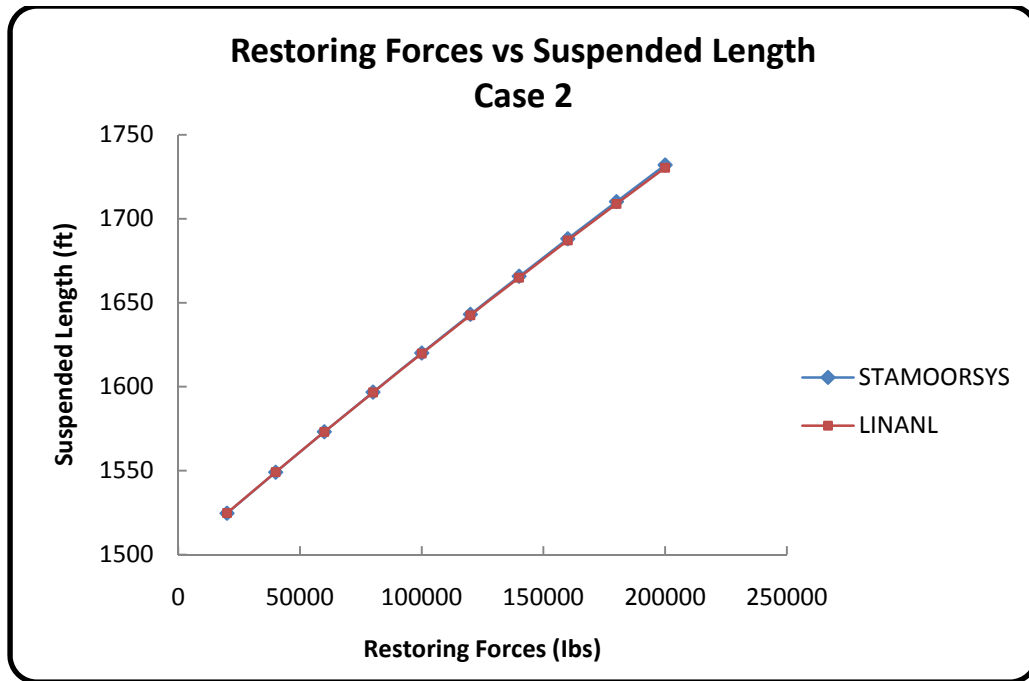


Fig. 4.10: Suspended lengths versus restoring forces for Case 2

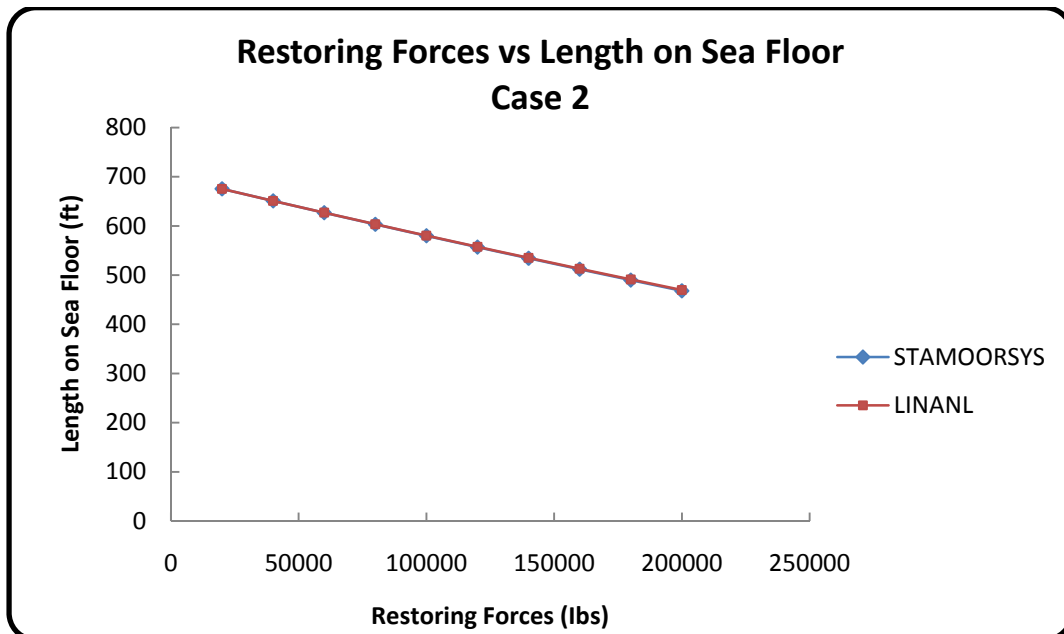


Fig. 4.11: Lengths on the sea floor versus restoring forces for Case 2

The third test case involves a second segment with a slightly lower axial stiffness (EA_0) than those in cases 1 and 2. LINANL is not designed to handle cases where the axial stiffness of any segment is representative of an extremely 'soft' segment. The program is mostly geared for lines with very high axial stiffness, and works very well if the stiffness is uniform in all segments. So for cases where axial stiffness of individual segments is remarkably different, the results produced by LINANL may be fairly inaccurate. Thus the reduction of axial stiffness of the second segment (case 3) is such that STAMOORSYS and LINANL can work within their intended scopes, beyond which there would be no basis for comparisons (figs. 4.12 through 4.16).

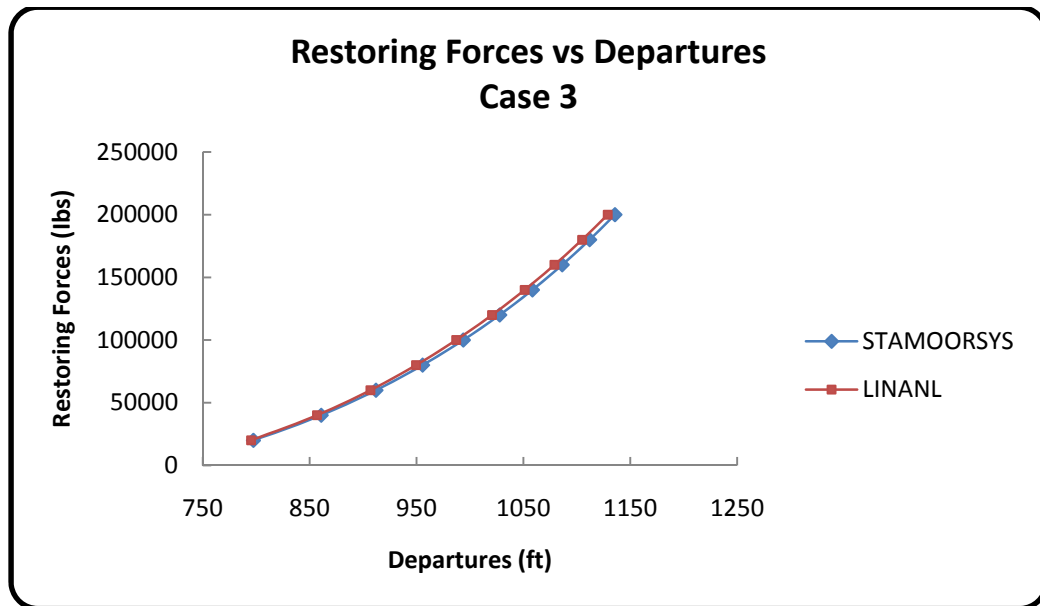


Fig. 4.12: Restoring forces versus departures for Case 3

Relative to the first and second cases, there are more significant differences in the computed departures, fairlead tensions and suspended lengths between LINANL and STAMOORSYS. It is logical to attribute these noticed deviations to the effect of the axial stiffness (EA_0) and / or weight per unit length, as these parameters are the only ones modified to make case 3 different from case 2. A comparison to a third program (Orcaflex) in case 4 offers more clarity to these

deviations. It is important to establish STAMOORSYS' capability to produce correct results for mooring lines with low axial stiffness (EA_0).

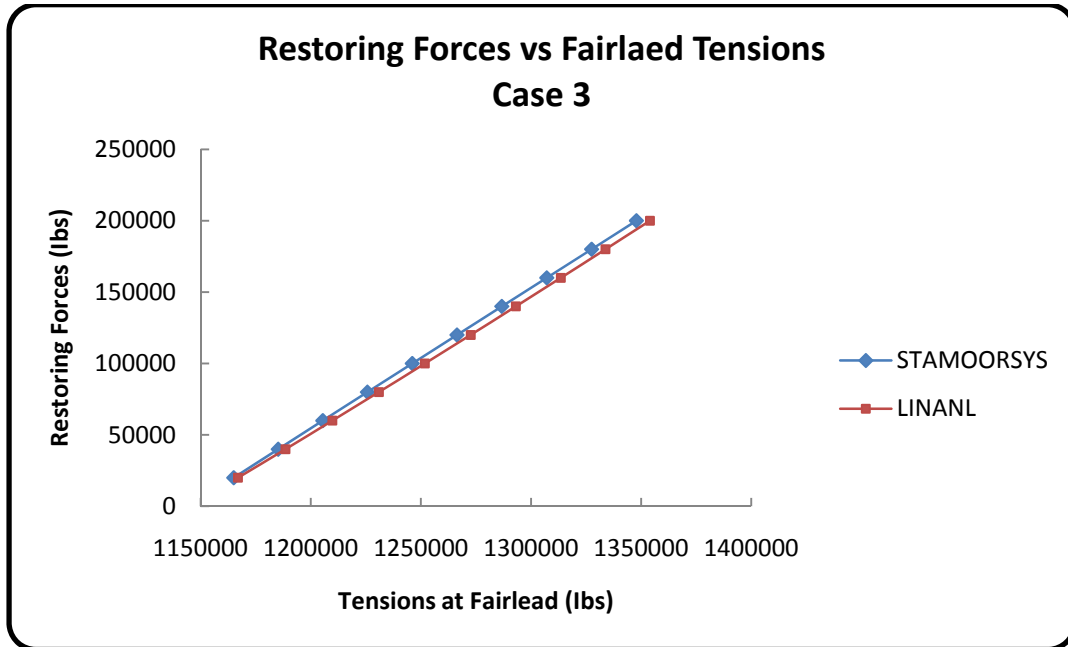


Fig. 4.13: Restoring forces versus fairlead tensions for Case 3

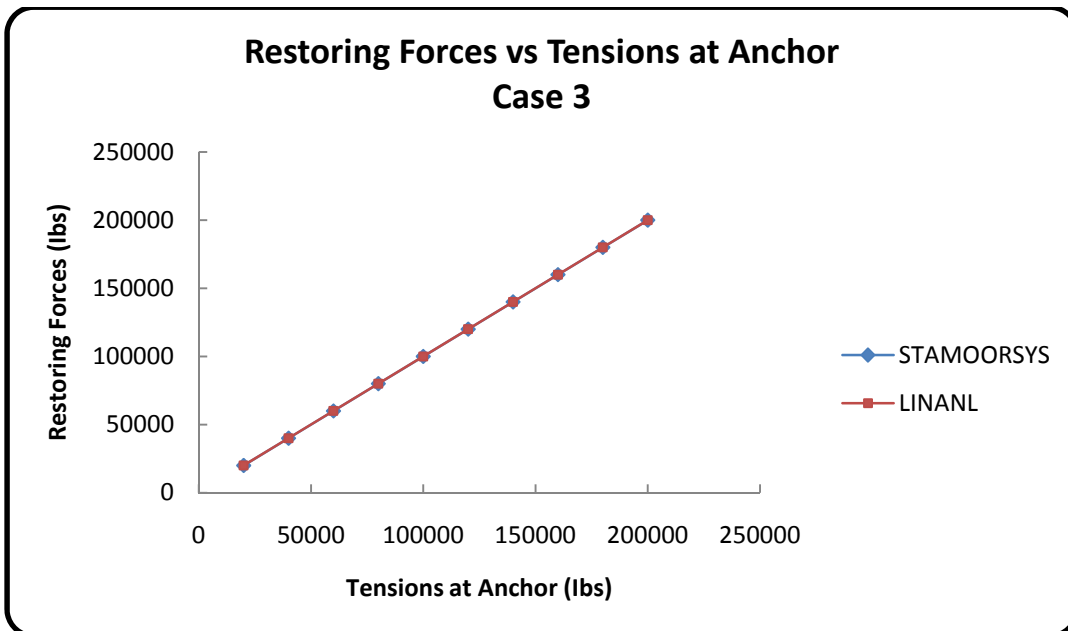


Fig. 4.14: Restoring forces versus tensions at the anchor for Case 3

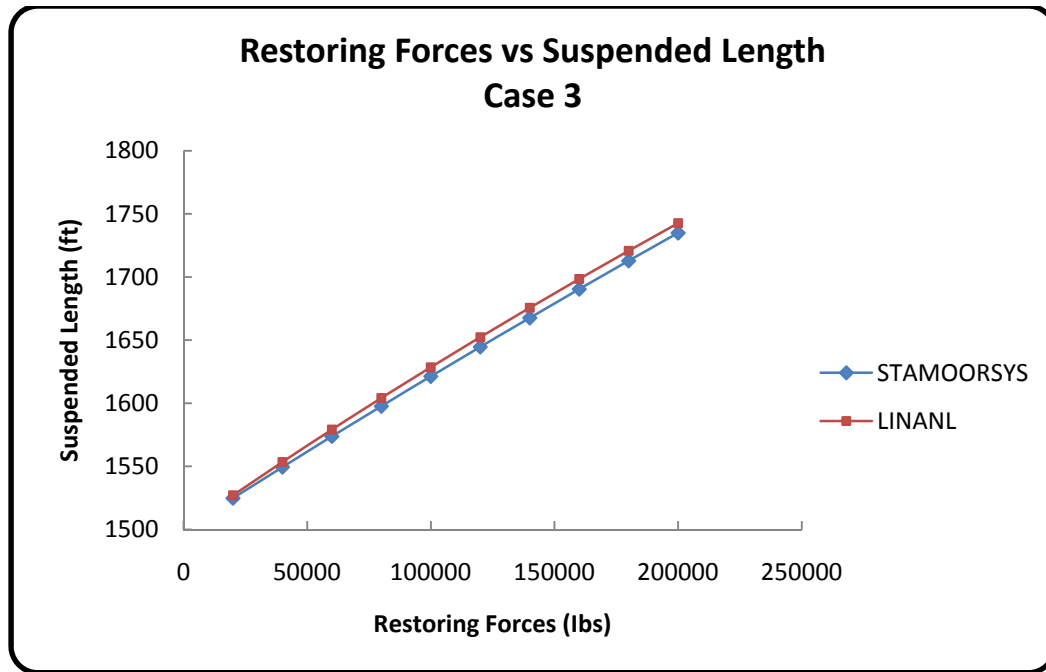


Fig. 4.15: Suspended lengths versus restoring forces for Case 3

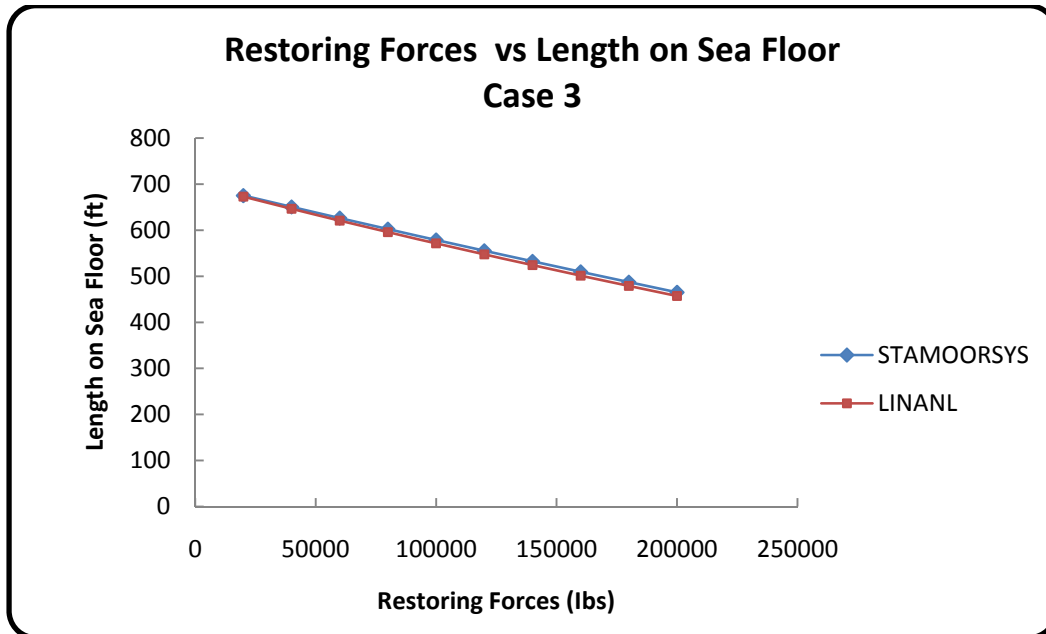


Fig. 4.16: Lengths on the sea floor versus restoring forces for Case 3

In general the comparisons between STAMOORSYS and LINANL for the first three cases are very close. Overall, the differences in computed values may be attributed to computational errors during numerical iterations. With the reason that the accuracy of the iterative solutions could be improved by the user in STAMOORSYS but not in LINANL, it is logical to suggest that the tolerance limit in LINANL is such that the iterative procedure does not converge with accurate values when large forces are applied to a line with relatively low axial stiffness.

A fourth case used in validating STAMOORSYS is considered, where a system is moored by a single line in a model test wave basin. The properties of the mooring system components are realistic for model test purposes (design of equivalent mooring systems). Table 4.5 summarizes the properties of the system components. Restoring forces used in analysis range from a minimum of 47500 lbs to a maximum of 2,892,400 lbs.

Table 4.5: Properties of mooring system components for test Case 4

SEGMENT	$EA_0(Ibs)$	$w(Ibs / ft)$	$L(ft)$	Fairlead Elevation (ft)
1	1.89E09	25	1684.7	1015.80
2	3.87E06	3042	201	
3	1.88E09	4135.40	15	

Using these values, single line analyses are performed with STAMOORSYS, LINANL and Orcaflex. One may ponder the non-use of Orcaflex in the validation test cases 1, 2 and 3 previously discussed. The availability of the program for this purpose is very limited as the only available license in the OTRC is shared by engineers working on design verification projects. Coupled with this fact, it is not so trivial to obtain local results from Orcaflex as it with LINANL. Knowledge

of how to use the software is required, and harvesting local results takes a relatively longer time compared to LINANL.

Single line analyses using the inputs in Table 4.5 produced the results displayed in figs. 4.17 and 4.18. The computed departures from all three programs fairly follow the same trend, over the range of restoring forces considered. The maximum percentage difference in departures computed using STAMOORSYS and Orcaflex is 0.36%. Between STAMOORSYS and LINANL, the maximum percentage difference is 1.70%. A significant deviation in computed departures is observed between LINANL and both STAMOORSYS and Orcaflex.

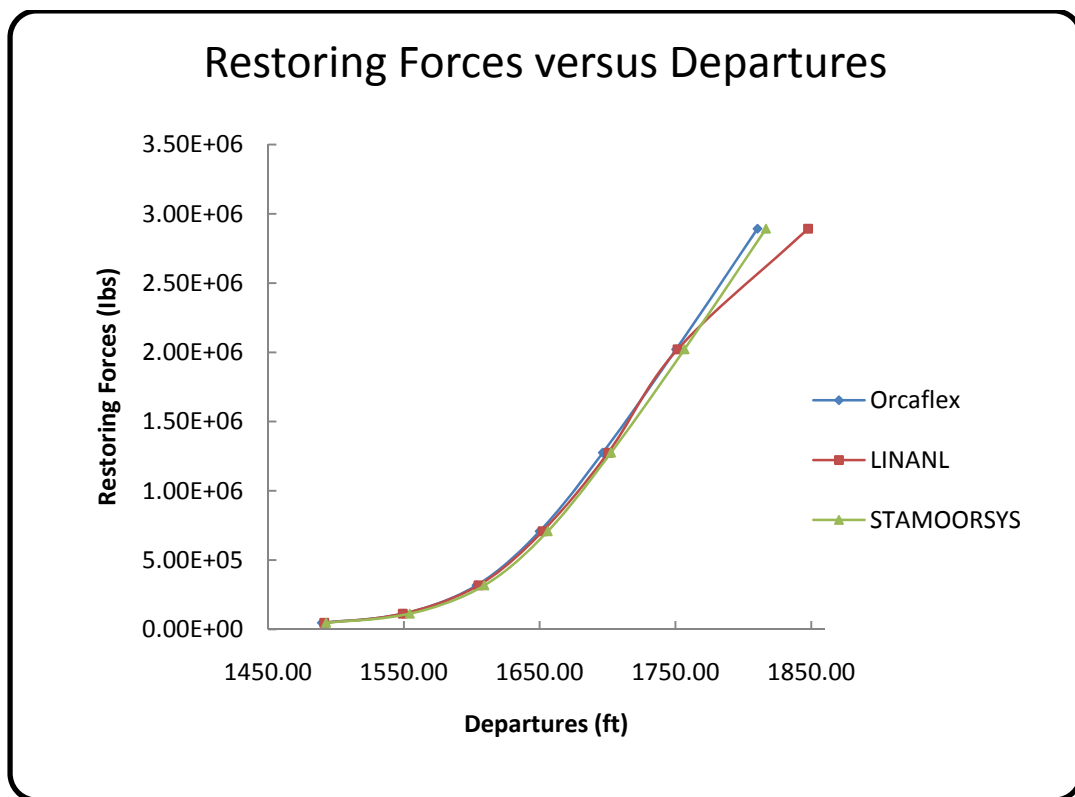


Fig. 4.17: Restoring forces versus departures for Case 4

Similar to fig. 4.6 in case 1, the deviation corresponds to the maximum force applied. For this force, Orcaflex and STAMOORSYS are in much stronger agreement. All three programs compute suspended lengths of 1900.7 ft (the

total length of the line) for all restoring forces applied. The departures obtained from all three programs are plotted against the fairlead tensions associated with them, in fig. 4.18. A more consistent agreement exists between STAMOORSYS and Orcaflex, than it does between LINANL and the other two programs. The curves suggest that STAMOORSYS is capable of producing correct results even for low axial stiffness (EA_0) and weights per unit length.

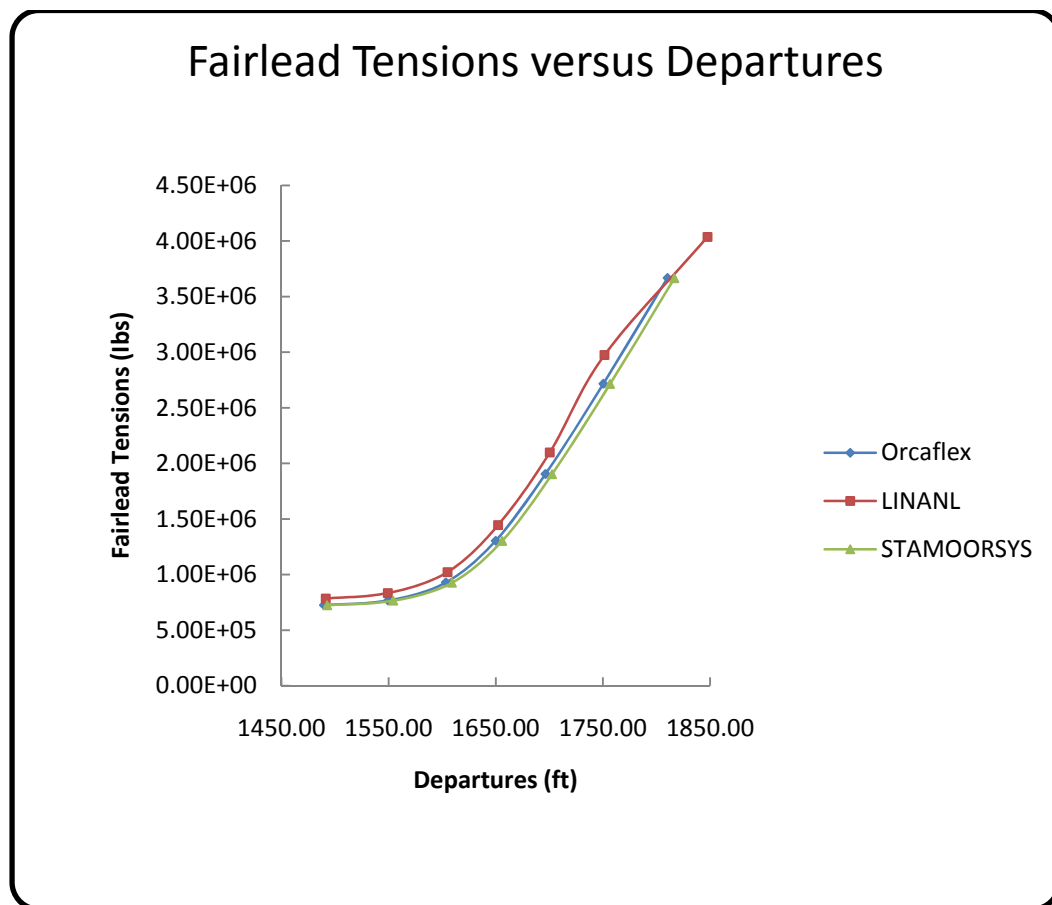


Fig. 4.18: Fairlead tensions versus departures for Case 4

Fairlead tensions computed by LINANL are slightly higher than those computed by STAMOORSYS and Orcaflex, and this deviation tends to increase as the departures (hence the forces) increase.

4.2 VALIDATION OF STAMOORSYS FOR STATIC GLOBAL ANALYSIS OF SPREAD MOORING SYSTEMS

Considering that the design of statically equivalent mooring systems ultimately leads to a comparison of results of static global analyses, it is necessary to validate STAMOORSYS using known results in this regard before an actual design case. This section discusses two validation cases, one of which is an example problem presented in Jones [5], where a spread mooring system is analyzed using MOORANL to obtain the horizontal global restoring forces on the floating vessel. MOORANL is a FORTRAN program for analysis of spread mooring systems. This example problem is repeated using STAMOORSYS and the results are compared. The second validation case is a comparison between STAMOORSYS and Orcaflex using equivalent mooring design results for a representative model floater. Using the unique combination of mooring system properties that led to a match (between prototype and equivalent) in the static global restoring force versus offset and global stiffness versus offset curves in Orcaflex, an effort is made to achieve the same match in STAMOORSYS.

First, consider a floating vessel with fairlead and anchor coordinates relative to the center of the floater as presented in Table 4.6. The floater is moored using four identical mooring lines. As presented in the example problem, each of the four lines is a single segment line with length of 1700 ft, uniform weight per unit length of 0.078 lbs / ft, and uniform axial stiffness (EA_0) of 200,000 lbs. The length of 1700 ft is mimicked in STAMOORSYS (because it handles only three-segment lines) as 200 ft of segment 1, 500 ft of segment 2 and 1000 ft of segment 3. The fairlead elevation relative to the sea bed / anchor point is 400 ft. For all three segments the same weights per unit length and axial stiffness as in MOORANL are input in STAMOORSYS to represent lines of uniform properties.

Table 4.6: Fairlead and anchor coordinates for example problem

LINE	FAIRLEAD COORDINATES		ANCHOR COORDINATES	
	X	Y	X	Y
1	50.00	75.00	1183.99	1208.99
2	-50.00	75.00	-1183.99	1208.99
3	-50.00	-75.00	-1183.99	-1208.99
4	50.00	-75.00	1183.99	-1208.99

Five horizontal offsets are applied to the vessel at a 45° heading to make the most loaded line in the system, line 3. The offsets range from 10 ft to 50 ft at increments of 10 ft. These data are entered in STAMOORSYS as inputs and a numerical value of 0.01 is used in the iterations. A preliminary range of restoring forces from 0 to 800 lbs, with 50 points for the preliminary restoring force versus departure curve is used in analysis. The results from the example problem produced using MOORANL are input into STAMOORSYS as the target curves to be matched (as would be done for a target / prototype mooring system).

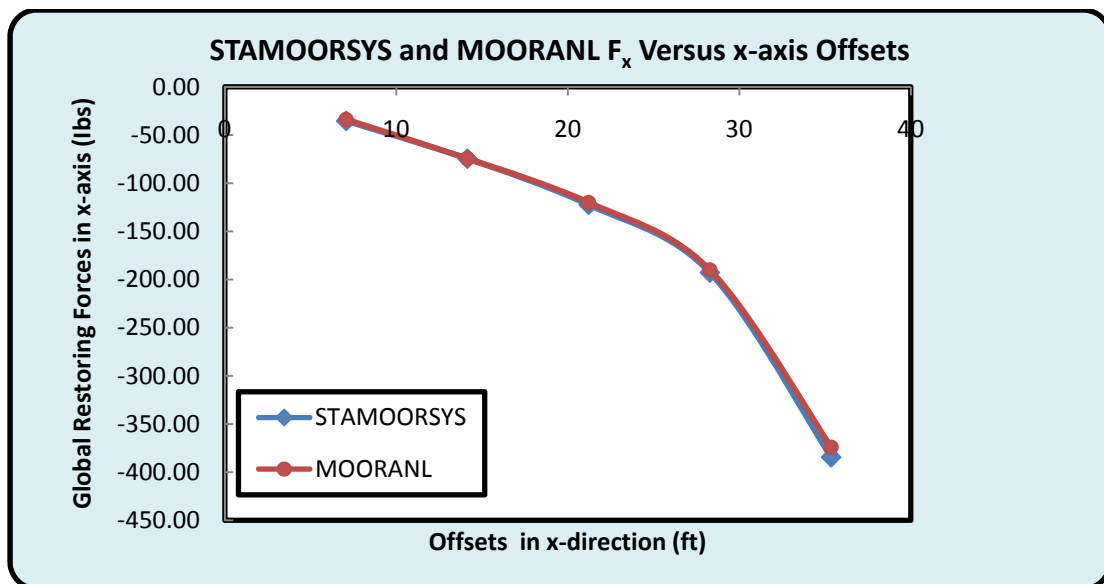


Fig. 4.19: MOORANL and STAMOORSYS x-axis global restoring force curves

Both MOORANL and STAMOORSYS compute the same global restoring forces in the x and y directions as shown in figs 4.19 through 4. 22; this is no surprise since the mooring system is symmetric about the center of the floater and the offsets are applied on a 45° heading. The maximum percentage difference between both programs is 4.1% for the global restoring forces.

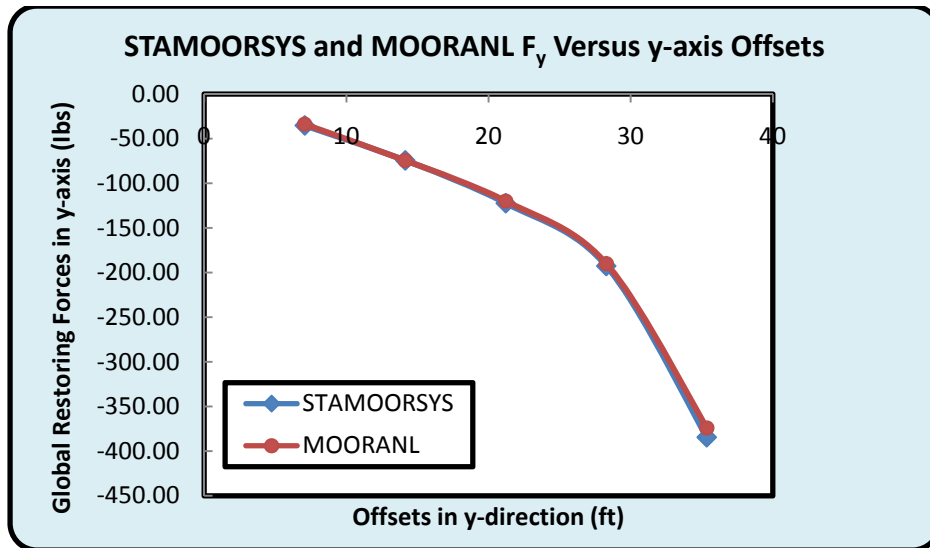


Fig. 4.20: MOORANL and STAMOORSYS y-axis global restoring force curves

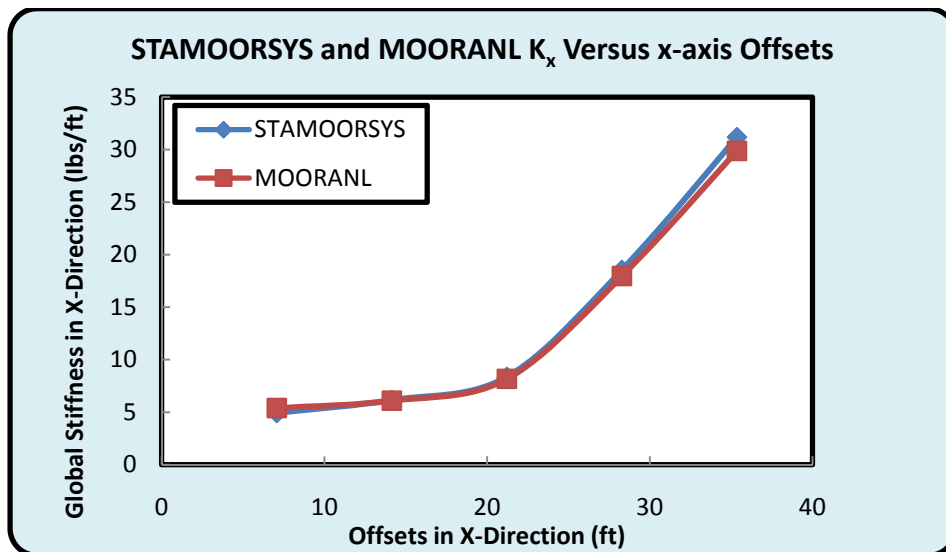


Fig. 4.21: MOORANL and STAMOORSYS x-axis global stiffness curves

For the global stiffness the maximum difference is 7.39%. The magnitudes of these differences are relatively low and these results suggest a good agreement between both programs, thereby validating STAMOORSYS.

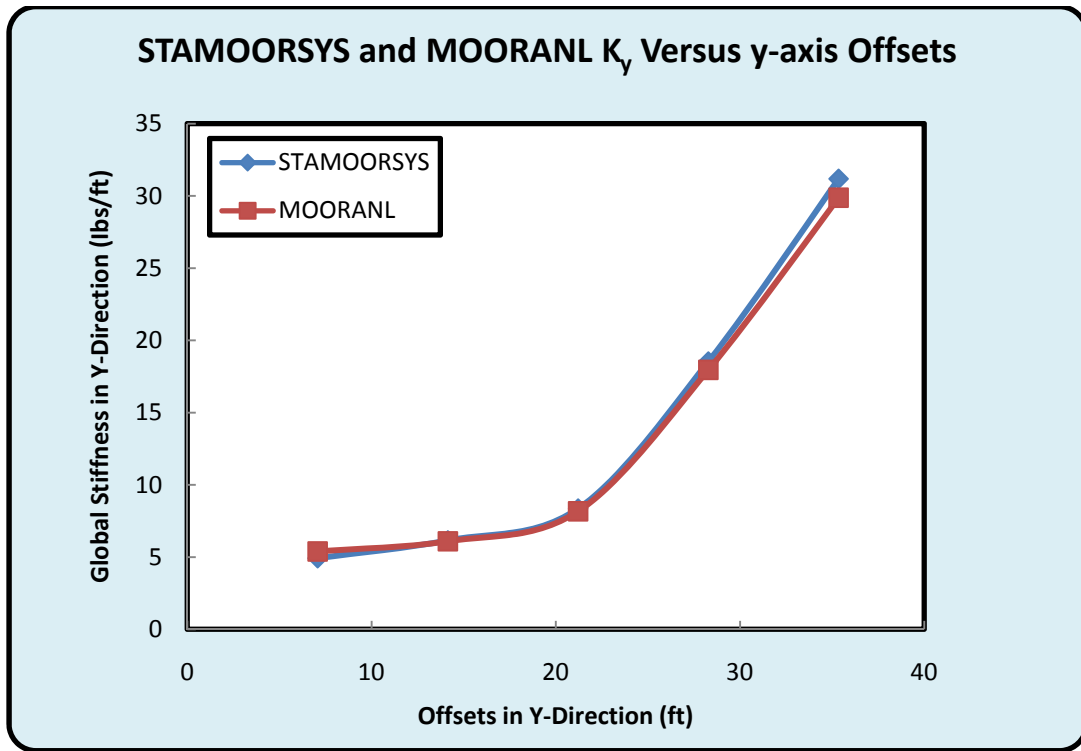


Fig. 4.22: MOORANL and STAMOORSYS y-axis global stiffness curves

Consider the second validation case where the properties of the mooring system components as used in Orcaflex are presented in Tables 4.7 and 4.8. Offset increments range from 0.10 to 242.82 ft in the x-direction only. The actual fairlead elevation relative to the anchor position is 1015.8 ft for all lines. Four lines are used in the analysis and all lines are identical. The input data is entered in STAMOORSYS and a 'numerical increment value in iteration' of 0.01 is used in running statics. A minimum preliminary restoring force of 0 and a maximum of 3,500,000 lbs are used with 500 points for the computation of the preliminary restoring force versus departure curve. Regarding the target plots from Orcaflex

to be the curves to be matched, these plots are entered into STAMOORSYS for comparison.

Table 4.7: Mooring line properties for global analysis validation using Orcaflex

SEGMENT	EA_0	w	L
1	1.89E09	25.87	1684.7
2	3.87E06	3042.00	201
3	1.88E09	4135.40	15

Table 4.8: Mooring line coordinates for global analysis validation using Orcaflex

LINE	FAIRLEAD COORDINATES (ft)		ANCHOR COORDINATES (ft)	
	X	Y	X	Y
1	43.84	43.84	1210.57	1210.57
2	-43.84	43.84	-1210.57	1210.57
3	-43.84	-43.84	-1210.57	-1210.57
4	43.84	-43.84	1210.57	-1210.57

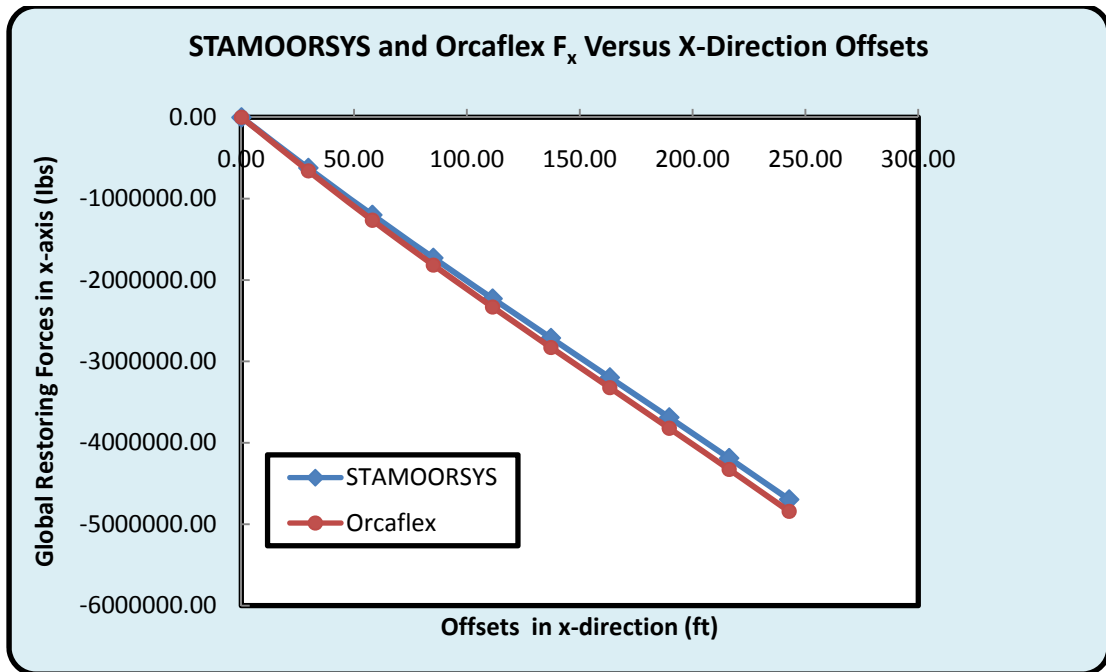


Fig. 4.23: Orcaflex and STAMOORSYS x-direction global restoring force curves

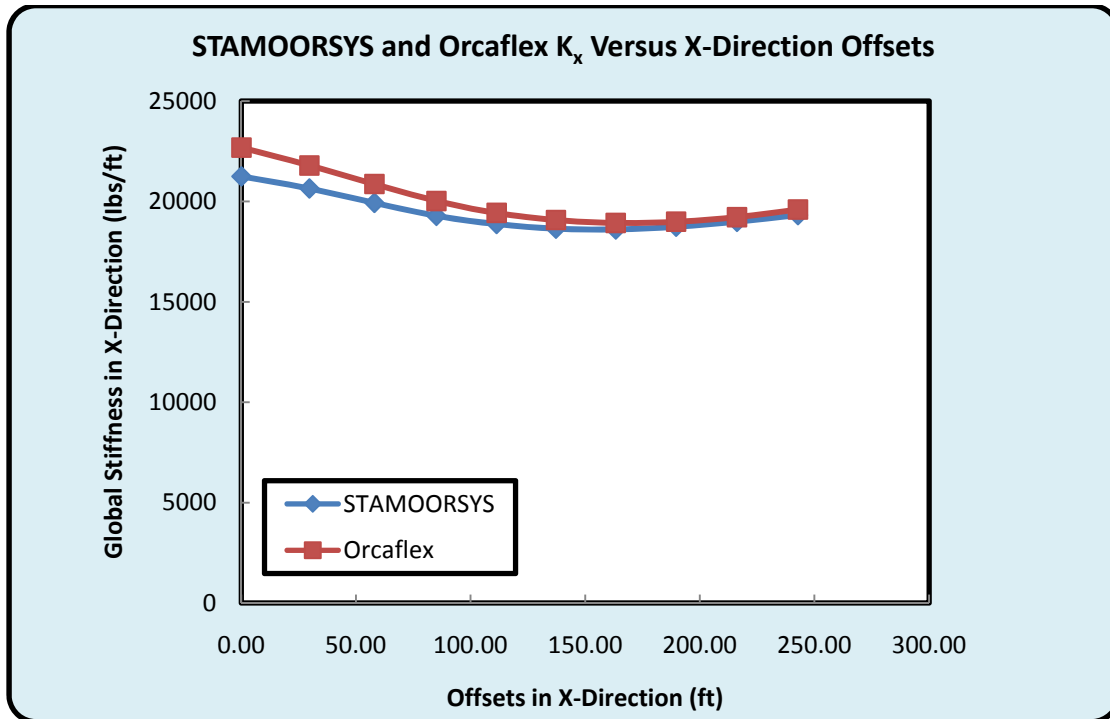


Fig. 4.24: Orcaflex and STAMOORSYS x-direction global stiffness curves

In comparing the global restoring forces (fig. 4.23) a maximum difference of 5.46% is computed while a maximum difference of 5.23% is computed for global stiffness (fig. 4.24). It is fair to infer that these differences are relatively low, and suggest a good agreement in the global static forces and stiffness in the mooring system between STAMOORSYS and Orcaflex.

To emphasize the importance of a high resolution (fine grid points) in the design of statically equivalent mooring systems, the global analysis verification exercise between STAMOORSYS and Orcaflex is repeated with 100 points used in computing the preliminary restoring force versus departure curve. Using a lower resolution (coarser grid points) the maximum percentage difference in global stiffness between STAMOORSYS and Orcaflex increases to 5.46%. Keeping the resolution high may incur more computation time, but it is certainly a good strategy that enhances the designer's search for a match in the static global response curves.

Considering the difference in the solution approach between Orcaflex and STAMOORSYS, there is bound to be some differences in the computed solutions. Orcaflex uses a numerical discrete element approach, where each element is treated as a lump mass. STAMOORSYS on the other hand is based on analytical solutions to the catenary equations. This fundamental difference in computation procedures suggests that there will always be differences in the obtained results, though these differences cannot be enormous if both programs apply their respective solution methods correctly.

4.3 DESIGN OF STATICALLY EQUIVALENT DEEPWATER MOORING SYSTEM

Armed with the approach discussed in the third chapter of this work, the goal in this section is to discuss a typical design case for a statically equivalent mooring system performed using STAMOORSYS. The basic information provided for

design includes the target global restoring force and stiffness curves obtained from the design of the prototype mooring system. These curves are computed over a specified range of offsets, and must be matched with tolerable errors by the equivalent mooring design over the same range of offsets. Engineering properties of the line segments of the prototype mooring system are also known, and these are considered in making good first guesses for the properties of the statically equivalent mooring system.

The prototype mooring is a 3x3 system (3 groups of 3 lines each) arranged symmetrically about the horizontal x-axis and with all lines identical. Each line consists of a 350 ft long upper platform chain segment followed by a 5940 ft long polyester rope segment followed by a 500 ft long lower anchor chain segment. The platform chain and anchor chain are both 4-1/4" chains with submerged weight of 132.2 lb/ft and axial stiffness of 235,319 kips. The polyester rope has submerged weight of 4.5 lb/ft and axial stiffness of 48,500 kips. The vertical distance from the seafloor to the fairleads is 4310 ft. Relative to the vertical axis of the spar, the fairlead radius is 46.02 ft and the anchor radius is 5328.5 ft. A plan view sketch of the prototype mooring system is shown in fig. 4.25.

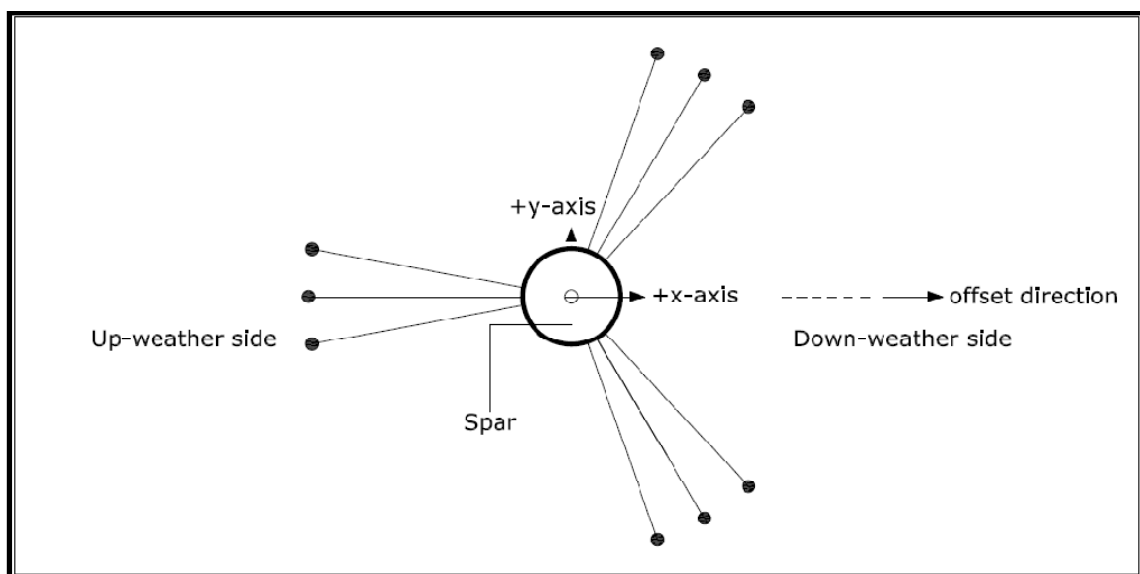


Fig. 4.25: Plan view sketch of prototype mooring system

The global coordinate system is located on the vertical axis of the spar and oriented such that the negative horizontal x-axis lines up with the central mooring line in one of the 3 groups. The spar will be tested with one weather environment only, one where the positive x-axis points down-weather. Therefore only the positive x-axis excursions of the spar are of interest in this design problem. Considering that the mooring arrangement is not symmetric about the horizontal y-axis, the force versus offset curve (for x-direction offsets) is not symmetric about zero offset. The target restoring force versus offset curve that is supposed to be matched is set up in STAMOORSYS for positive x-axis offset values associated with negative horizontal restoring forces.

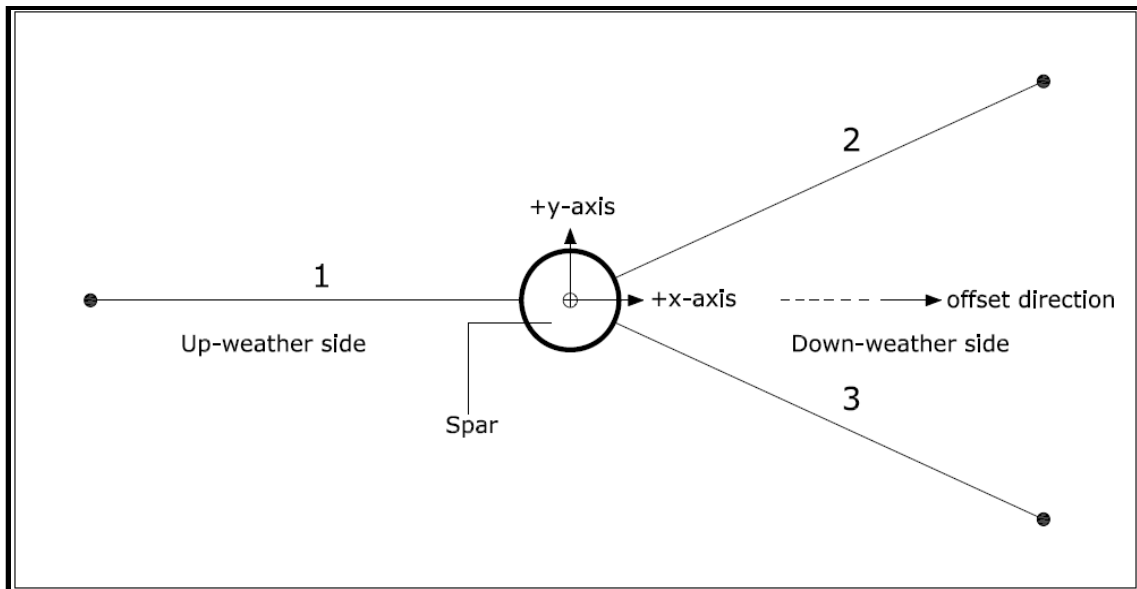


Fig. 4.26: Plan view sketch of equivalent mooring set-up

The objective is to design a 3-line equivalent mooring system (as shown in fig. 4.26) that matches the horizontal force versus offset curve and the horizontal stiffness versus offset curve of the prototype mooring with the following tolerances:

- Over the horizontal offset range from 15.56 ft to 251.50 ft, the global horizontal restoring force curve for the equivalent mooring should match that of the prototype to within 5%
- Over the horizontal offset range from 15.56 ft to 251.50 ft, the global horizontal stiffness curve for the equivalent mooring should match that of the prototype to within 10%.

The model of the spar will be built with the fairleads at the same location as the prototype, and so the fairlead coordinates (x, y) in feet for lines 1, 2 and 3 will be (-46.02, 0.00), (23.01, 39.85) and (23.01, -39.85) respectively. Since the model will be tested in the OTRC basin, the vertical distance from the fairleads to the basin floor will be 495 ft and the anchor radius must not exceed 1,440 ft. Each line will consist of a load (tension cell) attached to the fairlead, followed by a coil spring and a length of stainless steel cable. In full scale units, the load cell will have a length of 13.125 ft, a submerged weight of 747 lb/ft and an axial stiffness of 700,000 kips. The steel cable will have a submerged weight of 346.12 lb/ft and an axial stiffness of 705,957 kips.

In order to design the statically equivalent mooring system it will be necessary to select values for:

- the length of the stainless steel cable attached between the anchor and the coil spring
- the length, submerged weight and axial stiffness of the coil spring
- the anchor locations.

The parameters of the equivalent mooring which are varied during the design process are the coordinates of the anchors relative to the center of the platform, the lengths of the line segments, the axial stiffness and submerged unit weight

of the coil spring. The preliminary range of restoring forces is also adjusted to increase the grid resolution during analysis.

To highlight some significant points, two design solutions are provided to this problem; one which has features which can be criticized and another which may be regarded as fully acceptable. For the first design solution provided, comparisons of global restoring force versus offset curves between the prototype and the statically equivalent mooring system are shown in figs 4.27 and 4.28. For the range of offsets considered, the maximum percentage difference in the computed global restoring forces between the prototype mooring system and the statically equivalent mooring system along the x-axis is 4.80%. The global stiffness curves of the prototype and equivalent systems differed by a maximum of 10.0%.

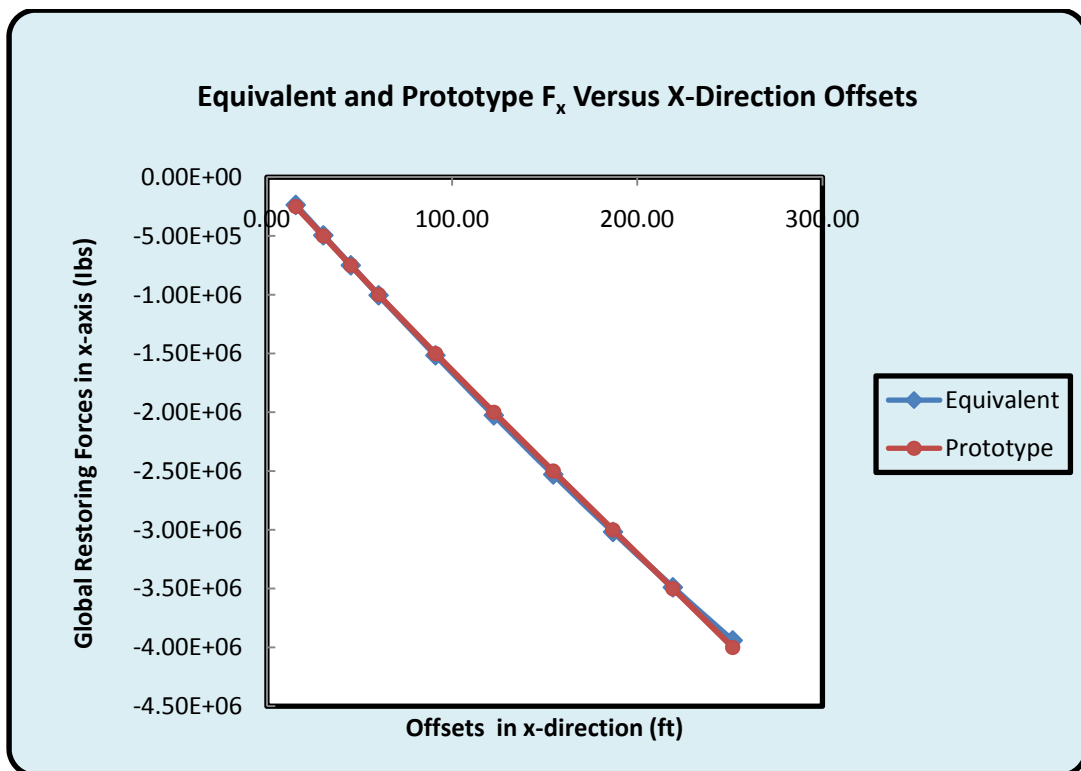


Fig. 4.27: Equivalent and prototype global restoring forces for design solution 1

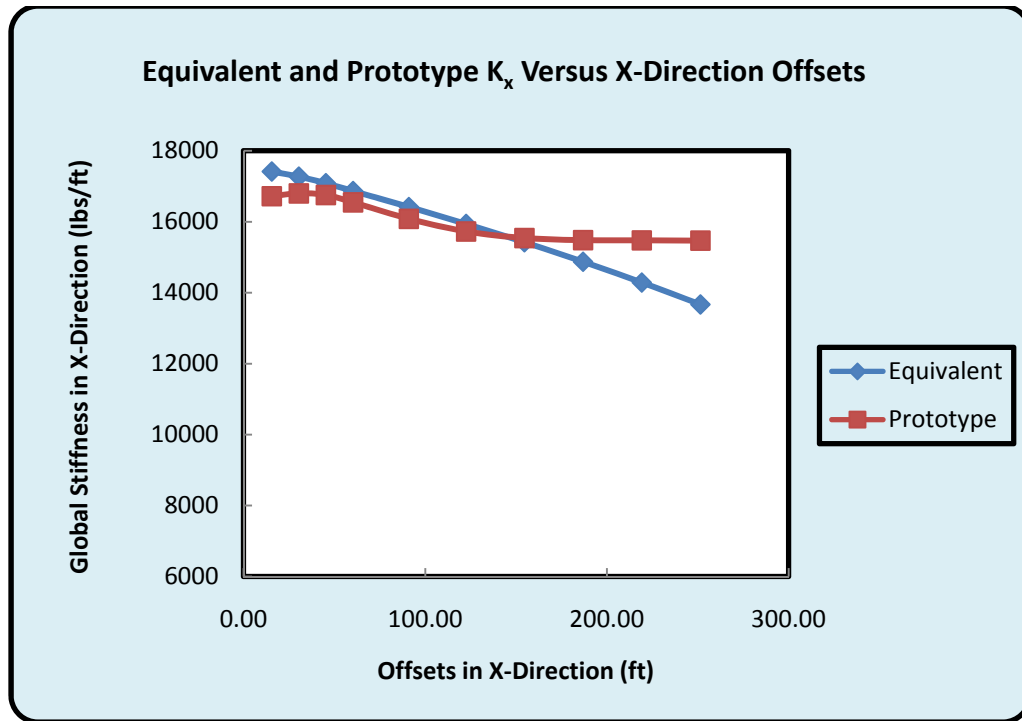


Fig. 4.28: Equivalent and prototype global stiffness for design solution 1

A summary of the properties of the designed statically equivalent system is given in Table 4.9. The solution consists of a symmetric arrangement of anchors about the horizontal x-axis, and this is required to ensure that under the action of a static force along the x-direction the vessel does not offset in the y-direction. The selected axial stiffness is within an acceptable range and the length of 700 ft can be achieved by connecting springs in series. However, a spring with submerged weight as low as 50 lbs/ft, cannot both produce the design stiffness and support the associated tensions in the line. Such springs are not commercially available, so this raises the issue of designing a system that theoretically satisfies the requirements but cannot actually be built.

Table 4.9: Properties of first equivalent mooring design solution

SEGMENT	EA_0 (lbs)	w (lbs/ft)	L (ft)	LINE	Anchor Coordinates	
					x (ft)	y (ft)
1	7.06E08	346.12	255	1	-1192.0	0.00
2	6.52E06	50	700	2	774.0	791.50
3	7.00E08	747.00	13.13	3	774.0	-791.50

Given that a numerical process is involved in the design simulations, it is important to emphasize that the accuracy of the design directly relates to the accuracy of both the numerical simulations and the adequacy of the grid resolution used. The design solution in Table 4.6 was obtained with a 'numerical increment value in iteration' of 0.1 and 100 grid points. On repeating the simulations using the same design results but with a numerical increment value of 0.01, the maximum difference in the global stiffness curves increased to 13.16% which is higher than the allowable value of 10.0%; this is unacceptable. This observation suggests the relevance of high accuracy in the numerical simulations. No alarming difference is observed with the number of grid points increased to 200. One may expect that with the very close match in the global restoring force versus offset curves (fig 4.27), a match between the stiffness curves is almost guaranteed for all offsets. The post processing done with the outputs of the first design solution suggests otherwise. Obtaining matching curves for the global restoring force and stiffness involves independent observation of both curves during the design process. It is easy to assume that because both curves often and inextricably respond to changes made to the properties of the mooring system, matching one within the required tolerance will automatically guarantee that the second will be satisfied as well. The reality however, is that the designer could still face a significant challenge in matching

say the stiffness curves within the specified tolerance, even when the global restoring curves have been matched to much lower than the required tolerance limit for all offsets in the specified range.

A more acceptable design solution is presented in Table 4.10. This second design still has the anchor positions symmetric about the horizontal x-axis. Compared to the first design solution, the second solution has a heavier and shorter coil spring that is slightly lower in axial stiffness, for the middle segment. The weight of the coil spring is such that it can resist the tensions in the mooring line and conveniently produce the design stiffness. Overall, this system is buildable in the OTRC wave basin.

Table 4.10: Properties of second equivalent mooring design solution

SEGMENT	EA_0 (lbs)	w (lbs/ft)	L (ft)	LINE	Anchor Coordinates	
					x (ft)	y (ft)
1	7.06E08	346.12	788.00	1	-1120.02	0.00
2	4.35E06	1374.26	294.94	2	560.01	969.97
3	7.00E08	747.00	13.13	3	560.01	-969.97

Compared to the global restoring forces and stiffness curves obtained in the first solution, those of the second solution are quite similar but with slight noticeable differences. The maximum percentage difference in global restoring forces between the prototype and equivalent systems is 4.86%. The maximum difference in the global stiffness curves is 6.29%. Figures 4.29 and 4.30 show the global restoring force and stiffness curves respectively.

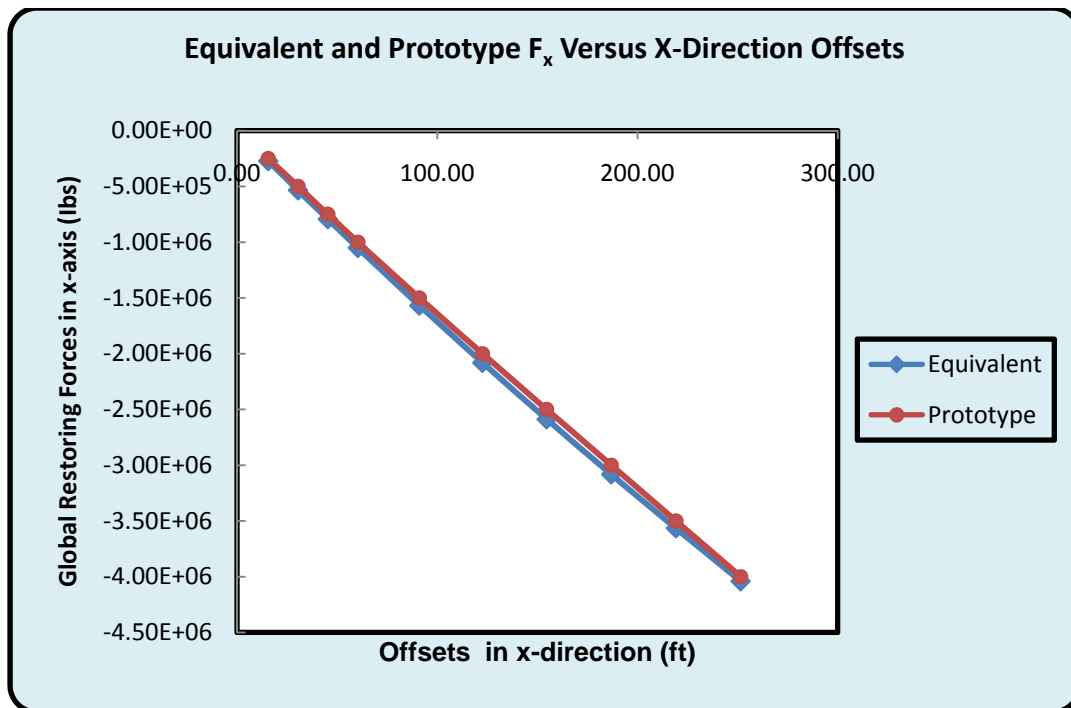


Fig. 4.29: Equivalent and prototype global restoring forces for design solution 2

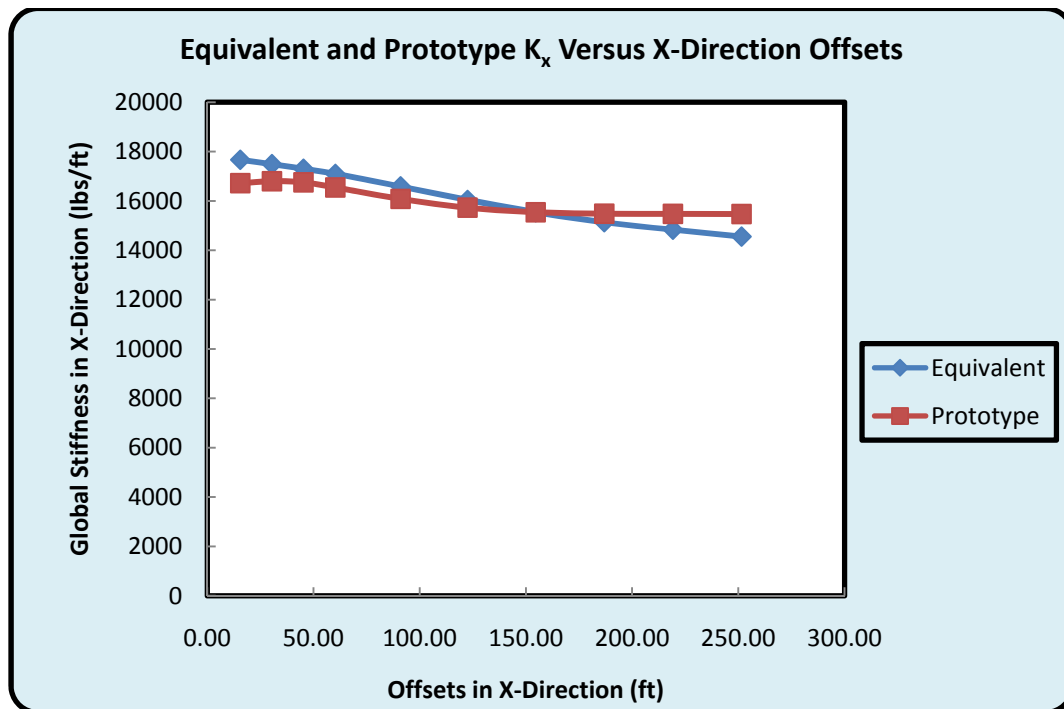


Fig. 4.30: Equivalent and prototype global stiffness for design solution 2

Considering the orders of magnitude of the computed percentage differences between these curves, it is fair to infer that the second design for the equivalent mooring system is sufficient for the spar testing project. The strong agreements between the equivalent and prototype curves suggest a strong basis for the comparison of dynamic responses obtained during model testing.

In practice, the designed equivalent system would be updated to compensate for the difference between the design properties and the as-built properties and adjustments in the wave basin. The updated design however does not differ significantly from the preliminary design of the statically equivalent mooring system.

The local results of static equilibrium for the second design solution are computed using the Set-up page in STAMOORSYS. These results include tensions at the anchors and fairleads, suspended line lengths, lengths of line on the sea floor and local restoring forces. Appendix B shows the local results of static equilibrium. The line configurations indicate that the system is a taut mooring system as all the lines are suspended for each applied offset, except for the last and largest offset at which about 3.5 ft of lines 2 and 3 is on the seafloor.

CHAPTER V

SUMMARY AND CONCLUSIONS

The importance of verifying designs of deepwater floating structures cannot be overemphasized. Measuring static and dynamic responses of floating structures during model testing offers proper insights on the behavior of the floater. This research embraces the hybrid method of design verification, which combines numerical simulations with model testing to reduce the level of uncertainties associated with model testing. One of the challenges in testing model floaters in the wave basin remains the spatial and depth limitations of wave tanks. For deepwater systems, direct scaling of the prototype mooring systems is often not possible and a mere truncation of the mooring system means that the moorings in the wave basin cannot impose the same static loads on the model floater, as the full depth moorings on the prototype structure. It is therefore necessary to design a statically equivalent mooring system that will impose the same static global loads on the model floater, as in the full depth system. To design this system, an efficient numerical tool is required.

Having identified the need for a fit-for-purpose tool in the design of statically equivalent mooring systems (which is a step in the hybrid verification process), STAMOORSYS has been produced through this research to meet this need. STAMOORSYS is a program for static analyses of spread mooring systems, specifically tailored to be easily used in the design of statically equivalent deepwater mooring systems. It accepts the properties of the mooring system components and other spatial data (e.g. anchor coordinates) as inputs, and uses these to statically analyze the mooring system for local and global responses (departures, restoring forces, stiffness, tensions and line configurations at static equilibrium). The program is geared for easy repetition of analyses in the effort to design (optimize) a statically equivalent mooring system, and this is achievable using the design page. For this reason the global restoring force and

global stiffness curves are provided in the design page, such that the designer can instantly visualize the global effects of alterations made to the system during design.

Without the consideration of certain factors from a realistic perspective, perhaps it may not be very easy to appreciate the advantages of STAMOORSYS regarding statically equivalent deep water mooring systems. Typical factors here include requirements from clients (owners of floating structure to be tested in the wave tank), time available to complete testing project, portability of the program and the effort required of a new user to understand and use STAMOORSYS compared to programs performing similar functions. Like many programs, the version of STAMOORSYS produced at this stage of the research project has some limitations, and these will also be discussed in this chapter.

5.1 ECONOMIC ADVANTAGES OF STAMOORSYS

As sponsor of this research project, the Offshore Technology Research Center reserves the right to use of this program. From personal communications with engineers (in the OTRC) involved with design verification processes such as that described in the third chapter of this work, it is possible and often the case that client requirements are stringent. The level of static equivalence to be achieved may be one with very high accuracy. Allowable errors between the target curves and those produced from the equivalent design is best kept at the minimum possible, to preserve the integrity of the basis for comparing dynamic responses. As STAMOORSYS is hosted in a Microsoft Excel spreadsheet, it is completely trivial to format cells such that the results displayed are to very high precision. STAMOORSYS offers both local and global results making comparisons easy and offering complete insight on static mooring configurations resulting from the given design properties of the system.

The current version of the program is only about 5938 KB in capacity, and thus can easily be carried about in a portable memory drive or even saved on a secure folder on a network to make it more readily accessible to the user(s). STAMOORSYS requires no additional hardware such as dongles for accessibility, and this is one less limitation.

Considering the fact that a new user (say, a new engineer on a project) may require the use of STAMOORSYS on a verification project, one does not have to worry so much about learning to use the program. The user interfaces in STAMOORSYS are self explanatory, and it is easy to move through the different pages of the program. Average knowledge of the use of Microsoft Excel would be just about adequate for a user to optimally put STAMOORSYS to use. This may not be so easy with other available programs performing similar or the same tasks; usually special knowledge of the software is required and this may take a while to grasp.

5.2 LIMITATIONS OF STAMOORSYS AND UP-COMING MODIFICATIONS

The current version of STAMOORSYS only addresses horizontal offsets and horizontal restoring forces on a floating vessel. For some floating structures (e.g. semi-submersibles) it is important to establish static equivalence in the vertical direction (relating to heave motions) as well as in the rotating plane relating to pitch motions of the floater. At a given offset location vertical restoring forces act on the floater causing it to tilt unevenly. Usually, the tilt versus offset curve experienced by the model floater in the wave basin comprises a steep slope which is not likely to be observed in the prototype structure. The local moments and vertical global restoring forces for the model floater must be compared to the local moments and vertical restoring forces of the prototype structure. Such capability should be added to the program to make it versatile enough to

address static equivalence in more directions of typical interest, for representative structures that could be tested in the OTRC.

An additional constraint in the current version of STAMOORSYS is that all lines attached to the vessel have the same fairlead and anchor elevations, and are of the same composition (EA_0 , w and L). Sometimes, it is not such a good idea to make lines on the up-weather side of the floater have the same properties as those on the down-weather side. It is desired to afford the user the opportunity to create each line composition such that it is unique. With such capability the optimization process is made more efficient, as the designer would have more properties to modify in the search for a match between the compared curves.

Not having enough information on commercially available components of mooring systems could lead to unbuildable designs, and eventually loss of time as such designs must be repeated. A database of properties of vendor mooring components (especially springs, cables and chains) could also be added to STAMOORSYS to speed the convergence to a buildable design. This will essentially point the designer(s) to the ranges of properties within which a buildable design solution can be obtained.

The current version of STAMOORSYS requires a manual optimization of the mooring system properties in search of a match in the global restoring force and global stiffness curves. With the in-built capability of Microsoft Excel to solve optimization problems, efforts will be made to enhance the optimization process in STAMOORSYS, such that design process is highly facilitated. The challenge in achieving this is handling the many design variables for the number of lines used in analysis. Additionally, using the optimizer in Excel to control the iterative computations in STAMOORSYS may not be very trivial. However, harnessing Excel's optimizer to enhance the design process is worth the effort considering that its computation speed is very high; this can save a lot of time.

5.3 CONCLUSIONS

Using the hybrid method of design verification to verify the designs of deepwater floating structures is greatly embraced by the industry. As exposed in the discussed literature in the second chapter of this work, the processes of modeling the model and designing a statically equivalent mooring system require efficient numerical tools. This research has provided a tool which is specifically tailored to perform one of the tasks required in the hybrid method.

STAMOORSYS has the capability of producing accurate results as shown in the comparisons made in the fourth chapter of this work. It is also very advantageous that the program offers the user a clear insight on the local effects of the chosen properties, as displayed under parameters such as suspended line lengths and length of the line on the sea floor. Being able to control the accuracies of the numerical simulations and grid resolutions is part of the program's strong capabilities. The interfaces of STAMOORSYS are created to minimize distractions in the design process which may arise from switching between windows and menus (as is the case in many other programs). Another unique advantage is being able to use the tools inherently available in Microsoft Excel, for any form of post processing which the designer / user may require. The user may also choose to save the spreadsheet for archival purposes after a particular project.

Although STAMOORSYS uses a numerical process in computing results of static equilibrium, the search for static equilibrium is a deterministic process. Many existing programs (especially finite element codes) use more approximate procedures in obtaining results. One of such techniques is specifying the anchor coordinates of the lines, and computing the coordinates of the top attachment point with numerical simulations and vice versa. The challenge with this procedure is that it is prone to inaccurate predictions of the touchdown point of

the mooring line. STAMOORSYS regards the touchdown point as a sensitive parameter in the numerical process, and thus the computation of this parameter is a lot more thorough than is obtainable in most other programs.

The major point of this research project has been to make life easier for the designers of statically equivalent deepwater mooring systems, by developing a tool specifically for this purpose. With the measure of achievement so far with STAMOORSYS, it is fair to say that the goal has been achieved to some extent, although more improvements (by eliminating the constraints discussed in section 5.2) to the program will make it even more useful.

REFERENCES

- [1] Stansberg, C. T., Karlsen, S. I., Ward, E. G., Wichers, J. E. W. and Irani, M. B., 2004, "Model Testing for Ultradeep Waters," OTC Conference, Houston, OTC 16587, pp. 1 - 8.
- [2] Department of Marine Technology, Norwegian University of Science and Technology, "Experimental Methods in Marine Hydrodynamics," January 2008, <http://www.ntnu.no/imt/research>.
- [3] McNatt, T. R., 1982, "Catenary Ocean Mooring Systems – Approaches to Analysis and Testing," IEEE Conference, **0197-7385/82/0000-0513**, pp. 517 - 518.
- [4] Jones, H. L., 1991, "Lecture notes on LINANL - Program for Static Analysis of Mooring Systems," Department of Civil Engineering, Texas A&M University, College Station, TX.
- [5] Jones, H. L., 1983, "MOORANL Users Guide - Program for Static Analysis of Spread Mooring Systems," Department of Civil Engineering, Texas A&M University, College Station, TX, pp. 48 - 54.
- [6] Orcina Limited, "Orcaflex Software," version 9.1a, Cumbria, UK.
- [7] Fernandez, J., 2008, "Reliability of Mooring Chains," Proceedings of TEKNA Conference on DP and Mooring of Floating Offshore Units, Alesund, Norway.
- [8] Richards, D., 2007, "Misrepresented Imports," Proceedings of the 7th International Rope Technology Workshop, College Station, TX.
- [9] Wu, S., 2007, "Taut-leg Mooring and Anchoring for Spars," Ocean Engineering Seminar, Texas A&M University, College Station, TX.
- [10] Kim, M. H., 2004, "Dynamic Analysis Tool for Moored Tanker-Based FPSO's Including Large Yaw Motions," Final Report Prepared for the Minerals Management Service under the MMS/OTRC Cooperate Research Agreement, <http://www.mms.gov>, pp. 2 - 4.

- [11] Luo, Y., Baudic, S., Poranski, P., Ormberg, H., Stansberg, C. T. and Wichers, J., 2004, "Prediction of FPSO Responses: Model Tests versus Numerical Analysis," OTC Conference, Houston, OTC 16585, pp. 1 - 7.
- [12] Stansberg, C. T., Ormberg, H. and Oritsland, O., 2002, "Challenges in Deep Water Experiments: Hybrid Approach," Transactions of the ASME, **124**, pp. 90 - 95.
- [13] Fylling, I. J. and Stansberg, C. T., 2005, "Model Testing of Deepwater Floating Production Systems: Strategy for Truncation of Moorings and Risers," Proceedings of 17th DOT Conference, Vitoria, Brazil, pp. 1 - 4.
- [14] Ormberg, H., Stansberg, C. T., Yttervik, R. and Kleiven, G., 1999, "Integrated Vessel Motion and Mooring Analysis Applied in Hybrid Model Testing," Proceedings of the 9th ISOPE Conference, Brest, France, **I**, pp. 339 - 346.
- [15] ITTC Specialist Committee on Deep Water Mooring, 1999, "Report from the Specialist Committee on Deep Water Mooring," 22nd ITTC Proceedings, Seoul, Korea & Shanghai, China, **II**, pp. 377 - 398.
- [16] Smith R. J. and MacFarlane, C. J., 2001, "Statics of a Three Component Mooring Line," Ocean Engineering, **28**(7), pp. 899 – 914.
- [17] Carbono, A. J., Menezes, I. F. M. and Martha, L. F., 2005, "Mooring Pattern Optimization using Genetic Algorithms," 6th World Congress of Structural and Multidisciplinary Optimization, Rio de Janeiro, Brazil, pp. 1 - 9.
- [18] Connaire A., Kavanagh K., and Ahilan R. V., 1999, "Integrated Mooring and Riser Design - Analysis Methodology," OTC Conference, Houston, OTC 10810, pp. 1 - 11.
- [19] Russell J. C. and Lardner T. J., 1997, "Statics Experiments on an Elastic Catenary," Journal of Engineering Mechanics, **123**(12), pp. 1322 - 1324.
- [20] Irvine, H. M., 1975, "Statics of Suspended Cables," J. Engrg. Mech. Div., ASCE, **101**(30), pp. 187 - 205.

- [21] Irvine, H. M. and Sinclair, G. B., 1976, "The Suspended Elastic Cable Under the Action of Concentrated Vertical Loads", *J. Solids Struct.*, **12**, pp. 309 - 317.
- [22] Francois, M., 2005, "Fiber Ropes for Station-keeping: Engineering Properties and Qualification Procedures," *IEEE Conference*, **2**, pp. 1623 - 1629.
- [23] Banfield S. J., Casey, N. F., Nataraja, R., 2005, "Durability of polyester deepwater mooring rope," *OTC Conference, Houston, I*, OTC 17510, pp. 1 - 9.
- [24] François, M., Davies, P., 2000, "Fibre rope deep water mooring: a practical model for the analysis of polyester mooring systems," *Rio Offshore Oil and Gas Conference, IBP* **247 00**.
- [25] Bureau Veritas, 1997, "Certification of Synthetic Fiber Ropes for Mooring Systems," *Bureau Veritas Certification Guidance Notes, NI* **432 DTO R00E**.
- [26] Casey, N. F. and Banfield, S. J., 2005, "Factors Affecting the Measurement of Axial Stiffness of Polyester Deepwater Mooring Rope Under Sinusoidal Loading," *OTC Conference, Houston, OTC* 17068, pp. 1 - 11.
- [27] Bowden G., 2004, "Stretched Wire Mechanics," work supported by Department of Energy, Geneva, pp. 1 - 8.
- [28] Irvine, H. M., 1981, "Cable Structures," *MIT Press, Cambridge, MA*, pp. 1-24.
- [29] Yang, W., 2007, "Hydrodynamic Analysis of Mooring Lines Based on Optical Tracking Experiments," *PhD dissertation in Ocean Engineering, Texas A&M University, College Station, TX*, pp. 48 – 49.

APPENDIX A

Appendix A1: Set-up Page in STAMOORSYS

STAMOORSYS Static Analysis of Spread Mooring Systems STAMOORSYS Static Analysis of Spread Mooring Systems STAMOORSYS Static Analysis of Spread Mooring Systems STAMOORSYS Static Analysis of Spread Mooring Systems

Select Units English

USE INPUT PARAMETERS

Length of Line Segments (ft)

Length of segment 1 215.00
Length of segment 2 700.00
Length of segment 3 15.11

Submerged weight per unit length of line (lb/ft)

Submerged wt. of seg 1 146.12
Submerged wt. of seg 2 50.00
Submerged wt. of seg 3 747.00

Coordinates of Anchors relative to Center of Platform (ft)

Line #	x	y
Line 1	1192.00	0.00
Line 2	176.00	791.50
Line 3	176.00	-791.50
Line 4		
Line 5		
Line 6		
Line 7		
Line 8		

Coordinates of Fairleads Relative to Center of Platform (ft)

Line #	x	y
Line 1	-60.02	0.00
Line 2	23.01	39.85
Line 3	23.01	-39.85
Line 4		
Line 5		
Line 6		
Line 7		
Line 8		

Stiffness of seg 1 7.00E+08
Stiffness of seg 2 6.52E+06
Stiffness of seg 3 7.00E+08

Initial assumptions for angles of inclination with reference to the horizontal (degrees)

Lowest end of seg 1 (at sea bed) 0.00
Lowest end of seg 2 0.00
Lowest end of seg 3 0.00

Vertical Distance From Fairlead to Seabed (ft)

At anchor point (at sea bed) 895.00

Coordinates of Vessel's Horizontal Offsets (ft)

Offset	x	y
HO1	13.56	0.00
HO2	30.48	0.00
HO3	45.32	0.00
HO4	60.12	0.00
HO5	75.01	0.00
HO6	122.53	0.00
HO7	154.41	0.00
HO8	188.84	0.00
HO9	219.20	0.00
HO10	251.50	0.00

Coordinates of Vessel's Vertical Offsets (ft)

Offset	x	y
VO1		
VO2		
VO3		
VO4		
VO5		
VO6		
VO7		
VO8		
VO9		
VO10		

Initial Headings of Lines (degrees) (relative to the horizontal)

Line #	Heading
Line 1	3.14
Line 2	6.79
Line 3	-6.79
Line 4	80.00
Line 5	80.00
Line 6	80.00
Line 7	80.00
Line 8	80.00

Preliminary Range of Restoring Forces (lb)

Minimum Force 0
Maximum Force 450000
No. of Points 100

Breaking Strength of Mooring Lines (lb)

Segment 1
Segment 2
Segment 3

No. of Lines to use in Analysis

Value 1

PROGRAM CONTROLS

Run Statics
Global Forces
Update Lines 1 to 4
Update Lines 5 to 8
Reset
Clear Inputs
Clear Outputs

CHECKS

Min. Departure (%)
Max. Departure (%)
Min. Pref. Departure (ft)
Max. Pref. Departure (ft)
Check Range is ok

Points with 1% Error

OUTPUT PARAMETERS

Preferred Departure in plane of line 1 (ft)

Line #	Value
D1	1161.34
D2	1176.46
D3	1191.30
D4	1206.30
D5	1216.99
D6	1248.51
D7	1300.39
D8	1332.86
D9	1365.18
D10	1397.48

Preferred Departure in plane of line 2 (ft)

Line #	Value
D1	1051.59
D2	1041.21
D3	1030.99
D4	1020.78
D5	1000.27
D6	979.76
D7	959.50
D8	939.74
D9	920.74
D10	902.47

Preferred Departure in plane of line 3 (ft)

Line #	Value
D1	1051.59
D2	1041.21
D3	1030.99
D4	1020.78
D5	1000.27
D6	979.76
D7	959.50
D8	939.74
D9	920.74
D10	902.47

Preferred Departure in plane of line 4 (ft)

Line #	Value
D1	1051.59
D2	1041.21
D3	1030.99
D4	1020.78
D5	1000.27
D6	979.76
D7	959.50
D8	939.74
D9	920.74
D10	902.47

RESTORING FORCES IN LINE 1 (lb)

Line #	Value
H1	207665.46
H2	254762.24
H3	287643.09
H4	313964.33
H5	338276.48
H6	360885.48
H7	382792.44
H8	404100.97
H9	424919.58
H10	445247.58

RESTORING FORCES IN LINE 2 (lb)

Line #	Value
H1	162767.88
H2	154367.05
H3	146416.13
H4	138872.21
H5	1226542.33
H6	1009980.44
H7	916973.81
H8	770589.00
H9	612132.82
H10	501231.24

RESTORING FORCES IN LINE 3 (lb)

Line #	Value
H1	162767.88
H2	154367.05
H3	146416.13
H4	138872.21
H5	1226542.33
H6	1009980.44
H7	916973.81
H8	770589.00
H9	612132.82
H10	501231.24

RESTORING FORCES IN LINE 4 (lb)

Line #	Value
H1	162767.88
H2	154367.05
H3	146416.13
H4	138872.21
H5	1226542.33
H6	1009980.44
H7	916973.81
H8	770589.00
H9	612132.82
H10	501231.24

RESTORING FORCES IN LINE 5 (lb)

Line #	Value
H1	207665.46
H2	254762.24
H3	287643.09
H4	313964.33
H5	338276.48
H6	360885.48
H7	382792.44
H8	404100.97
H9	424919.58
H10	445247.58

RESTORING FORCES IN LINE 6 (lb)

Line #	Value
H1	207665.46
H2	254762.24
H3	287643.09
H4	313964.33
H5	338276.48
H6	360885.48
H7	382792.44
H8	404100.97
H9	424919.58
H10	445247.58

RESTORING FORCES IN LINE 7 (lb)

Line #	Value
H1	207665.46
H2	254762.24
H3	287643.09
H4	313964.33
H5	338276.48
H6	360885.48
H7	382792.44
H8	404100.97
H9	424919.58
H10	445247.58

RESTORING FORCES IN LINE 8 (lb)

Line #	Value
H1	207665.46
H2	254762.24
H3	287643.09
H4	313964.33
H5	338276.48
H6	360885.48
H7	382792.44
H8	404100.97
H9	424919.58
H10	445247.58

TENSION AT ANCHOR (lb)

Anchor #	Value
TA1	2692096.90
TA2	2620861.01
TA3	2464504.82
TA4	2077115.11
TA5	1841862.00
TA6	1634577.24
TA7	1462790.45
TA8	1274906.14
TA9	1075689.64
TA10	873889.18

TENSION AT FAIRLEAD (lb)

Fairlead #	Value
FL1	274144.18
FL2	287197.78
FL3	298812.25
FL4	313620.61
FL5	330539.47
FL6	349769.49
FL7	391924.53
FL8	421844.36
FL9	450505.61
FL10	478215.61

COMPUTED WATER DEPTH (ft)

Water Depth #	Value
WD1	495.06
WD2	495.18
WD3	495.30
WD4	495.04
WD5	495.30
WD6	495.06
WD7	495.02
WD8	495.06
WD9	495.13
WD10	495.19

GLOBAL FORCES IN Z-AXIS (lb)

Force #	Value
Fz1	-236601.19
Fz2	-494756.17
Fz3	-790104.30
Fz4	-1006064.81
Fz5	-1151422.54
Fz6	-1265181.14
Fz7	-1328784.61
Fz8	-1351763.19
Fz9	-1488349.73
Fz10	-194598.88

GLOBAL FORCES IN X-AXIS (lb)

Force #	Value
Fx1	0.00
Fx2	0.00
Fx3	0.00
Fx4	0.00
Fx5	0.00
Fx6	0.00
Fx7	0.00
Fx8	0.00
Fx9	0.00
Fx10	0.00

GLOBAL FORCES IN Y-AXIS (lb)

Force #	Value
Fy1	0.00
Fy2	0.00
Fy3	0.00
Fy4	0.00
Fy5	0.00
Fy6	0.00
Fy7	0.00
Fy8	0.00
Fy9	0.00
Fy10	0.00

STRENGTH CHECK!

Maximum Tension in Segment 1 (lb)

Line #	Value
Line 1	478215.91
Line 2	58621.86
Line 3	57068.33
Line 4	
Line 5	
Line 6	
Line 7	
Line 8	

Maximum Tension in Segment 2 (lb)

Line #	Value
Line 1	477928.30
Line 2	58621.86
Line 3	58621.46
Line 4	
Line 5	
Line 6	
Line 7	
Line 8	

Maximum Tension in Segment 3 (lb)

Line #	Value
Line 1	478215.91
Line 2	58621.87
Line 3	591638.07
Line 4	
Line 5	
Line 6	
Line 7	
Line 8	

STAMOORSYS Static Analysis of Spread Mooring Systems STAMOORSYS Static Analysis of Spread Mooring Systems STAMOORSYS Static Analysis of Spread Mooring Systems STAMOORSYS Static Analysis of Spread Mooring Systems

Appendix A2: Design Page in STAMOORSYS

STAMOORSYS Static Analysis of Spread Mooring Systems STAMOORSYS

USER INPUT PARAMETERS

Length of Line segments (Feet)

Length of segment 1	255.00
Length of segment 2	700.00
Length of segment 3	13.33

Submerged weight per unit length of line (lbs/ft)

Submerged wt. of seg-1	346.12
Submerged wt. of seg-2	50.00
Submerged wt. of seg-3	747.00

Axial Stiffness of Mooring Lines - EA (lbs)

Stiffness of seg-1	7.06E+08
Stiffness of seg-2	6.52E+06
Stiffness of seg-3	7.00E+08

Numerical increment value in iteration (Feet)

Value: 0.1

No. of Lines to use in Analysis

Value: 3

Preliminary Range of Restoring Forces (lbs)

Minimum Value of Force	0
Maximum Value of Force	4500000
No. of Points	100

Coordinates of Anchors relative to Center of Platform (Feet)

	X	Y
Line 1	-1192.00	0.00
Line 2	774.00	791.50
Line 3	774.00	-791.50
Line 4		
Line 5		
Line 6		
Line 7		
Line 8		

Coordinates of Target Offsets Used in Prototype Design (Feet)

	X	Y	Z
1	15.56	0.00	0.00E+00
2	30.48	0.00	0.00E+00
3	45.32	0.00	0.00E+00
4	60.32	0.00	0.00E+00
5	91.01	0.00	0.00E+00
6	122.53	0.00	0.00E+00
7	154.61	0.00	0.00E+00
8	186.88	0.00	0.00E+00
9	219.20	0.00	0.00E+00
10	251.50	0.00	0.00E+00

Global Restoring Forces for Prototype System to be Matched (lbs)

	F _x	F _y	F _z
1	-250000		0
2	-500000		0
3	-750000		0
4	-1000000		0
5	-1500000		0
6	-2000000		0
7	-2500000		0
8	-3000000		0
9	-3500000		0
10	-4000000		0

PROGRAM CONTROLS

Run Statics

Update Lines 1 to 4

Update Lines 5 to 8

Reset

Clear Inputs

Clear Outputs

THIS CHECK MUST BE SATISFIED.

Min. Departure (ft)	902.47
Max. Departure (ft)	1397.48
Min. Pref. Departure (ft)	473.13
Max. Pref. Departure (ft)	1397.51
Check!	Range is ok

THIS CHECK MUST BE SATISFIED.

Points with >= 5% Error	0
-------------------------	---

HORIZONTAL COMPONENT OF LINE TENSIONS, FOR LINES 1 to 4

OUTPUT PARAMETERS

Global Force in X-Axis (lbs)	
Fx1	-238532.49
Fx2	-497299.43
Fx3	-751061.22
Fx4	-998398.82
Fx5	-1515942.07
Fx6	-2025107.15
Fx7	-2530631.04
Fx8	-3015924.24
Fx9	-3486349.75
Fx10	-3942849.12

Global Force in Y-Axis (lbs)

Fy1	0.00
Fy2	0.00
Fy3	0.00
Fy4	0.00
Fy5	0.00
Fy6	0.00
Fy7	0.00
Fy8	0.00
Fy9	0.00
Fy10	0.00

Global Force in Z-Axis (lbs)

Fz1	
Fz2	
Fz3	
Fz4	
Fz5	
Fz6	
Fz7	
Fz8	
Fz9	
Fz10	

Global Stiffness in X-Axis (lbs/ft)

Equivalent K ₁	17474.08885
Equivalent K ₂	17218.2844
Equivalent K ₃	16792.8484
Equivalent K ₄	16613.95943
Equivalent K ₅	16513.41952
Equivalent K ₆	15958.05075
Equivalent K ₇	15399.18371
Equivalent K ₈	14796.39138
Equivalent K ₉	14343.80166
Equivalent K ₁₀	13905.66614

Global Stiffness in Y-Axis (lbs/ft)

Equivalent K ₁	#DIV/0!
Equivalent K ₂	#DIV/0!
Equivalent K ₃	#DIV/0!
Equivalent K ₄	#DIV/0!
Equivalent K ₅	#DIV/0!
Equivalent K ₆	#DIV/0!
Equivalent K ₇	#DIV/0!
Equivalent K ₈	#DIV/0!
Equivalent K ₉	#DIV/0!
Equivalent K ₁₀	#DIV/0!

Global Stiffness in Z-Axis (lbs/ft)

Equivalent K ₁	#DIV/0!
Equivalent K ₂	#DIV/0!
Equivalent K ₃	#DIV/0!
Equivalent K ₄	#DIV/0!
Equivalent K ₅	#DIV/0!
Equivalent K ₆	#DIV/0!
Equivalent K ₇	#DIV/0!
Equivalent K ₈	#DIV/0!
Equivalent K ₉	#DIV/0!
Equivalent K ₁₀	#DIV/0!

TENSIONS AT FAIRLEADS FOR LINES 1 to 4

OUTPUT PARAMETERS

Tension at Fairlead 1 (lbs)	
TF1	2748175.05
TF2	2875900.53
TF3	3001242.05
TF4	3126672.68
TF5	3393013.79
TF6	3664569.82
TF7	3944102.87
TF8	4222613.68
TF9	4502768.70
TF10	4788710.35

Tension at Fairlead 2 (lbs)

TF1	1815035.16
TF2	1729259.49
TF3	1645829.43
TF4	1563520.90
TF5	1387603.41
TF6	1219325.19
TF7	1053508.98
TF8	895190.22
TF9	742777.80
TF10	595765.03

Tension at Fairlead 3 (lbs)

TF1	1815035.16
TF2	1729259.49
TF3	1645829.43
TF4	1563520.90
TF5	1387603.41
TF6	1219325.19
TF7	1053508.98
TF8	895190.22
TF9	742777.80
TF10	595765.03

Tension at Fairlead 4 (lbs)

TF1	
TF2	
TF3	
TF4	
TF5	
TF6	
TF7	
TF8	
TF9	
TF10	

Target Stiffness in X-Axis (lbs/ft)

Prototype K ₁	16718.84939
Prototype K ₂	16798.15714
Prototype K ₃	16753.84683
Prototype K ₄	16545.54914
Prototype K ₅	16080.33748
Prototype K ₆	15726.04926
Prototype K ₇	15539.96695
Prototype K ₈	15481.61669
Prototype K ₉	15474.72787
Prototype K ₁₀	15466.91927

Target Stiffness in Y-Axis (lbs/ft)

Prototype K ₁	#DIV/0!
Prototype K ₂	#DIV/0!
Prototype K ₃	#DIV/0!
Prototype K ₄	#DIV/0!
Prototype K ₅	#DIV/0!
Prototype K ₆	#DIV/0!
Prototype K ₇	#DIV/0!
Prototype K ₈	#DIV/0!
Prototype K ₉	#DIV/0!
Prototype K ₁₀	#DIV/0!

Target Stiffness in Z-Axis (lbs/ft)

Prototype K ₁	#DIV/0!
Prototype K ₂	#DIV/0!
Prototype K ₃	#DIV/0!
Prototype K ₄	#DIV/0!
Prototype K ₅	#DIV/0!
Prototype K ₆	#DIV/0!
Prototype K ₇	#DIV/0!
Prototype K ₈	#DIV/0!
Prototype K ₉	#DIV/0!
Prototype K ₁₀	#DIV/0!

DEPARTURES IN THE PLANE OF THE LINE

OUTPUT PARAMETERS

Preferred Departure in Plane of Line 1 (Feet)

D1	1161.54
D2	1176.46
D3	1191.30
D4	1206.30
D5	1236.99
D6	1268.51
D7	1300.59
D8	1332.86
D9	1365.18
D10	1397.48

Preferred Departure in Plane of Line 2 (Feet)

D1	1051.59
D2	1041.21
D3	1030.99
D4	1020.78
D5	1000.27
D6	979.76
D7	959.50
D8	939.78
D9	920.74
D10	902.47

Preferred Departure in Plane of Line 3 (Feet)

D1	1051.59
D2	1041.21
D3	1030.99
D4	1020.78
D5	1000.27
D6	979.76
D7	959.50
D8	939.78
D9	920.74
D10	902.47

Preferred Departure in Plane of Line 4 (Feet)

D1	
D2	
D3	
D4	
D5	
D6	
D7	
D8	
D9	
D10	

Resultants of Horizontal Offsets (Feet)

Offset 1	15.56
Offset 2	30.48
Offset 3	45.32
Offset 4	60.32
Offset 5	91.01
Offset 6	122.53
Offset 7	154.61
Offset 8	186.88
Offset 9	219.20
Offset 10	251.50

GLOBAL RESTORING FORCE PLOTS

Equivalent and Prototype F_x Versus X-Direction Offsets

Equivalent and Prototype F_y Versus Y-Direction Offsets

Equivalent and Prototype F_z Versus Z-Direction Offsets

PLOTS OF GLOBAL STIFFNESS

Equivalent and Prototype K_x Versus X-Direction Offsets

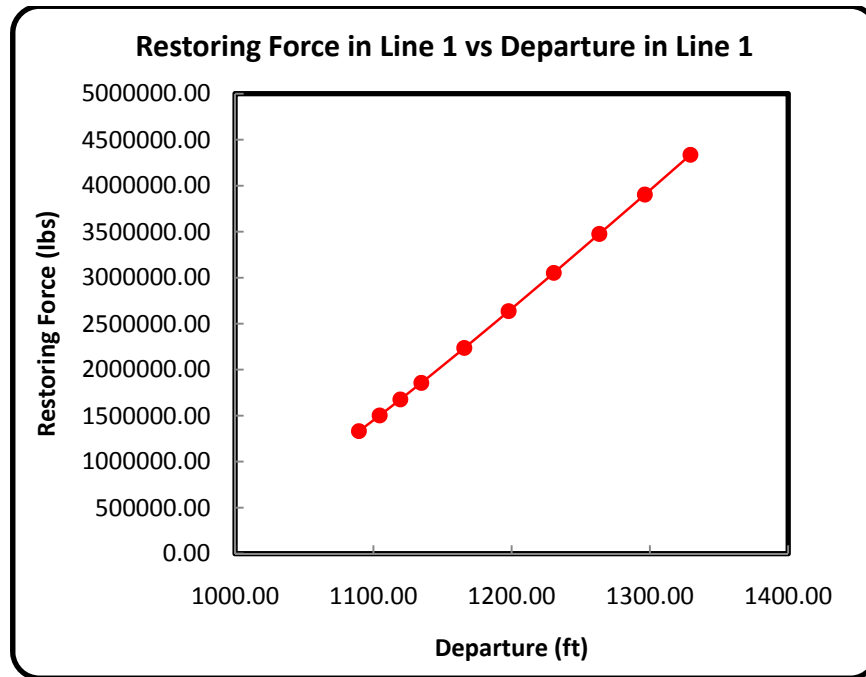
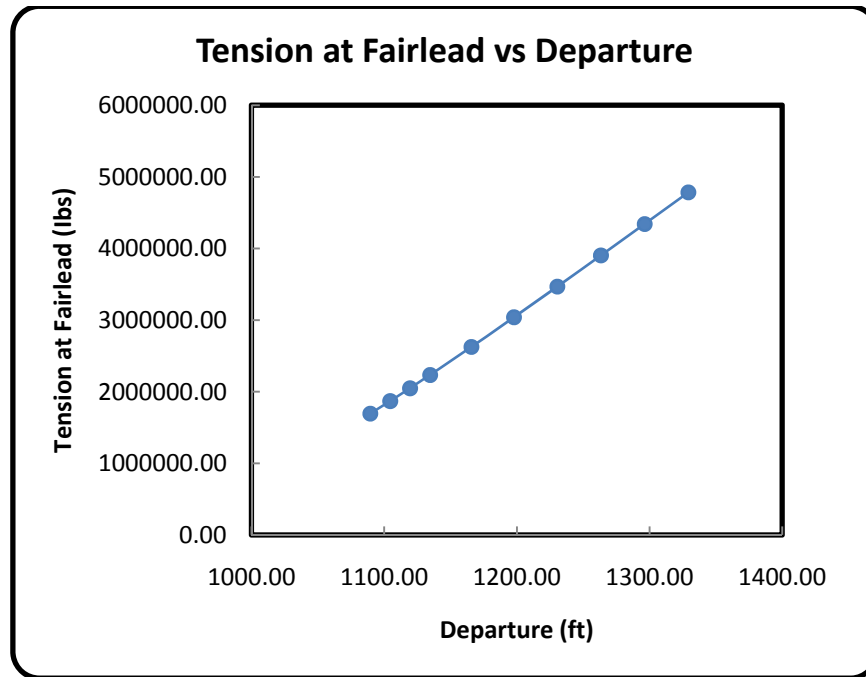
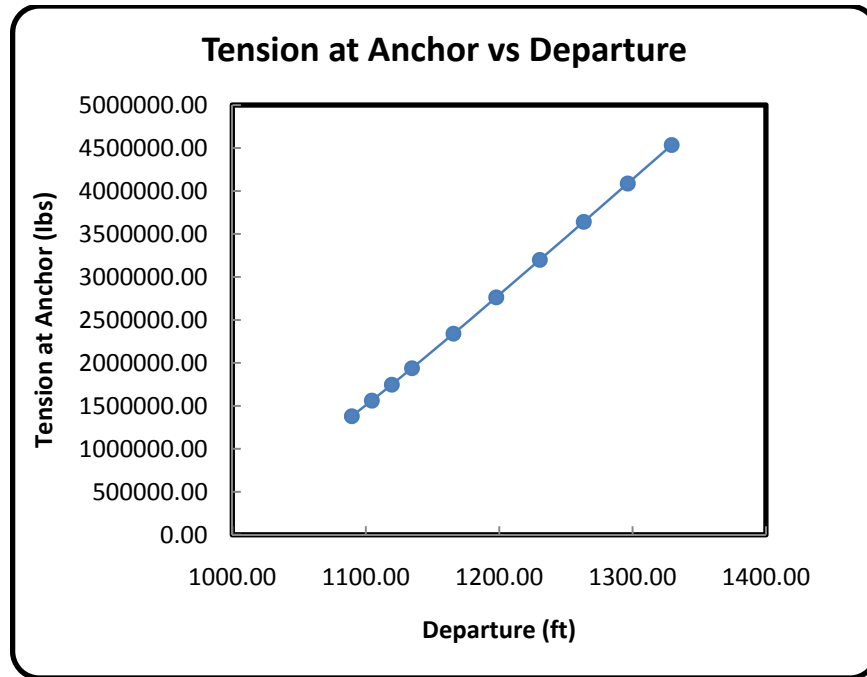
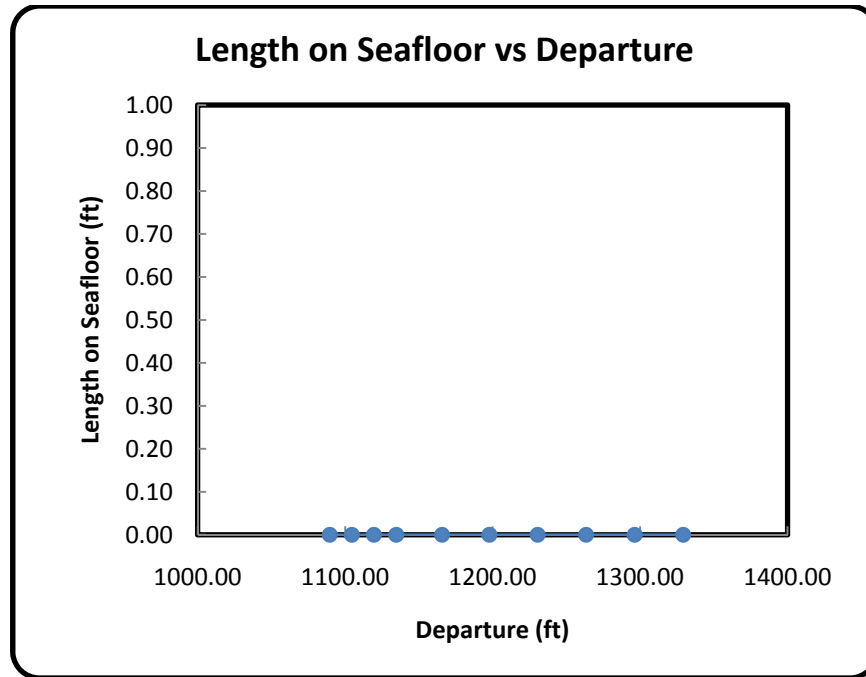
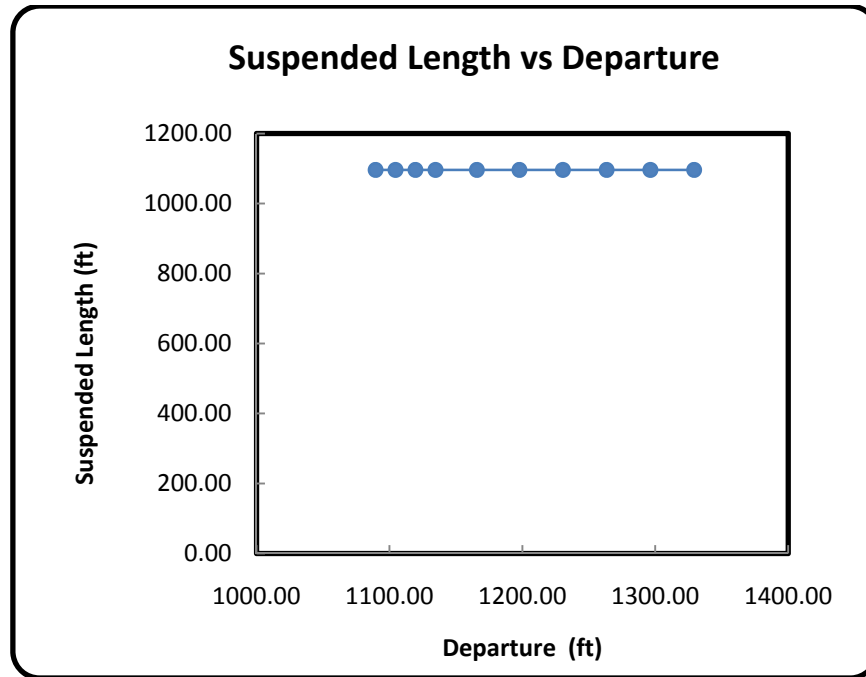
Equivalent and Prototype K_y Versus Y-Direction Offsets

Equivalent and Prototype K_z Versus Z-Direction Offsets

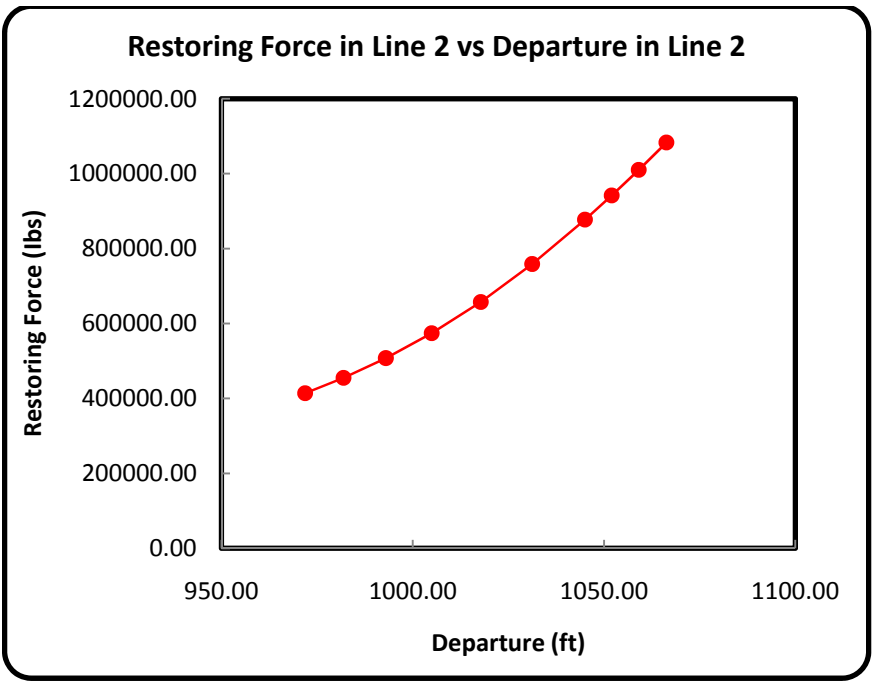
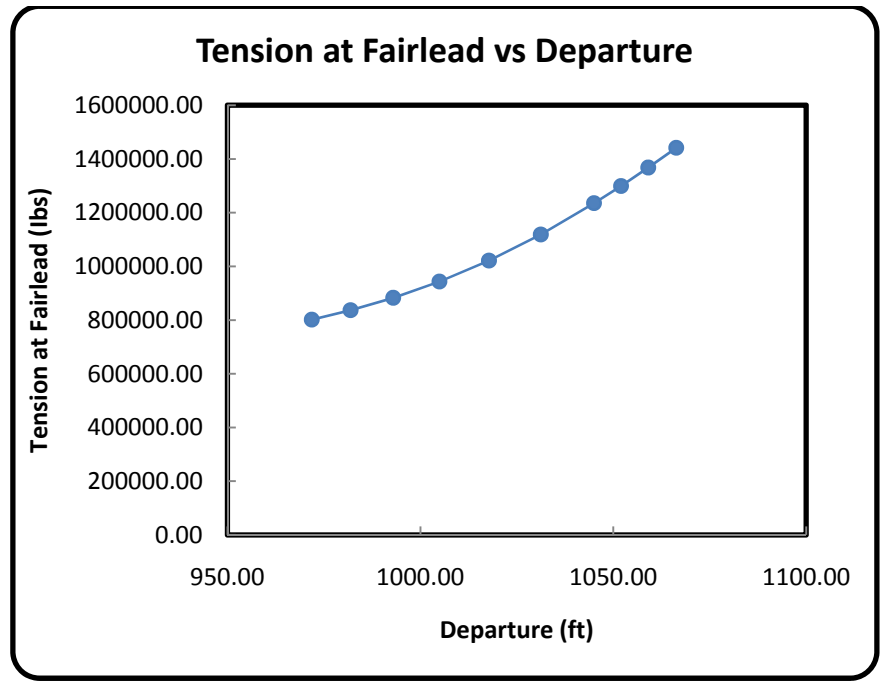
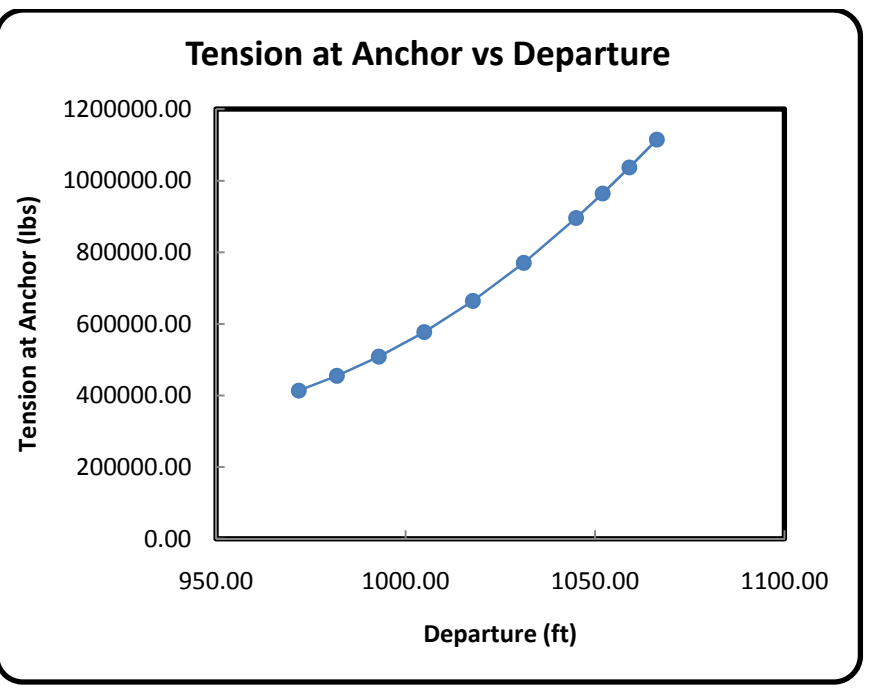
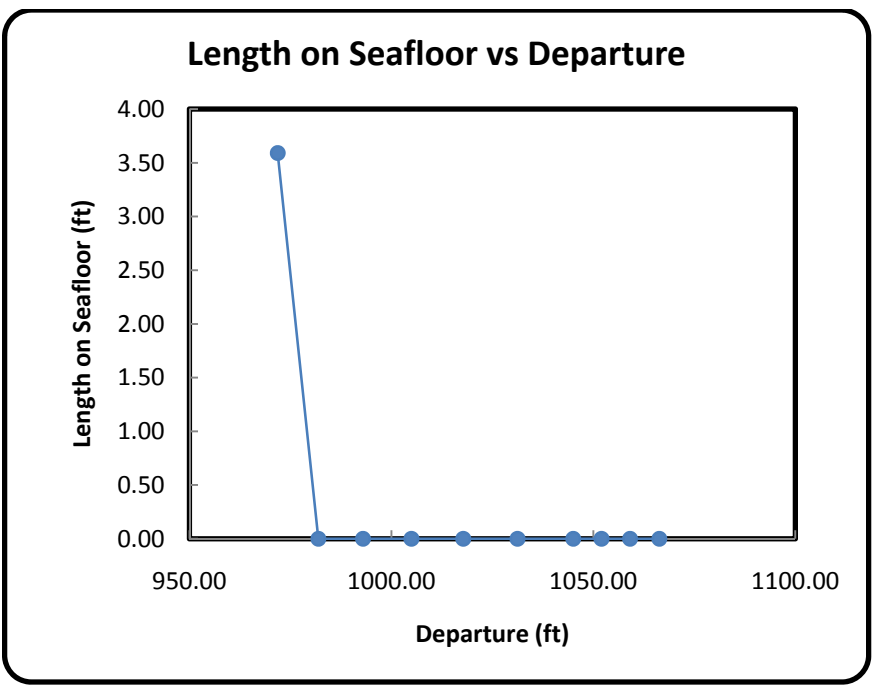
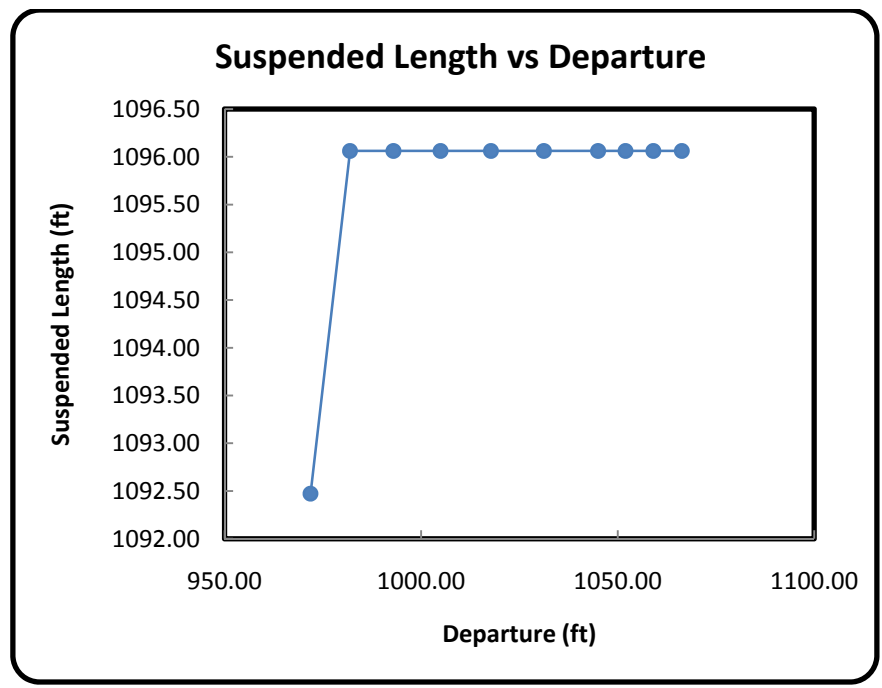
STAMOORSYS Static Analysis of Spread Mooring Systems STAMOORSYS

APPENDIX B

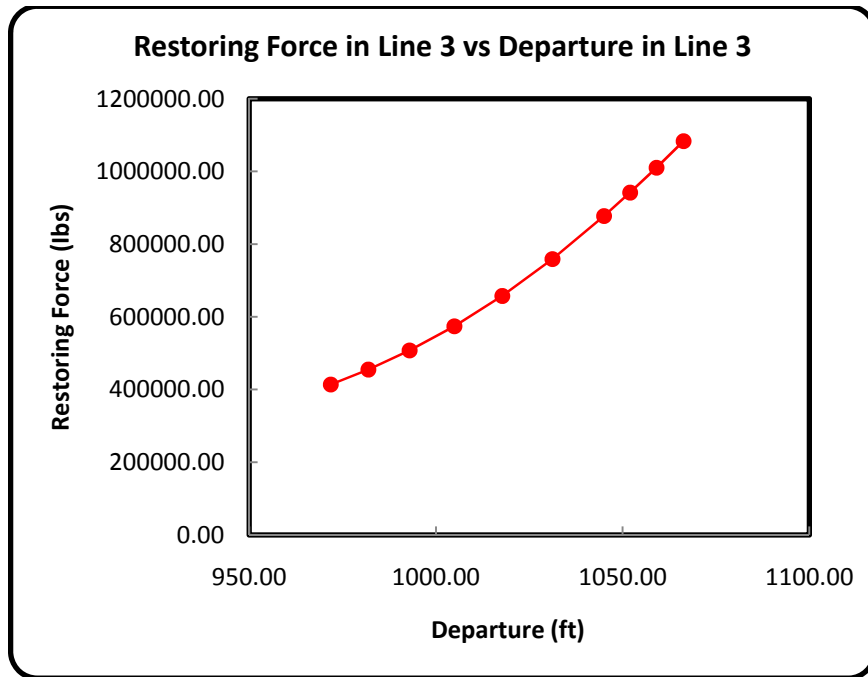
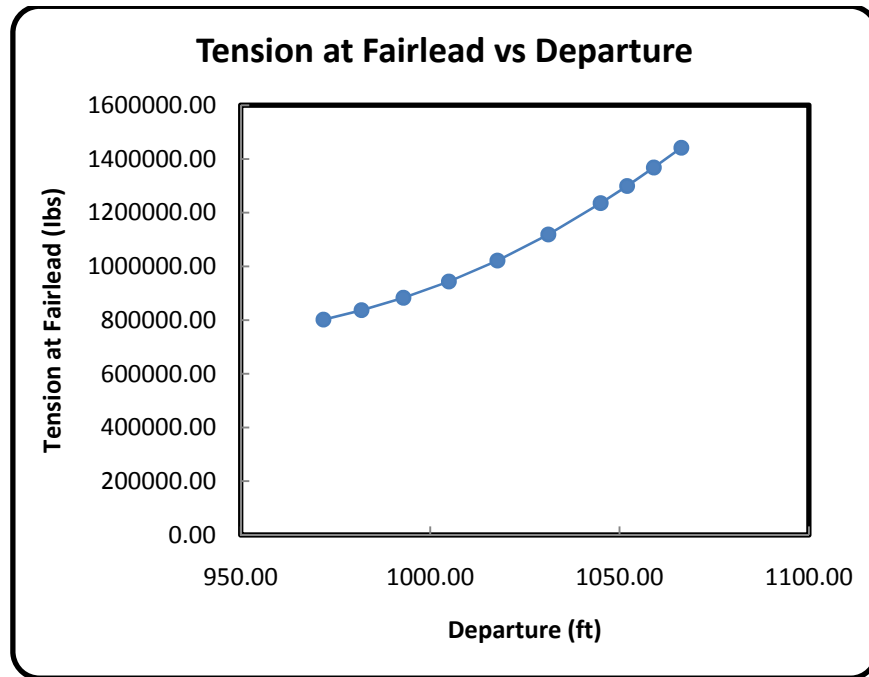
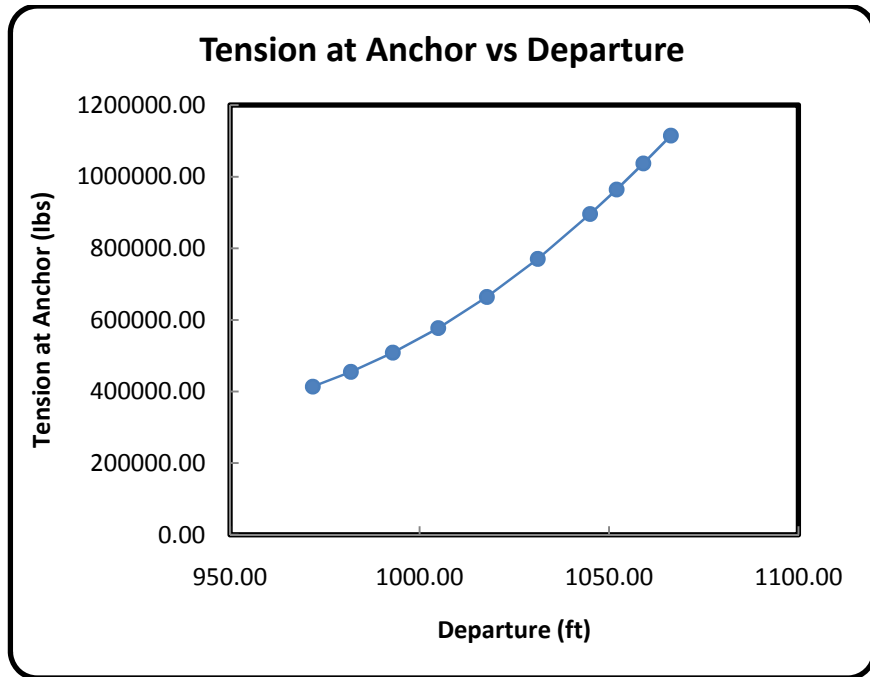
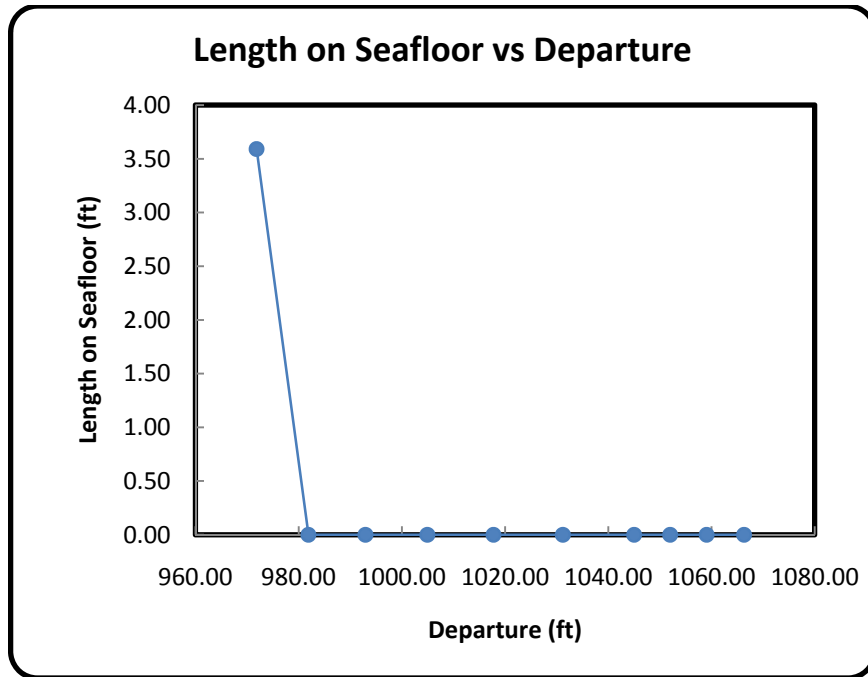
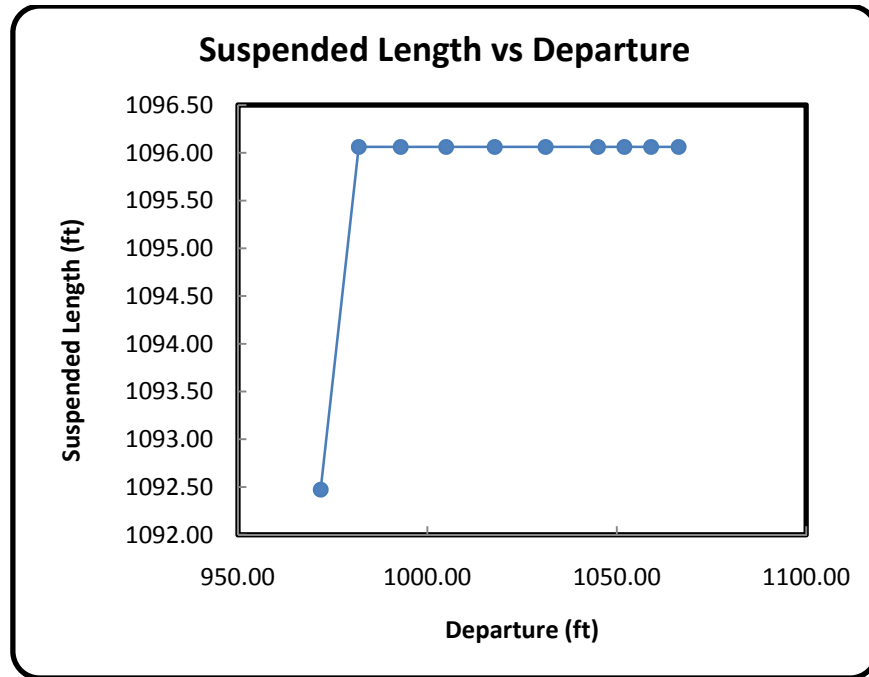
Appendix B1: LOCAL RESULTS FOR LINE 1



Appendix B2: LOCAL RESULTS FOR LINE 2



Appendix B3: LOCAL RESULTS FOR LINE 3



VITA

IKPOTO ENEFIOK UDOH

Research Assistant, Offshore Technology Research Center

Coastal and Ocean Engineering, Texas A&M University

3136 TAMU, Texas 77843-3136

USA

put247@yahoo.com

EDUCATION

M.S., Ocean Engineering, Texas A&M University, 2008

B.Eng., Civil and Environmental Engineering, University of Port Harcourt, 2004

RECOGNITIONS / AWARDS

D. Michael Hughes Scholarship Award, Ocean Engineering Program, Texas A&M University, 2007.

Akwa Ibom State Scholarship Award, Nigeria, 2006.

Federal Government Scholarship Award, Nigeria, 2002.

PROFESSIONAL MEMBERSHIPS AND LEADERSHIP POSITIONS HELD

President, Offshore Technology Research Center Graduate Students Forum (OTRCGSF), Texas A&M University, USA (2007 – Present)

Current Member, American Society of Civil Engineers (ASCE)

General Parade Commander, National Youth Service Corps (NYSC), Zamfara State, Nigeria (2005 – 2006)